MAY 2017

M.Sc. in Civil Engineering

YUSUF JAMAL ABDULRAHMAN

UNIVERSITY OF GAZİANTEP

GRADUATE SCHOOL OF

NATURAL & APPLIED SCIENCES

A NUMERICAL STUDY ON THE LINKED COLUMN FRAME STRUCTURAL SYSTEMS

M. Sc. THESIS

IN

CIVIL ENGINEERING

BY

YUSUF JAMAL ABDULRAHMAN

MAY 2017

A Numerical Study on the Linked Column Frame Structural Systems

M.Sc. Thesis

in

Civil Engineering

University of Gaziantep

Supervisor

Assoc. Prof. Dr. Esra METE GÜNEYİSİ

by

Yusuf Jamal ABDULRAHMAN

May 2017

REPUBLIC OF TURKEY
UNIVERSITY OF GAZİANTEP
GRADUATE SCHOOL OF
NATURAL & APPLIED SCIENCES
CIVIL ENGINEERING DEPARTMENT

Name of the thesis: A Numerical Study on the Linked Column Frame Structural Systems

Name of the student: Yusuf Jamal ABDULRAHMAN

Exam date: 18.05.2017

Approval of the Graduate School of Natural and Applied Sciences

Prof. Dr. A. Necmeddin YAZICI
Director

I certify that this thesis satisfies all the requirements as a thesis for the degree of Master of Science.

Prof. Dr. Abdulkadir ÇEVİK
Head of Department

This is to certify that we have read this thesis and that in our consensus opinion it is fully adequate, in scope and quality, as a thesis for the degree of Master of Science.

Assoc. Prof. Dr. Esra METE GÜNEYİSİ
Supervisor

Examining Committee Members:	Signature
Assoc. Prof. Dr. Ali Fırat ÇABALAR	....
Assoc. Prof. Dr. Esra METE GÜNEYİSİ	....
Assoc. Prof. Dr. Kasım MERMERDAŞ	....

I hereby declare that all information in this document has been obtained and presented in accordance with academic rules and ethical conduct. I also declare that, as required by these rules and conduct, I have fully cited and referenced all material and results that are not original to this work.

Yusuf Jamal ABDULRAHMAN

ABSTRACT

A NUMERICAL STUDY ON THE LINKED COLUMN FRAME STRUCTURAL SYSTEMS

ABDULRAHMAN, YUSUF JAMAL
M.Sc. in Civil Engineering
Supervisor: Assoc. Prof. Dr. Esra METE GÜNEYİSİ
May 2017
104 pages

The idea of using the frame with the linked column in the earthquake resistant structures is a new issue and considered as one of the novel types of seismic protection systems. In this study, the nonlinear behavior of the moment resisting frame (MRF) and the linked column frame (LCF) were investigated comparatively based on the pushover and time history analysis. To this aim, 3-story and 6-bay steel frame models with and without the linked columns were studied. The LCF models were designed as one linked column (LCF1), three linked columns (LCF3), five linked columns (LCF5) and seven linked columns (LCF7). The spacing between the linked column was also altered as 1, 2 and 3 m for all models. Thus, a total of 13 different frame models (covering a bare MRF and 12 LCFs) was taken into account. The capacity curve, story displacement and drift variation, time history plots, and plastic hinge formation for all structures were evaluated. In the time history analysis, three different earthquake ground motions were used. The case studied MRF was observed to be the most vulnerable under the earthquakes. However, it was pointed out that by introducing the link column into the frame, the seismic demands were successfully controlled, depending mainly on the number and spacing of the linked columns.

Keywords: Earthquake, Linked column, Moment resisting frame, Nonlinear behavior, Spacing.

ÖZET

BAĞLANTILI KOLON ÇERÇEVELİ YAPISAL SİSTEMLER ÜZERİNE NÜMERİK BİR ÇALIŞMA

ABDULRAHMAN, YUSUF JAMAL
Yüksek Lisans Tezi, İnşaat Mühendisliği
Danışman: Doç. Dr. Esra METE GÜNEYİSİ
Mayıs 2017
104 sayfa

Depreme dayanıklı yapılarda bağlantılı kolon çerçeve kullanma kavramı yeni bir konudur ve yeni bir sismik koruma sistemi türü olarak düşünülmüştür. Bu çalışmada, moment aktaran çerçeve ve bağlantılı kolon çerçevelerinin doğrusal olmayan davranışı, itme ve zaman tanım alanındaki analizlere dayalı olarak karşılaştırmalı olarak araştırılmıştır. Bu amaçla, bağlantılı kolonları olan ve olmayan 3 katlı 6 açıklıklı çelik çerçeve incelendi. Bağlantılı kolon çerçeve modelleri, bir bağlantılı kolon, üç bağlantılı kolon, beş bağlantılı kolon ve yedi bağlantılı kolon olarak tasarlandı. Bağlantılı kolonlar arasındaki mesafe tüm modeller için 1, 2 ve 3 m olarak değiştirildi. Böylece, toplam 13 farklı çerçeve modeli (referans bir moment aktaran çerçeve ve 12 bağlantılı kolonlu çerçeveleri kapsayan) dikkate alınmıştır. Tüm yapılar için kapasite eğrisi, kat deplasmanı ve ötelenme değişimi, zaman tanım alanı çizimleri ve plastik mafsal oluşumları değerlendirildi. Zaman tanım alanındaki analizlerde üç farklı deprem yer hareketi kullanılmıştır. Araştırmada kullanılan moment aktaran çerçevenin deprem etkisinde en savunmasız olduğu gözlemlenmiştir. Bununla birlikte, bağlantılı kolonların çerçeveye dahil edilmesiyle, bağlantılı kolon sayısına ve aralığına bağlı olarak sismik talepler başarıyla kontrol edilmiştir.

Anahtar Kelimeler: Deprem, Bağlantılı kolon, Moment aktaran çerçeve, Doğrusal olmayan davranış, Aralık.

To My Parents

ACKNOWLEDGEMENT

Firstly, praises to Allah, the Almighty, on whom ultimately we depend for sustenance and guidance. I am ever grateful to Lord, the Creator and the Guardian, and to whom I owe my existence.

I would like to express my sincere thanks to my supervisor, Assoc. Prof. Dr. Esra METE GÜNEYİSİ, for all of her help, patience, valuable advices and her kind guidance. I'm very grateful and honored to work under her academic guidance.

I would like to take a chance to thank all of my friends here in Gaziantep and those who are back home at Erbil, for their continuous support, motivation and Help, they were right by my side whenever I needed them at every stage of my thesis.

Finally, I am very grateful to my parents, my brothers and my sisters, for their continues love, support and dedication, and to my wife Bafren B. Ahmed, for her Love, patience and endless support for finishing my work.

TABLE OF CONTENTS

Page

LIST OF FIGURES

Page

LIST OF TABLES

Page

LIST OF SYMBOLS/ABBREVIATIONS

ADAS	Additional Damping and Stiffness devices
AISC	American Institute of Steel Construction
ASCE	American Society of Civil Engineers
BRB	Buckling Restrained Braces
CBF	Concentrically Braced Frames
EBF	Eccentrically Braced Frames
FEMA	Federal Emergency Management Agency
IMF	Intermediate Moment Frames
LCF	Linked Column Frame
MRF	Moment Resisting Frame
OMF	Ordinary Moment Frames
RC	Reinforced Concrete
SMF	Special Moment Frame
SMRF	Special Moment Resisting Frame
TADAS	Triangular Additional Damping and Stiffness devices

CHAPTER 1

INTRODUCTION

1.1 General

The main aim of study the linked column frame system is based upon providing different levels of safety against different levels of earthquake actions. For example, under high intensity seismic activities to avoid the total or partial collapse; under mid intensity seismic activities to bound the damage in repairable states, and under low intensity activities to return to the occupancy rapidly or to remain in the elastic state (Turkish Earthquake Code, 2007). For this purpose, in addition to the conventional structural systems such as steel shear panel devices (Nakashima, 1995; Nakashima et al., 1995; Miyama et al., 1996; Shimizu et al., 1998; Tanaka et al., 1998), buckling-restrained braces (BRBs) (Saeki et al., 1996; Aiken et al., 1999; Iwata et al., 2000; Sabelli et al., 2003), and additional damping and stiffness devices (ADAS) and triangular additional damping and stiffness devices (TADAS) (Tsai et al., 1993; Dargush and Soong, 1995; Tena-Colunga, 1997), at first, in the study of Dusicka and Iwai (2007), the link column frame structural system with the aim of taking the role of bracing in steel structures and also with the aim of observing damage in link members which can be replaceable was suggested. New structural systems that provides the dissipation of the earthquake energy efficiently have been still investigated. The notion of using the linked column frame (LCF) constitutes one of these novel systems, that have gained interest on it in the recent years.

1.2 Description

The linked column frame system as a novel system mainly has two energy dissipation mechanisms in itself such as the link column system and the moment resisting frame. The main aim in the design of LCF is to dissipate energy within the link members and decrease the inelastic deformation demand and consequently damage in the other structural members of the moment resisting frame as shown in Figure 1.1 (Malakoutian et al., 2012). In the literature, there are limited studies examining the behavior of LCF experimentally and also analytically. For instance, at first, in the study of Dusicka and Iwai (2007), the link column frame structural system with the aim of taking the role of bracing in steel structures and also with the aim of observing damage in link members which can be replaceable was suggested. Also, in their study as shown in Figure 1.2, the different column base support conditions were taken into account in comparison of the LCFs with special moment resisting frames. Additionally, in the study of Malakoutian et al. (2012) the design procedure for LCF was suggested, and in a new study (Malakoutian et al., 2013), the results of the full-scale investigates regarding LCF and exhaustive determinate element modeling of these experimentally tested LCFs were given. In another study, the response modification, the over strength and deflection amplification factors for LCFs were determined considering different design parameters (Malakoutian et al, 2016). On the other hand, in the literature there are studies investigating the utilization of linked column frame systems in reinforced concrete structures. For example, in the study of Shelton and Hemalatha (2016) the link beams, which were constructed as reinforced concrete, were designed to connect with the columns by the use of bolted connections. Their effects on the behavior of 4, 7 and 10 storey three dimensional reinforced concrete structures were studied. Similarly, in the study of Lydia and Hemalatha (2013), the effectiveness of the implementation of the linked reinforced concrete beams in different locations in the lateral resistance of a two dimensional reinforced concrete frame were examined.

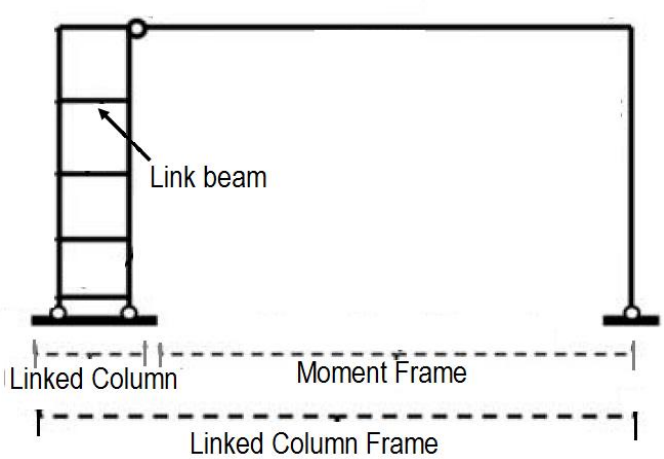

Figure 1.1 Schematic view of Linked Column Frame (LCF) system (Malakoutian et al., 2012)

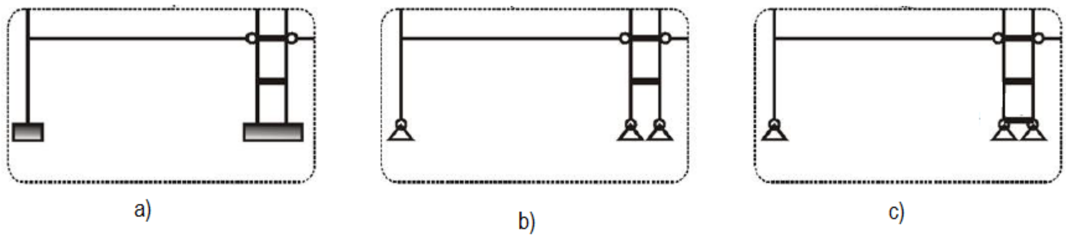

Figure 1.2 LCF systems with different support conditions: a) fixed, b) pin, c) pin and linked (Malakoutian et al., 2013)

1.3 Scope of work

In this study, the comparative evaluation of 3-story and 6-bay steel linked column frames with the moment resisting frame were conducted. For this parametric study, one linked column (LCF1), three linked column (LCF3), five linked column (LCF5) and seven linked column (LCF7) frames having link beam length of 1, 2 and 3 m were considered. Thus, different frame models (a bare MRF and 12 LCFs) were analyzed through nonlinear static (pushover) and nonlinear dynamic analysis. Consequently, from the analysis, the capacity curves, the maximum story displacement demand, the maximum inter-story drift demand and the variation of roof displacement with time, plastic hinge patterns for all structures were examined, comparatively.

1.4 Outline of the thesis

This thesis has 5 chapters:

Chapter 1 Introduction: which is contained the introduction and background of the LCF frame systems and scope of works.

Chapter 2 Literature review: which is included in the previous research on structural systems, seismic load effecting on structural systems, and linked column frame structural system.

Chapter 3 Methodology: in this chapter the analytical model of structures which is included design procedures, prototype designs details, description of the development and modeling techniques of the link; and nonlinear analysis included nonlinear static (pushover) and time history analysis.

Chapter 4 Results and discussion: Discussed the results which is out come from nonlinear analysis of MRF and LCFs corresponding Sap2000 modeling.

Chapter 5 Conclusions: Provides a conclusion of the results for analyzed different models.

CHAPTER 2

LITERATURE REVIEW

2.1 Structural systems

The structural framing of a building has gravity and lateral loads to reflect. Therefore, concurrently with the preparation of the floor and roof framing plans, the architect should define how to provide lateral load resistance to the structure. The peak point for designing structural system is load that effected on the choosing the material and properties which is lateral forces made by earthquake shaking are resisted by the structure frame and by the relative improving of seismic resistant design and detailing provided (FEMA P-749, 2010).

2.1.1 Bearing wall and shear wall systems

Structural wall carried vertical support for the building's weight and lateral resistance of the building's. This structural are generally used for warehouses, low-rise commercial buildings of concrete, residential construction, wood construction, and masonry (Figure 2.1) (FEMA P-749, 2010).

In building frame systems, shear walls used to struggle lateral loads and provide lateral stiffness beside extreme side-sway. Also used to provide lateral strength and stiffness in arrangement with a steel braced system. The reinforced concrete shear walls are more common in commercial buildings, also shear walls can be made from wood (PCI, 1992; Doran, 2013).

For designing shear walls and bearing walls as interior and exterior and their anchorage the force shall be equivalent to 40% of the short retro design haunted response acceleration SDS times the weight of wall, W_c, normal to the surface, with a minimum force of 10% of the weight of the wall. Interlink of wall elements and links to supporting framing systems shall have thermal changes, rotational capacity, or sufficient strength to resist shrinkage, adequate ductility, and variance foundation settlement where collective with seismic forces (ASCE/SEI 7–10, 2013).

Figure 2.1 A three-story masonry bearing wall building (FEMA P-749, 2010)

2.1.2 Building frame systems

A common type of structural system on structural steel and concrete for constructing buildings are building frames. In this system the columns and beams typically will providing the building's weight. Providing lateral resistance is carried by braces which is diagonal steel members that spread between the columns and beams to provide horizontal stiffness or by masonry, concrete, or timber shear walls that deliver lateral resistance but without carrying weight of the structure. The diagonal braces using form some building frame structures in natural and plain fragment of the building design as is the case for the tall building (FEMA P-749, 2010).

2.1.3 Moment-resisting frame systems

Generally, it is using for structural steel and reinforced concrete construction. In frame system, the weight of the structure and strength and stiffness needed to resist lateral forces carryout by the horizontal beams and vertical columns. While using rigid connections between the columns and beams, the strength and stiffness are achieved to avoid columns and beams from rotating relative to one other. A steel MRF building under construction shown in (Figure 2.2) (FEMA P-749, 2010).

There are three types of steel moment frames are ordinary moment frames (OMF), special moment frame (SMF) and intermediate moment frames (IMF). SMFs are ordinary to withstand significant inelastic deformations when subjected to the forces resulting from motions of the design earthquake. The inelastic deformation capacity of IMFs is more limited when compared to SMFs. OMFs are less ductile than IMFs, and are expected to have limited ductility within their components and connections. Steel moment resisting frames, especially their fully welded connections, were heavily and unexpectedly damaged during the 1994 Northridge and the 1995 Kobe earthquakes. Before the development of any yielding in the beams many of these connections failed because of absence of confirmation of considerable plastic deformation, and therefore achieved poorly.

This sudden and varied damage facilitated to conduct immediate examinations of pre Northridge connections after the earthquake. Examinations by Popov et al. (1998), Hajjar et al. (1998), Shuey et al. (1996) and Uang et al. (1998) replicated all the major types of damage seen in the field, and also presented little or no plastic deformation. Varied research following the Northridge Earthquake recognized a number of factors that donated to the premature fractures experimental after the earthquake. This included factors connected to the connection configuration and factors connected to the welding, as well as others. Some of these factors have suggestions in developing the linked column frame (LCF) and are debated in the following sections. Comprehensive reports were produced on design, retrofit, analysis and construction inspection of moment resisting frames (FEMA-354, 2000; FEMA-352, 2000; FEMA-350, 2000; FEMA-351, 2000; FEMA-353, 2000; FEMA-355 C, 2001) by the SAC Joint Venture Partnership and through support by the Federal Emergency Management Agency (FEMA).

Figure 2.2 High rise steel moment frame structure under construction (FEMA P-749, 2010)

Liao et al. (2007) release on ABAQUS advanced a three-dimensional finite-element model to evaluate effects of connection fractures of seismic load accurately considering pre and post Northridge connections to evaluate the performance on 3-story MRF, contribution of gravity frame as well as the effects of panel zone and column deformations on building performance. The results show that as probable the pre-Northridge building has much higher failure possibility in all performance categories from immediate occupancy to initial collapse, for that reason is much exposed to future seismic excitation due to connection fractures.

2.1.4 Dual systems

Dual systems, a sparing alternative to moment-resisting frames, are commonly used for high buildings. Dual system structures feature a mixture of moment-resisting frames and concrete, masonry, or steel walls or steel braced frames. The vertical support for the weight and a ration of the lateral resistance of the structure carried out by the moment-resisting frames which is lateral resistance mostly delivered by masonry, concrete, or steel walls or by steel braced frames. Sometimes frame-shear wall interactive system's name is given to dual systems (FEMA P-749, 2010).

2.1.5 Cantilever column systems

Sometime in low-rise structures and in the top story of tall structures, the cantilever column system is used. In these structures, where they are restrained from rotating the columns cantilever will be upward from their base. The lateral resistance to earthquake forces and building's weight will be in vertical support carried by the column. In past earthquake the structures which are used this system have performed poorly, that's make most uses in the zones which have high seismic activity (FEMA P-749, 2010).

2.1.6 Concentrically and Eccentrically Braced Frames

First developing in the concentrically and eccentrically braced frames was in the early 1970s in Japan. which is investigating and component levels in the United States was in 1980s at the University of California, Berkeley that concluded a series of experimental and analytical studies (Roeder and Popov, 1977; Malley and Popov, 1983; Hjelnstad and Popov, 1983; Kasai and Popov, 1986; Whittaker et al., 1987; Ricles and Popov,1987; Ricles and Popov, 1989; Engelhardt and Popov, 1992).

Concentrically braced frames (CBFs) are a type of preventing lateral loads structure systems through a vertical concentric truss system, the axes of the members supporting concentrically at the joints. Because of the CBFs can provide high strength and stiffness, it tends to be effective in preventing lateral forces. These appearances may less favorable seismic response in the results with the low drift capacity and higher accelerations. In the seismicity areas, steel or composite structural CBFs are a common structural system. To form a vertical truss seeing columns, braces, and beams are arranged in the CBFs systems. By truss action the lateral earthquake forces will be resists in this system, also develops ductility by inelastic effect in braces. When braces perform in elastic range the CBFs system is measured as the most stiffness efficient. The lateral stiffness starts humiliating and an irregular response is developed when the inelastic response is initiated. speed of production, managed fabrication process and qualified to the reduced cost are the approval of the CBFs system. Even though the advantages mentioned above, poor energy preoccupation and dissipation through inelastic response are comparatively shown in the CBFs. This system unproductive and untrustworthy for seismic applications because of poverty of compressive strength, progressive respite of braces, and untimely fracture. The concentrically braced frames classifies to ordinary or special. Extensive qualification about elements or connections cannot be seen in Ordinary concentric braced frames. Generally, it's used in the areas that have low seismic risk. Instead, for the areas in high seismic risk the special concentrically braced frames are mostly used mostly. The goal of the concentrically braced frame design is warranted satisfactory ductility (i.e., to stretch without breaking suddenly) The commonly used CBF shapes are shown in Figure 2.3. The V-braced frames of Figures 2.3d and 2.3e are also known as chevron-braced frames (Sabelli et al., 2003).

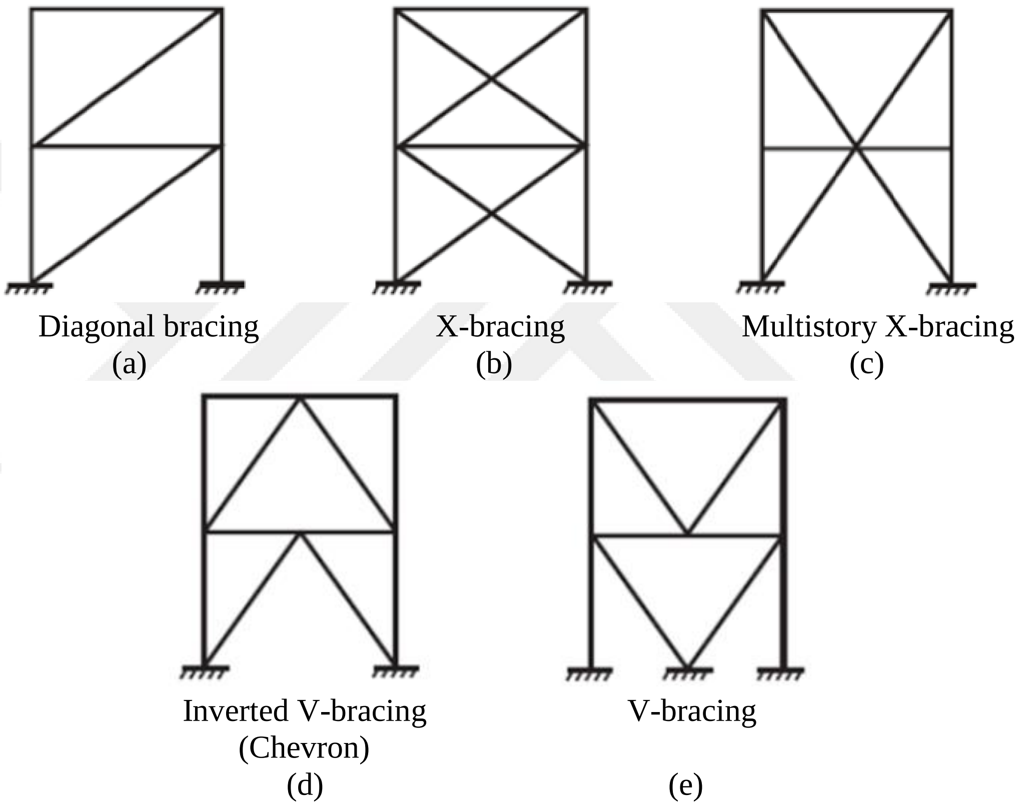

Figure 2.3 Different configurations of CBFs (Sabelli et al., 2003)

Between moment frame (high ductility and stable energy dissipation capacity) and concentrically braced frames (high elastic stiffness) can be observed the eccentrically braced frames (EBFs) as a hybrid system. The advantages and minimize the disadvantages of these two systems are combined in the EBFs. In EBFs, shear forces established in the ductile steel link and forces are transmitted to the brace members through bending. The link is considered to action as a fuse by yielding and also dissolving energy during averting buckling of the brace members. Stylish links provide a stable source of energy dissipation. In eccentrically braced steel frames, different brace shapes are used where the links are identified by the dimension *e* such as shown in Figure 2.4 V-bracing, K-bracing, X-bracing and Y-bracing (Malakoutian et al., 2013).

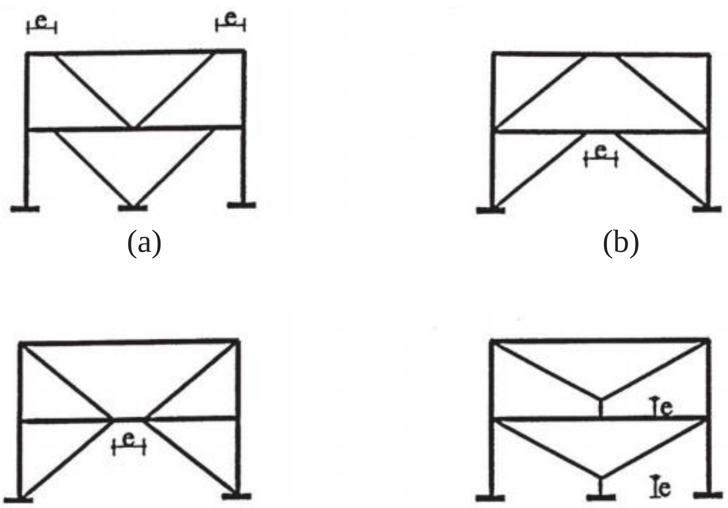

(a) (b) (c) (d)

Figure 2.4 Different types of eccentrically braced steel frames: a) V-Bracing, b) K-Bracing, c) X-Bracing, and d) Y-Bracing (Ghobarah and Elfath, 2001)

Pincheira and Jirsa (1995) studied the performance of reinforced concrete (RC) buildings under five earthquake ground motion records dignified on firm and soft soils for three, seven and twelve story. As shown in (Figure 2.5) Structures were reformed with three different reintegration structures; X-bracing, post tensioned bracing, and addition of structural infill walls. In relations of stiffness and strength improvement, the response of original structures compared with all methods. Analysis results presented that was observed that it was possible to choose from different brace arrangements while the solution is not unique to provide satisfactory seismic performance. All the retrofitting methods for three-storey building, showed acceptable performance for all ground motions. The structural wall provided acceptable performance for seven and twelve storey buildings, however, bracing systems did not arrange for the expected performance for all ground motion records. Brace systems could affect axial load levels on RC members harmfully, so for such cases, it could be important to improve axial load abilities of RC members. For the post tensioned brace case, the supply of internal forces on RC members are narrowly related with bracing shape, brace size and initial level of brace pre-stress.

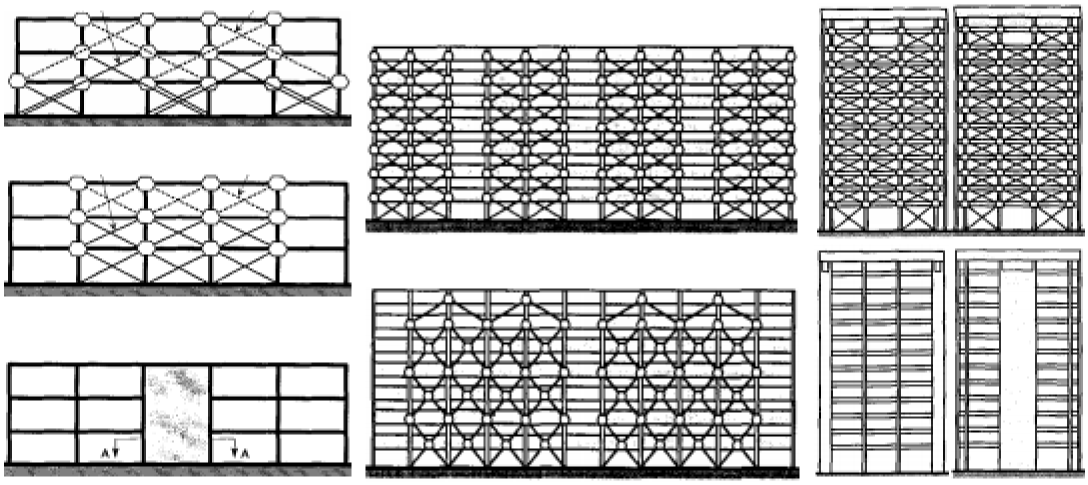

Three Story Building Seven Story Building Twelve Story Building

Figure 2.5 Retrofitted frame model of examined buildings (Pincheira and Jirsa, 1995)

Ghobarah and Elfath (2001) used different ground motion records for a low rise not ductile reinforced concrete structure to get seismic performance. Reinforced concrete designed as a three storey office building; (a) inverted-V bracing with vertical steel links (eccentric), (b) different alignment of first case, and (c) concentric inverted-V-bracing as shown in (Figure 2.6). Analysis results presented that: (case E2) inverted-V bracing with vertical steel links resulted in higher lateral loading capacity than V1 and E1 cases which is V1 provided the highest increase in stiffness. Under the load commanded by earthquake ground motions, less damage and deformation was seen in cases E1 and E2. For bracing systems an important factor is a link deformation angle that could be reserved under an acceptable shear deformation limit. Under seismic loads, plastic mechanism of the structure was expressively allied with the distribution of braces over the structure.

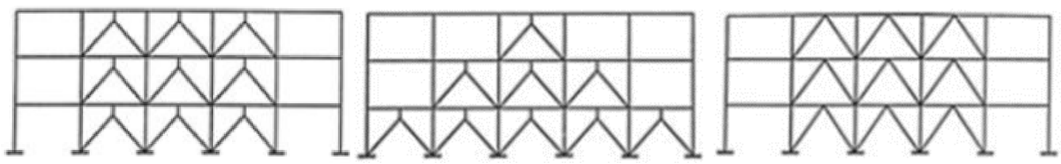

(a) E1 (b) E2 (c) V1

Figure 2.6 Applied rehabilitation system (Ghobarah and Elfath, 2001)

Najafi and Tehranizadeh (2017) addressed the demand of choosing resourceful length of link-beam for the models with eccentrically braced frames, which is used seismic resisting systems, in vision of reducing the amount of distribution in structural responses. The valuation has been piloted by the help of the suggested equations allowing for different height of structures exposed to far and near-field ground motions. By the help of β-unzipping method, reliability assessment of the EBF frames supports confirming suggested equations allowing for failure probability for each model. There is very acceptable conformity for the efficient length of link-beam achieved based on deterministic analyzing by the help of the proposed equations and probabilistic analysis by the help of β-unzipping method which illustrates accuracy and practicality of the introduced equations. The pushover analysis was performed based on the FEMA356 and the diagrams for models by varying number of stories and by the length of link-beams equal to 0.5 and 3.0 m are presented in (Figure 2.7) pushover results for the models by different number of stories and length of link-beams.

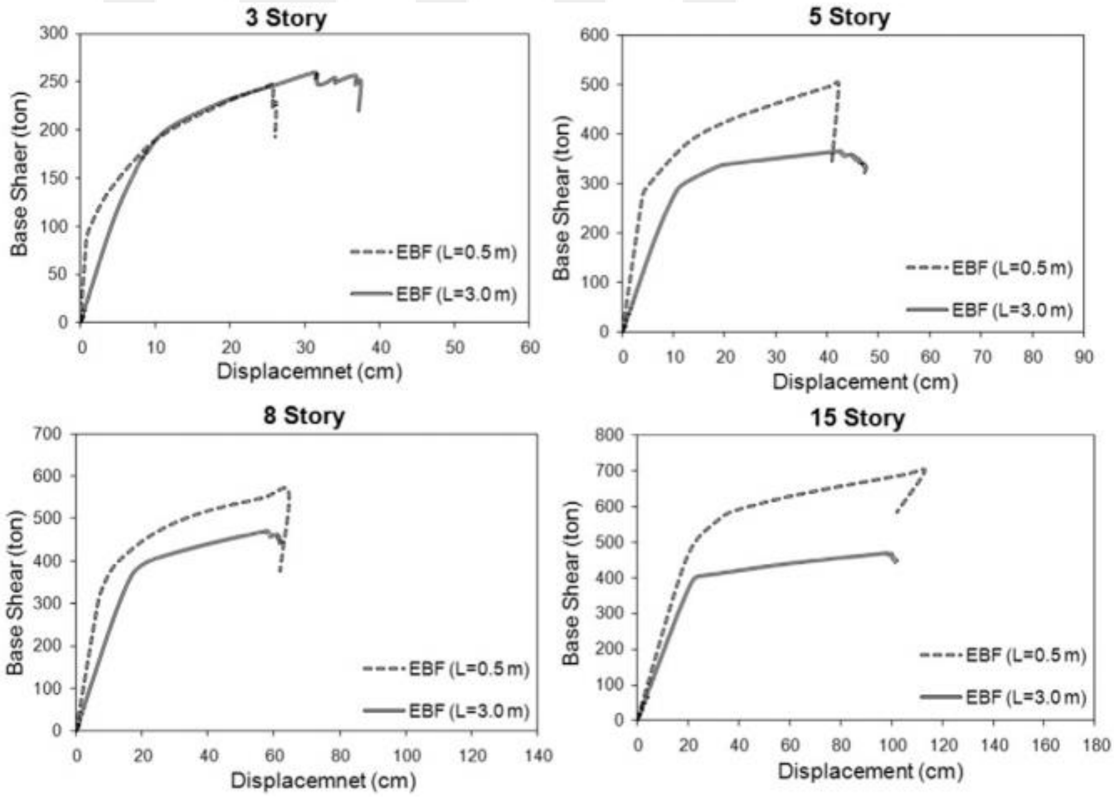

Figure 2.7 Pushover diagrams for models by different number of stories and length of link-beams (0.5 m, 3.0 m) (Najafi and Tehranizadeh, 2017)

Budiono et al. (2017) mainly, focused of earthquake load for performance of link elements in the eccentrically braced frame (EBF) as lateral force protection above the effects of remaining stress over Investigational tests were showed in two stages: First, two links were tested, a standard link that corresponds with the AISC 341–10 as detailed in (Figure 2.8) and a modified link; second, the Neutron Diffraction technique using the equipment of DN1 at Center of Science and Technology of Advanced Material – National Nuclear Energy Agency (PSTBM-BATAN) to remaining stress capacity of the link element. In the first stage, the performances of both links were studied based on the remaining stress distribution. On and around the “k area”, the crack on the standard link is opening because of the amount of tensile stresses, so that it decreases the performance of the link element. To avoid the opening of crack that may occur on the web plate around the “k area”, the link need to improve by replacing the stiffener of the vertical web with the horizontal stiffener, so that it can be improved the performance of the link elements.

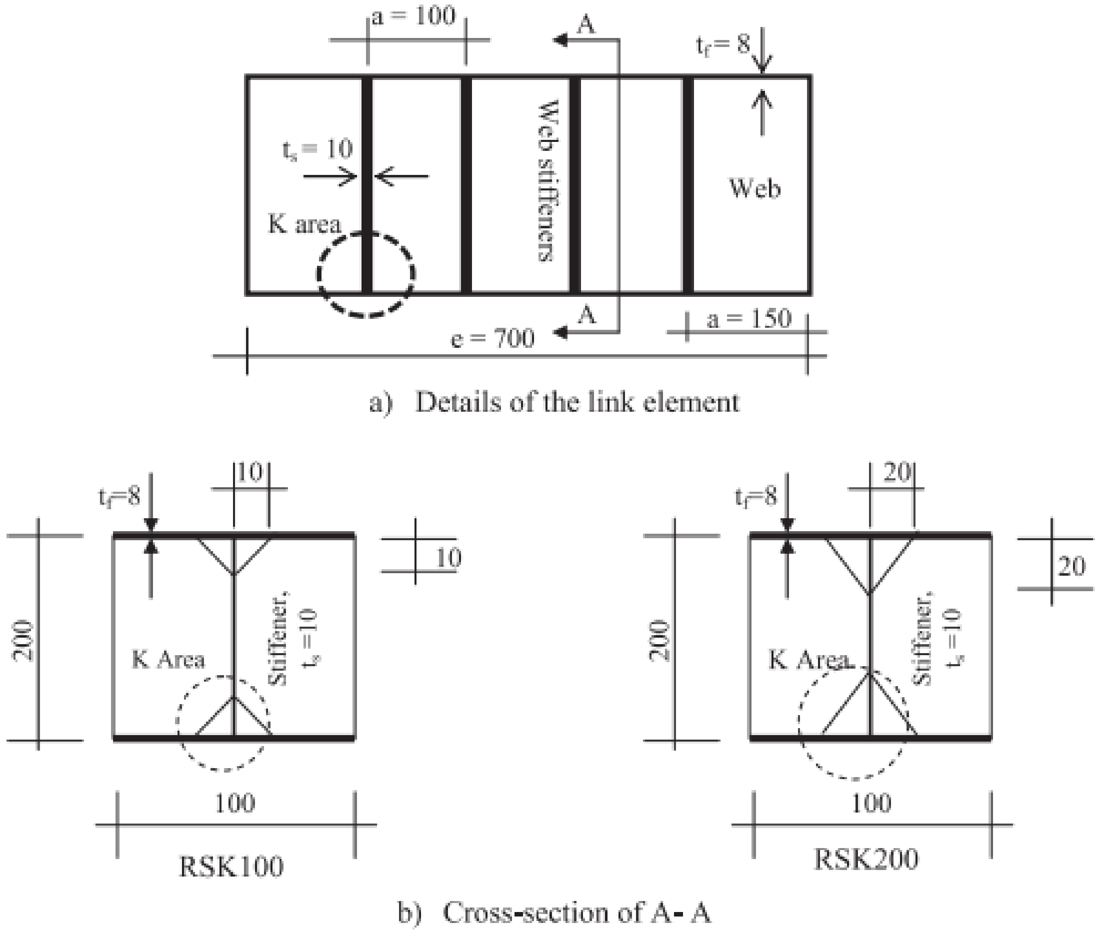

Figure 2.8 Variation of k area extent from the measured samples (in mm) (Budiono et al., 2017)

Based on the above results, from the study of Budiono et al. (2017) the following conclusions were drawn:

a) The remaining stress (Figure 2.9) distribution arrangement in the welding area, for both in the transversal or longitudinal direction has the same result that was performed by research. Furthermore, on the area around the weld toe, the remaining stress has positive value (tensile stress) that nonstop decreases in the Heat Affected Zone area and turns to negative with increasing distance to the weld toe point. This is because of the received heat in the area of weld toe is far bigger than on the external area.

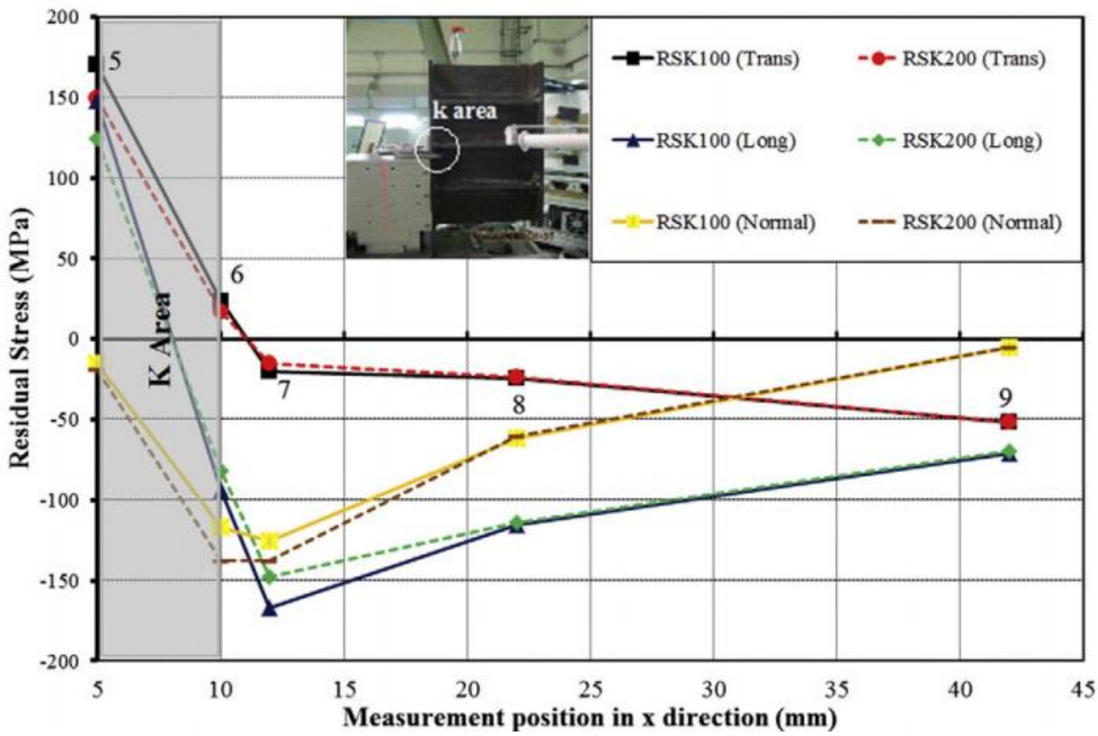

Figure 2.9 Results of measurements of both samples (Budiono et al., 2017)

b) by using the Neutron Diffraction method, achieved value of tensile stress shown that capacity of the yield stress of the material in the weld toe area is between of 75 to 85% and between 50 and 60% of the yield stresses in the longitudinal and transversal directions incline to decrease on the Heat Affected Zone area.

c) An increasing in the ductility of the link element is achieved, through improved link element performance by the adding of the horizontal stiffener, that was performed acceptable to avoid the “k area” which may cause high tensile stress. Moreover, buckling process confirmed to slow down by strengthening the flange end plate. (Figure 2.10) shows that the improved link element has developed performance compared to the standard link. because the ductility value can be increased by avoiding the “k area” that has high tensile stress value, the link element performance may increase.

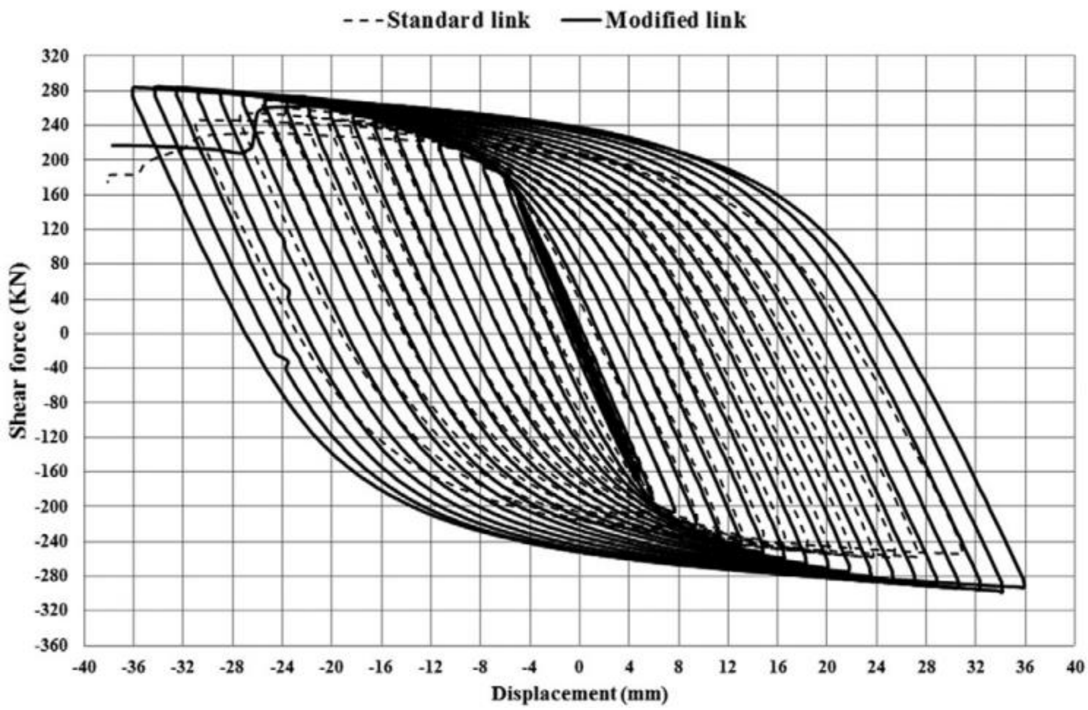

Figure 2.10 A comparison between the hysteretic curve of the standard and modified links (Budiono et al., 2017)

2.2 Seismic load effecting on structural systems

During several past earthquakes, satisfactory seismic performance was presented in the steel structures. In fact, such structures can be developed to resist earthquakes very successfully due to their advantageous mass to stiffness ratio, maintainable energy captivation capacity, and ductility. However, unforeseen damage was restricted mainly in braced bays of CBFs and beam to column links of welded MRFs during recent earthquakes varied brittle fracture was detected in framed structures (AIJ, 1995; Youssef et al., 1995).

Damage analyses observed many structural lacks also at the foundation levels. Definitely, three kinds of failure were detected in base column plate links, that is: excessive deformation of base plates, failure of welds at base plates and damage to anchor bolts. The causes of such damage may be credited to the preparation in Japan to design standard column base links as pin-supported, i.e., no moment transfer at the column base (AIJ, 1995; Azizinamini and Ghosh, 1996).

In Japan a very popular material structural is steel. In the past earthquakes, several tall buildings prepared in the steel frames and have endured a large number of earthquakes without severe damage, instance the great Kanto earthquake in 1923 and Tokachi-Oki in 1968. Though, some damage was continued by medium rise steel buildings during the Miyagiken-Oki earthquake in 1978, mainly the damage because of the fracture of bolted bracing connections. Conversely, a government building which is seventeen story amongst many other steel and composite structures endured with no informed structural damage. The limited ductility and conforming hard fractures in new CBFs exhibited in the fracture of link elements or bracing elements. Instance, damage in braces contained of: net fracture at bolt holes, severe alteration of unstiffened beam in chevron braces (Figure 2.11) and the fracture of welded links and web tear-out (Figure 2.12) (DiSarno and Elnashai, 2002).

Figure 2.11 Damage to nonductile braces in Kobe earthquake: net fracture at bolt holes (left) and severe distortion of unstiffened beam in chevron braces (right) (Naeim, 2001)

Figure 2.12 Damage to nonductile braces in the Kobe earthquake: fracture of welded links and web tear-out (left) and fracture of welded links (right) (Naeim, 2001)

Northern Iran in the June 21, 1990 have an earthquake (M=7.7 and PGA=0.65g) which was the worst seismic incident of this century in heavily populated areas. More than 40,000 people was dead, 100,000 injured and left more than half million homeless, causing the worst economic loss in the history of the nation (Nateghi, 1997). Extensively damaged was contained in medium rise steel frames for residential buildings. These residential constructions five story MRFs were built in the 1980s; with special semi-rigid beam to column links (Khorjinee) and infill walls covering in between the framing. Khorjinee links contain of continuous beams set on top of seat angles, which are welded to both sides of the columns (Figure 2.13) (Nateghi, 1995).

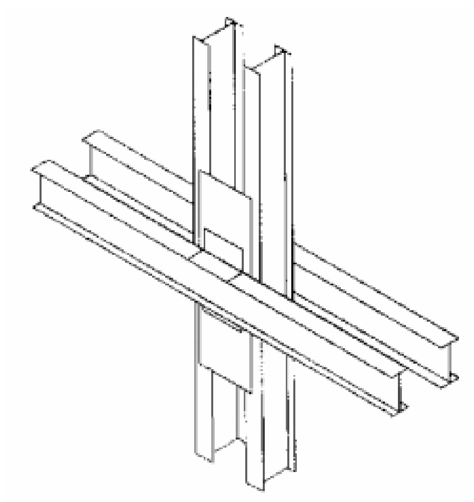

Figure 2.13 Classic Khorjinee beam to column link used in Iran (Nateghi, 1995)

Steel, steel-encased and steel-infilled reinforced concrete buildings are very extensively used in Japan. Of these, unbraced frames knowledgeable the most severe damage; 34 braced in two orthogonal directions, 134 were braced only in one direction and 432 buildings were completely unbraced. In addition, many of these buildings employed shop-welded beam-to-column links and cold-formed hollow sections (Figure 2.14) (DiSarno and Elnashai, 2002).

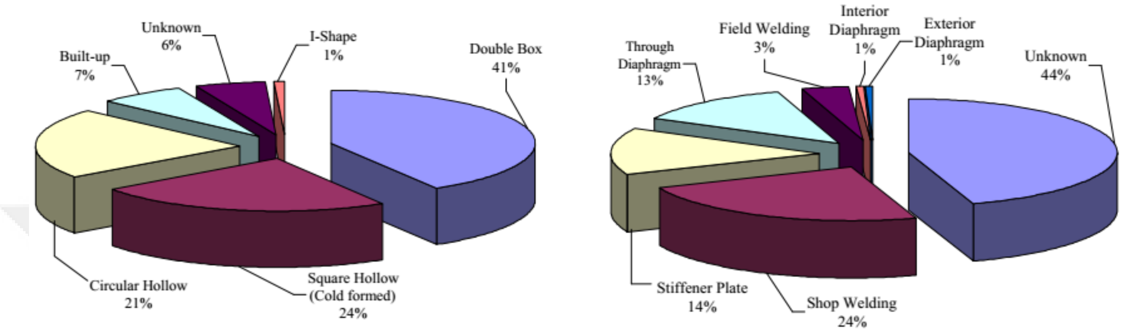

Figure 2.14 Kind of columns (left) and beam-to-column links (right) used in damaged steel and composite buildings in Japan (Nakashima et al., 1998)

The Chi-Chi earthquake in the September 21, 1999 caused severe damage and collapse to many building structures in Taiwan. However, mostly RC buildings were harmfully affected (Figure 2.15) with the lateral resisting systems composed by MRFs (Naeim et al., 2000; FEMA 355E, 2000).

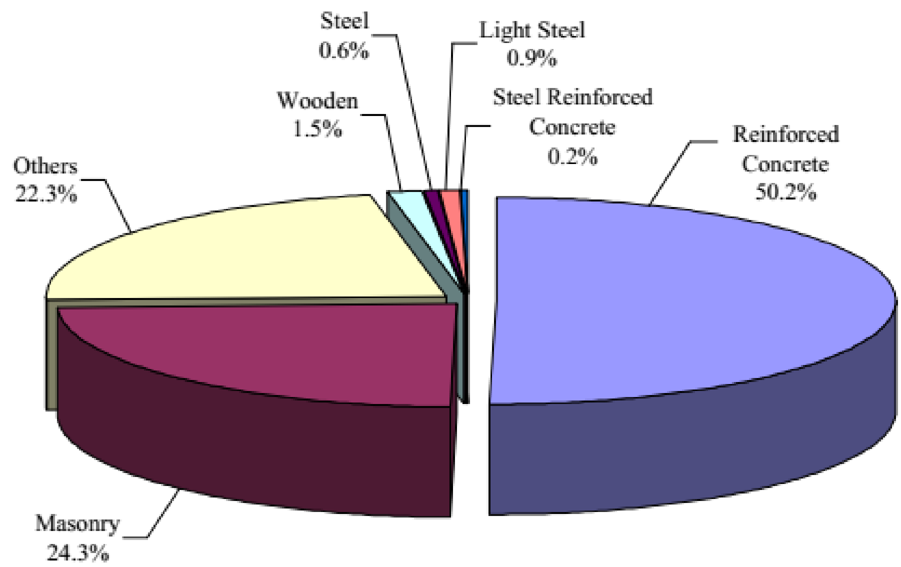

Figure 2.15 Damage detected in building structures in Taiwan (FEMA 355E, 2000)

2.3 Linked column frame structural system

Many systems proposed on development of various advanced structural systems and components to reduce earthquakes loads and make more easily repaired following moderate. These include the improvement of buckling-restrained braces (BRBs) (Saeki et al., 1996; Aiken et al., 1999; Iwata et al., 2000; Sabelli et al., 2003), triangular added damping and stiffness devices (TADAS) (Tsai et al., 1993; Dargush and Soong, 1995; Tena-Colunga, 1997) the steel shear panel devices (Nakashima, 1995; Nakashima et al., 1995; Miyama et al., 1996; Shimizu et al., 1998; Tanaka et al., 1998), and added damping and stiffness devices (ADAS). These systems are able to focus all damage in a ductile element, which is reusable and relatively easily repaired, allowing the main structure, including the gravity load resisting system, to keep on fundamentally elastic and undamaged. Residual drifts may also be relatively small in such systems since the elastic response of the nearby framing will help to at least partially recenter the system. Likewise, the linked column frame (LCF) system, which utilizes links that are envisioned to yield in shear and provide a plastic mechanism that limits the internal forces and safeguards the columns and gravity frame, may reach three behavior levels: elastic behavior, quick repair where the whole structure remains undamaged, collapse prevention where the links plastically deform, while the gravity frame remains undamaged, where plastic hinges also happen in beams of the moment frame (Malakoutian, 2013).

Ramadan and Ghobarah (1995) recommended that the bolted end plate connections offer a promising and economic alternative to fully welded link-to-column connections. Testing conducted that links with effectively designed bolted connections unremitting the same displacement demands and degenerate nearly the same amount of energy as links with shop welded end plate connections. Link end plate behavior is prejudiced by various parameters containing bolt slip, end plate thickness, and link-to-end plate weld design. Bolt slip causes connections to dissipate a lower amount of energy, and in shear links the effects of bolt slip are exaggerated due to the large shear loads enforced on the bolts. To eliminate the effects of bolt slip, it is recommended that bolted end plate connections be designed to slip critical standards.

Nader et al. (2002) and Goodyear and Sun (2003) suggested the linked column frame systems, designed and developed for tall bridge towers such as that of the new east spans of the San Francisco Oakland Bay Bridge.

Arce (2002) reconnoitered the impact of the flange width-to-thickness ratio on the rotation capacity and overstrength of links in EBFs. Sixteen links with four different wide flange sections and a wide variety of link lengths were tested at the University of Texas, Austin. The test setup consisted of a link welded to end plates that were bolted to a large beam and a large column as shown in (Figure 2.16). The column was pushed up to induce a shear force and near-equal end moments in the link. The same beam and column were used throughout the testing; only the link section was replaced for each test. The predominant failure mode observed in these tests was the fracture of the link web initiating at the end of the stiffener welds. Overstrength data collected in these tests suggest that the current overstrength factors specified in the provisions for design of braces are reasonable. Sections with high ratios of flange to web areas did not exhibit unusually high overstrength factors, at least within the range of flange to web area ratios typical of rolled W- shapes.

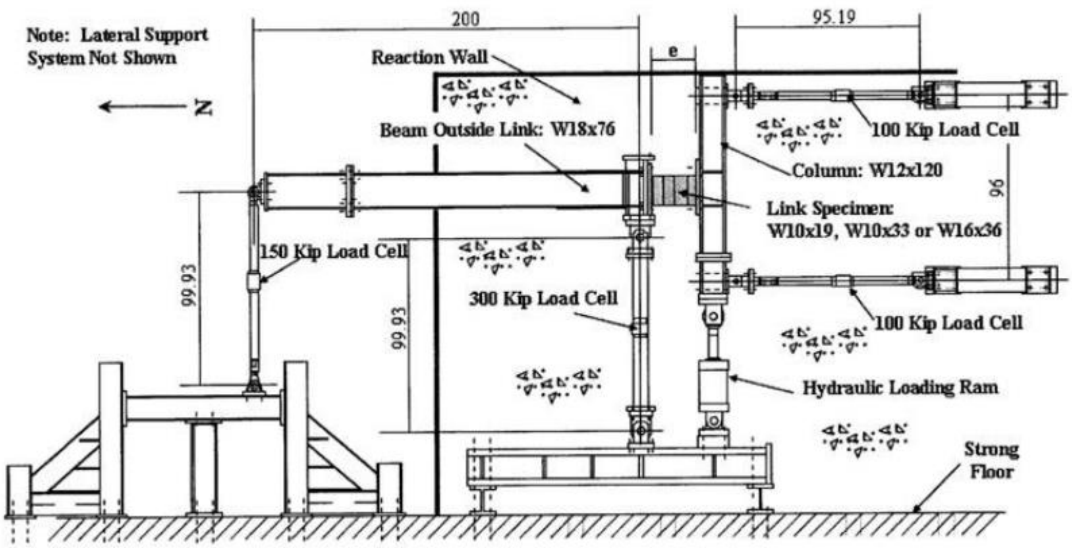

Figure 2.16 Experimental set-up (Arce, 2002)

Richards and Uang (2002;2004) performed a finite element modeling of EBF links and EBF systems to address flange width-thickness limits stiffener spacing requirements and inelastic rotation demands. Nonlinear response history analyses were performed for nine eccentrically braced frames subjected to 20 earthquake records scaled to represent design events. Results were used to quantify the cumulative rotation demands on links in EBFs as a function of link length and system geometry and to develop a revised experimental loading that simulated the expected demands. Result of detailed finite element analysis, similar to these shown in Figure 2.17, of various link geometries were used to verify requirements of preventing web and flange local buckling.

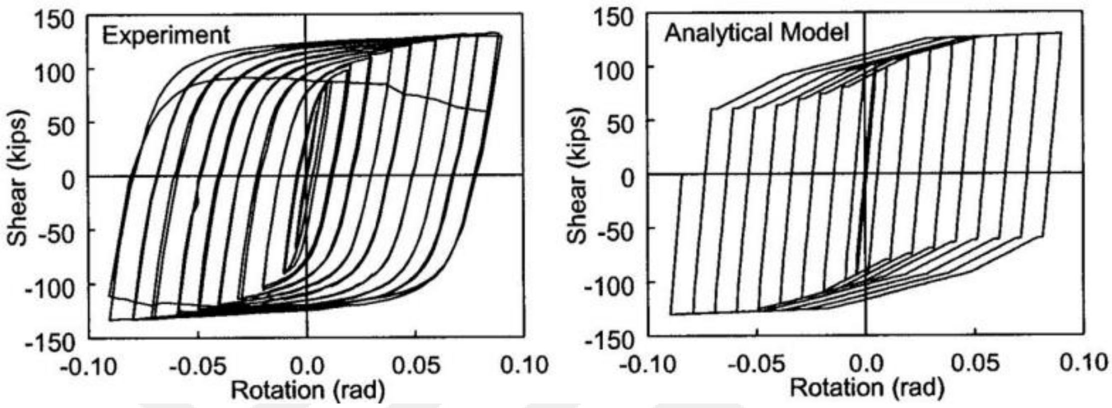

Figure 2.17 Comparison between experimental and analytical results (Richards, 2004)

Okazaki et al. (2005) designed the links in these frames to deform in elastically at performance levels below that of the frame so as to concentrate damage at the location of the link. To reduce lateral load demands during seismic events, shear links have been used as energy dissipaters in eccentrically braced frame for buildings and major bridges. Requirements for link design are given in the 2005 AISC Seismic Provisions for Structural Steel Buildings, and the maximum design link rotation is specified according the to the length ratio of the link.

Okazakia and Engelhardtb (2007) proposed cyclic loading tests of the performance of link beams in steel EBFs. They constructed thirty-seven link examples from five different wide-flange sections, all of ASTM A992 steel, with link length changing from short shear yielding links to long flexure yielding links. The incidence of web fracture in shear yielding link specimens led to further study on the cause of these fractures. Since the link web fracture seemed to be a phenomenon unique to modern rolled shapes, the potential role of material properties on these fractures is debated. Based on the test data, a change in the flange slenderness limit is proposed. The link over strength factor of 1.5, as assumed in the current U.S. code provisions, appears to be reasonable. The cyclic loading history used for testing was found to significantly affect link performance (Figure 2.18).

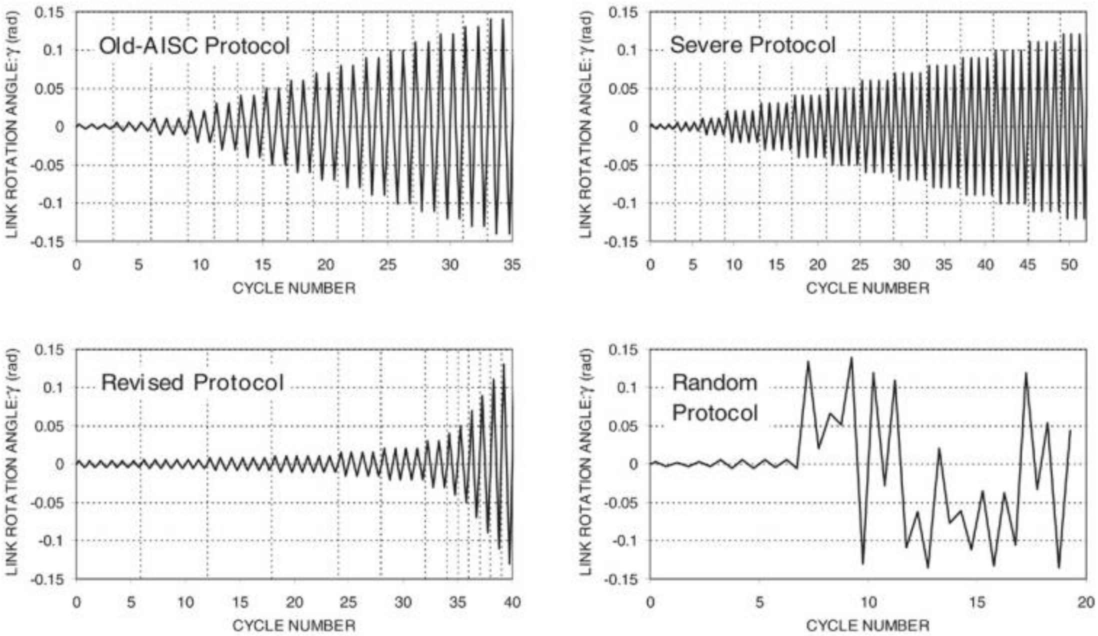

Figure 2.18 Loading protocols (Okazakia and Engelhardtb, 2007)

Test explanations also suggest new techniques for link stiffener design and detailing for link-to-column connections. As presented in results of this test program clearly that the loading protocol used (Figure 2.19) to test EBF links has a very large effect on the inelastic rotation attained by the links. Since the loading protocol as such a large effect on link test results, it is important that loading protocols realistically reflect demands caused by actual earthquake loading. Such a loading protocol for EBF links was recently developed by Uang and Richards (2003;2004), and has been adopted by the 2005 AISC Seismic Provisions. A number of shear yielding links tested in this program failed due to fracture of the link web. Explanations from this program suggest that the loading history and stiffener arrangement have limited influence on the link web fracture. One method is to increase the distance from the k-line of the rolled link section to the termination of the stiffener to link web fillet weld. Based on the test results, it is recommended that stiffener welds be terminated a distance of at least five times the web thickness from the k-line of the link section. Another method to delay web fracture is to restrain both sides of the link web using stiffeners without placing welds directly to the web.

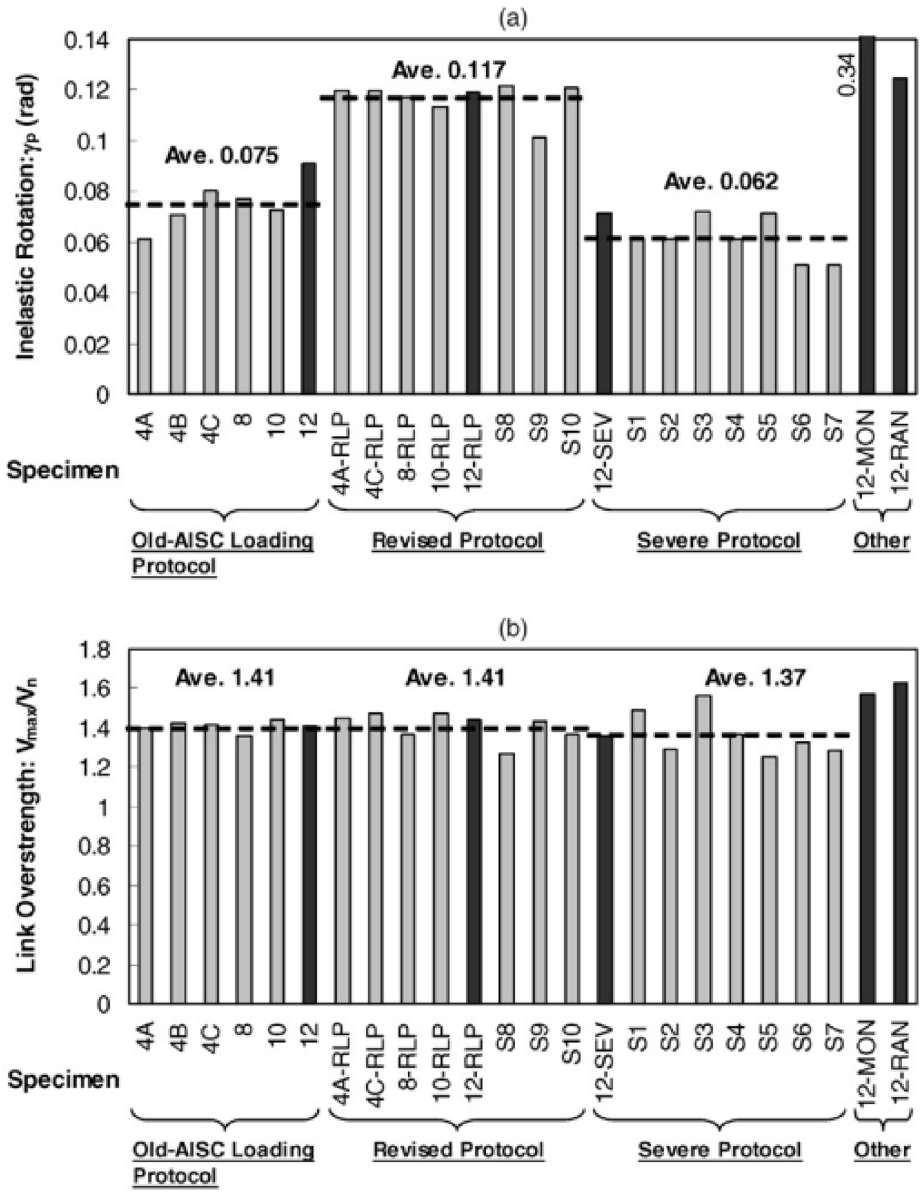

Figure 2.19 Performance of shear yielding links: (a) inelastic rotation and (b) overstrength factor (Okazakia and Engelhardtb, 2006)

Dusicka and Iwai (2007) introduced link column frame system (LCF), a structural steel framing system free of diagonal bracing and intended to provide rapid return to occupancy following an earthquake. The LCF system is inspired by EBFs, and the bridge towers described previously. They developed 3-story linked column frames for the building layout used by the SAC research project (FEMA-353, 2000). Each frame considered had different column base fixidity (Figure 2.20). They compared the global pushover results for these models with the pushover results (Figure 2.21) of a special moment resisting frame (SMRF) building developed as part of the SAC project as a post-Northridge design. Moreover, in order to prevent any column damage, all columns in the LCF system are pinned at the foundation while an additional link is added between the linked columns near the foundation to help control story drift demands at the bottom level. As further, in all LCF's, columns were protected from yielding. Due to low stiffness of SMRFs its designs is controlled by satisfying maximum story drift requirements, resulting in the use of deep beams and columns. However, the larger stiffness of LCF makes it possible to reduce the structural sections and the corresponding steel weight for the frame. The work described herein builds on this initial study of the LCF system.

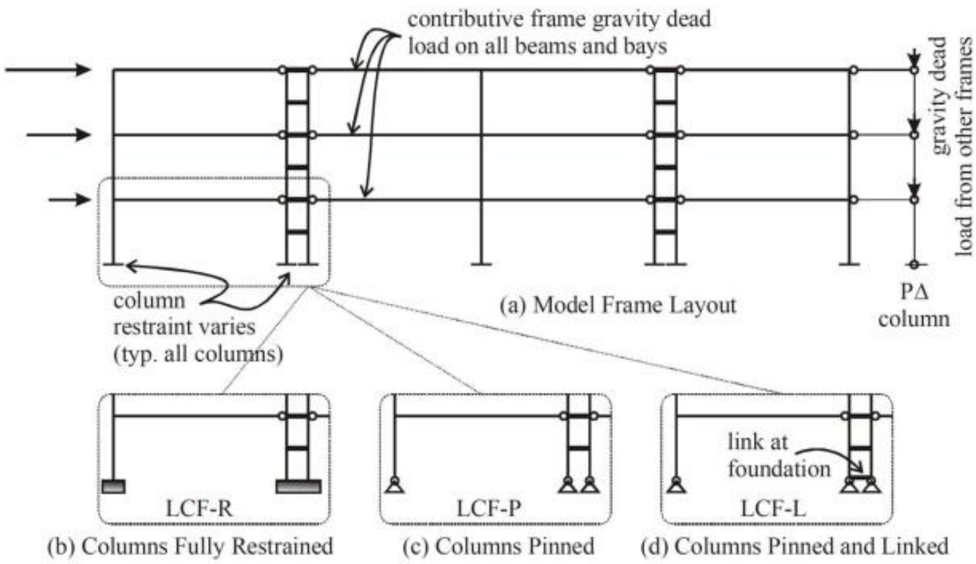

Figure 2.20 Numerical model layout with different column boundary (Dusicka and Iwai, 2007)

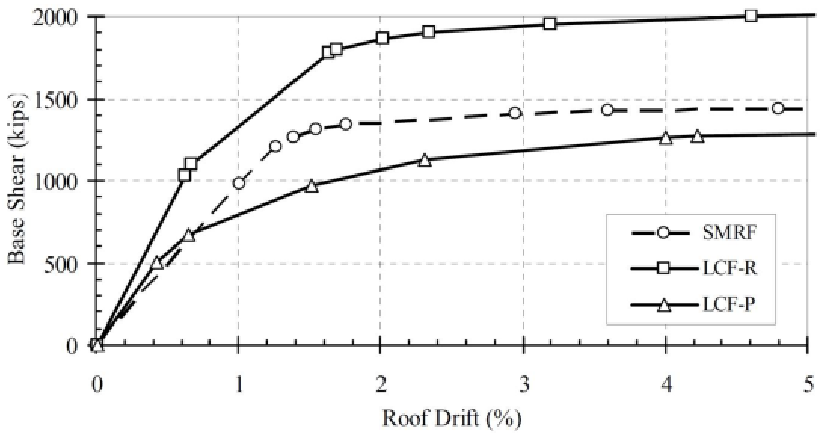

Figure 2.21 Pushover response of LCF in comparison with SMRF (Dusicka and Iwai, 2007)

Lewis (2010) investigated the link component of the LCF system. Specifically, the usefulness of using shear and flexure dominated rolled w-sections with bolted endplate connections was tested. End stiffeners were delivered to shift plastic strain away from the bolted end plates, and recommendations for middle link stiffeners were taken from the 2005 AISC Seismic Provisions for links in Eccentrically Braced Frame. It was determined that end stiffeners were effective in moving plastic strain towards the center of the links, and bolted end plates allowed for rapid and relative ease of link replacement; however residual stresses from middle stiffener welds resulted in web fracture failure in all shear dominated links tested. This design allows for an increase in web thickness without increasing the shear strength of the link, resulting in a web which is continually stiffened. The spacing of the two web plates and stiffness of the core material influence the out-of-plane rigidity of the web, allowing flexibility in design. This innovative stiffening technique eliminates the need for transverse web stiffeners which have been shown to introduce ductility related performance issues. Intermediate web stiffener welds have been shown to change the characteristics of the base metal in the link web, resulting in the initiation of web fracture. The basic concept of the composite link can be seen in (Figure 2.22) The following sections provide a literature review on EBF links and sandwich webs and discuss in detail the numeric modeling and experimental testing conducted on composite link specimens.

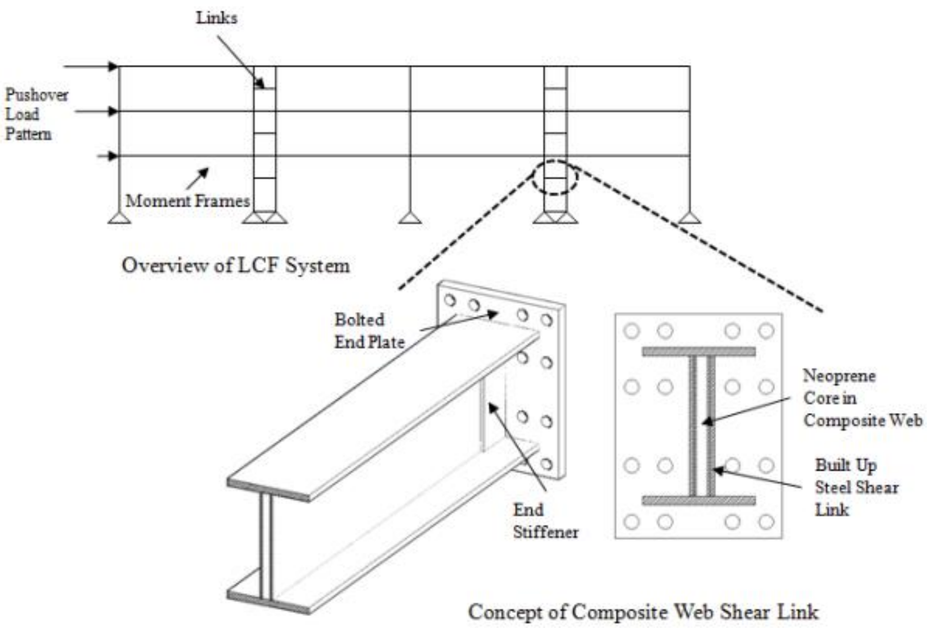

Figure 2.22 Link column frame overview (Stephens, 2011)

Dusicka and Lewis (2010) developed joined end-plate particulars with stiffeners at the link ends that are parallel to the beam web and joined to the link flanges and end plate (Figure 2.23) that contained of full-scale tests and comprehensive finite element modeling. For connecting the stiffeners and links to the end-plates, fillet welds are used. To make sure the link can be easy replace ability, the columns bolted with the end-plates. As shown in Figure 2.23, links using these particulars have achieved big rotations in full-scale experiments, achieving rotations are 0.07 rads for the flexural link and 0.10 rads for the shear links. The parallel web stiffeners successfully reduce the flange and web strains at the link ends, averting failure of the end-plate welds and ensuring yielding of the webs and flanges away from the end-plates. For assessment, similar links were tested with joined end-plates but before failure, lacking the parallel web stiffeners and achieved rotations of 0.04 rads for flexural and 0.055 rads for shear links of the end-plate weld. As shown in the Figure 2.24 this proves the effectiveness of adding the parallel web stiffeners and unstable the failure mode of the link.

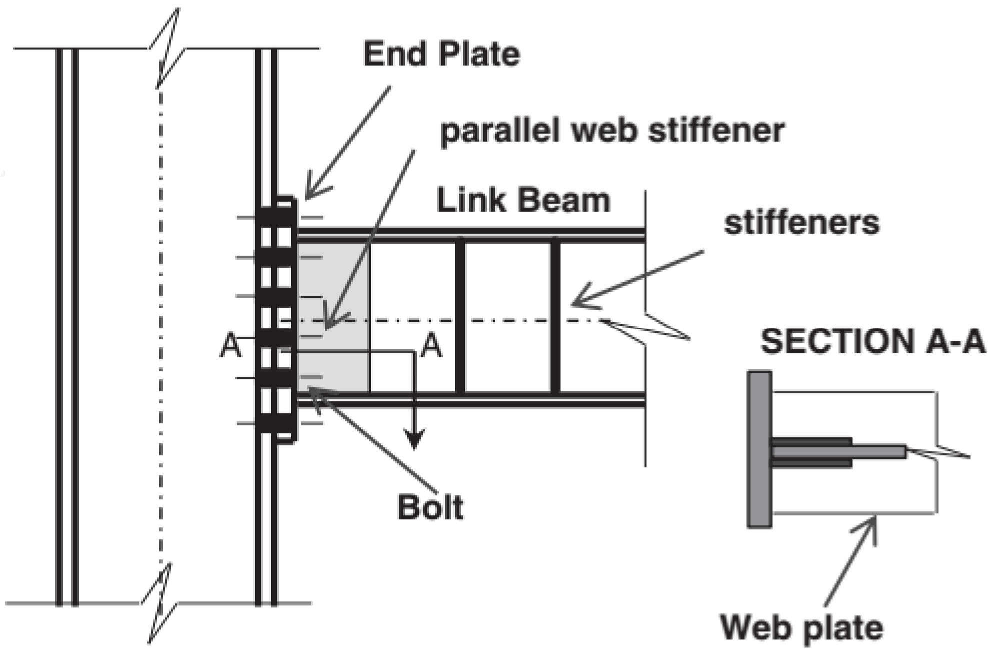

Figure 2.23 Link-to-column connection detail with bolted end-plate and parallel web stiffeners (adapted from Dusicka and Lewis (2010))

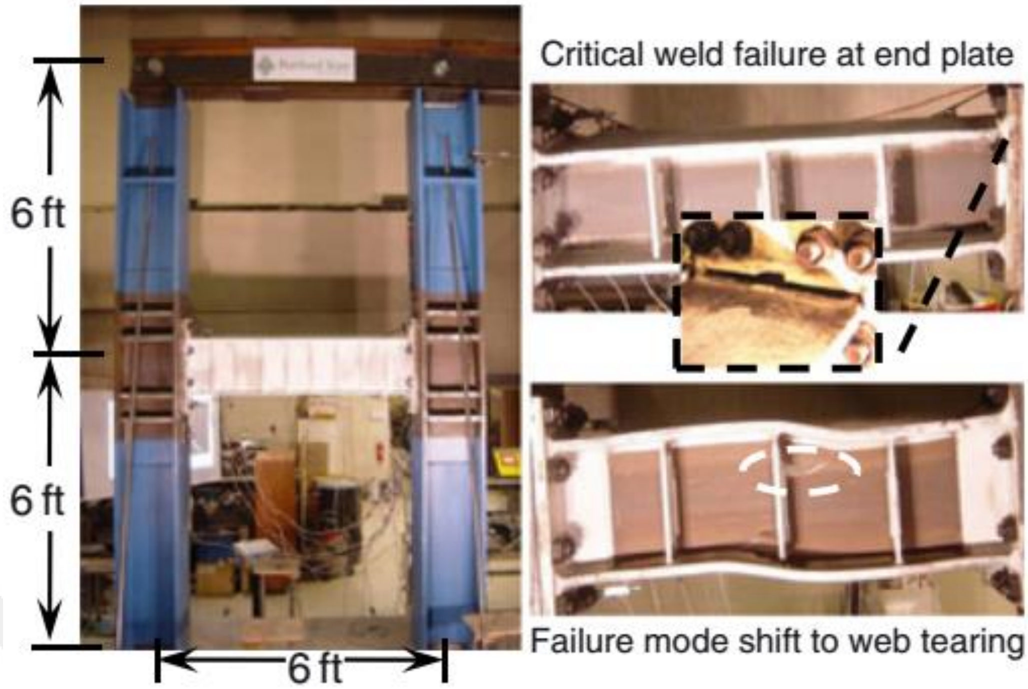

Figure 2.24 Test set-up and link failure modes for bolted end plate links with and without parallel web stiffeners (Dusicka and Lewis, 2010)

Stephens (2011) focused on moving from discrete transverse web stiffening to continuously stiffened webs in built up shear links. Built up links were designed to yield in shear when subjected to severe cyclic loading, however the webs of the links were designed using two metal sheets joined by an elastic core. These composite “sandwich” webs allowed for an increase in web thickness (and inherent flexural rigidity) without increasing the shear strength of the links. Numerical and experimental investigations were conducted to assess the performance of composite sandwich links subjected to severe loading. Improved web behavior in sandwich links achieved in numerical results that the core material was given an elastic modulus greater than 5000 psi. Due to manufacture limitations, experimental specimens were fabricated with a core material elastic modulus of 1000 psi. These specimens did not perform as well as unstiffened base case links in terms global hysteretic behavior or ductility.

Malakoutian et al. (2012) used the structural analysis software OpenSees (Mazzoni et al., 2009) to designing linked column frame as a new lateral load resisting system (Figure 2.25) and discussing following an earthquake event. The new system (LCF) can provide rapid return to occupancy. The replaceable links are designed to develop plastic hinges and placed between closely spaced columns, which is combined with a secondary moment frame. The material stress-strain performance is specified for flexural and axial response and applied to the fibers. The shear stress-strain performance is specified for the shear response, and basically multiplied by the shear area, which for wide-flange sections is the web area (Malakoutian, 2011). A series of 3-, 6- and 9-story LCF was designed for nonlinear response history analysis. The result show that (Figure 2.26) all LCFs achieved the key design objectives, specifically, after a 50% in 50 year event that no repair is needed, which is only minor link yielding was detected, also rapid return to occupancy by replacing the damaged links is reached for a 10% in 50 hazard level as plastic hinging was successfully limited to the links and for 2% in 50 year hazard level the collapse prevention is achieved since the story drifts were generally less than 5%. Additionally, even though most LCF designs were drift controlled, for the 10% in 50 year earthquakes all story drifts were less than 2% from response history analyses (Figure 2.27), which estimated the design seismic demands. This performance for the design seismic demands is acceptable. System level experiments using NEES infrastructure and hybrid simulation are underway to verify these conclusions.

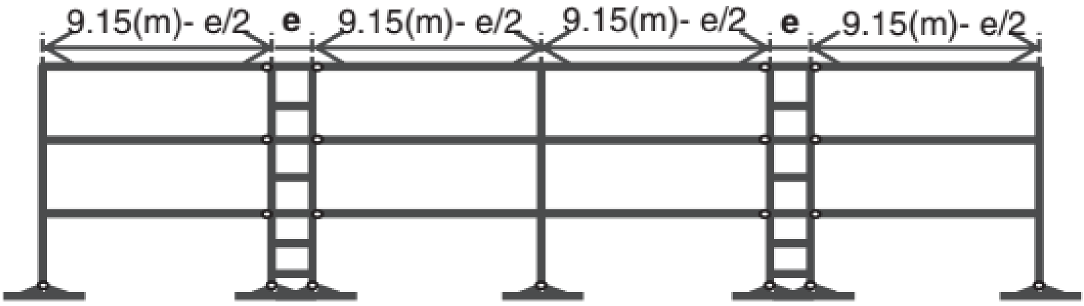

Figure 2.25 LCF model based on SAC model (Malakoutian et al., 2012)

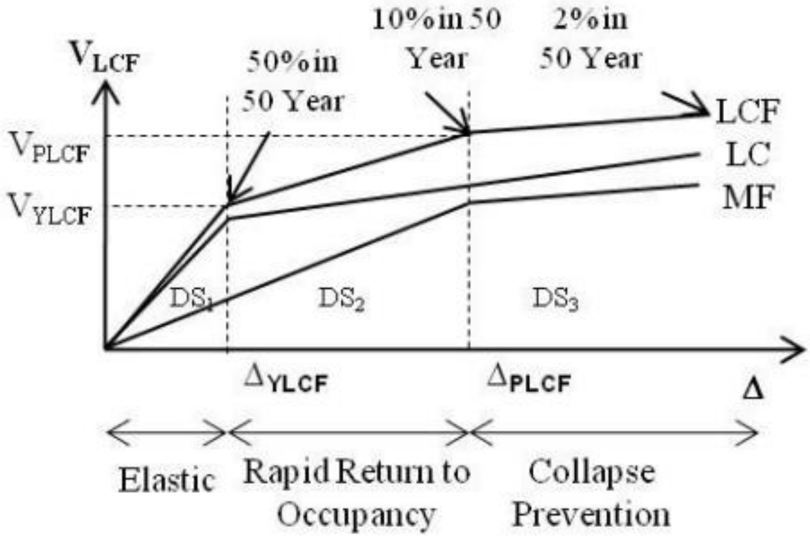

Figure 2.26 Idealized LCF and component pushover curves (Malakoutian et al., 2012)

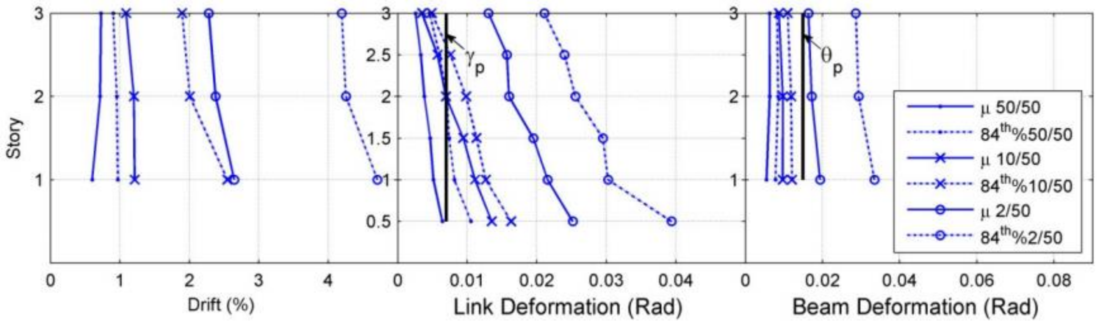

Figure 2.27 Median and 84th percentile story drift results for 3-, 6- and 9-story LCF buildings (Malakoutian et al., 2012)

Malakoutian et al. (2013) proposed the linked column frame (LCF) system to preventing seismic load to limit seismic damage, comparatively easily replaced elements. To limit seismic forces and provide energy dissipation, designed the linked columns via link yielding, while preventing damage to the moment frame under certain earthquake hazard levels. A design method is recommended that ensures plastic hinges develop in the links of the linked columns at a significantly lower story drift than when plastic hinges develop in the moment frame beams. The large drift difference helps enable design of this system for two separate performance states: rapid return to occupancy, where only link damage happens and relatively simple link replacement is possible, and collapse prevention, where both the links and the beams of the moment frame may be damaged. A series of 3-story, 6-story, and 9-story prototype LCF buildings were designed using the proposed design approach (Figure 2.28).

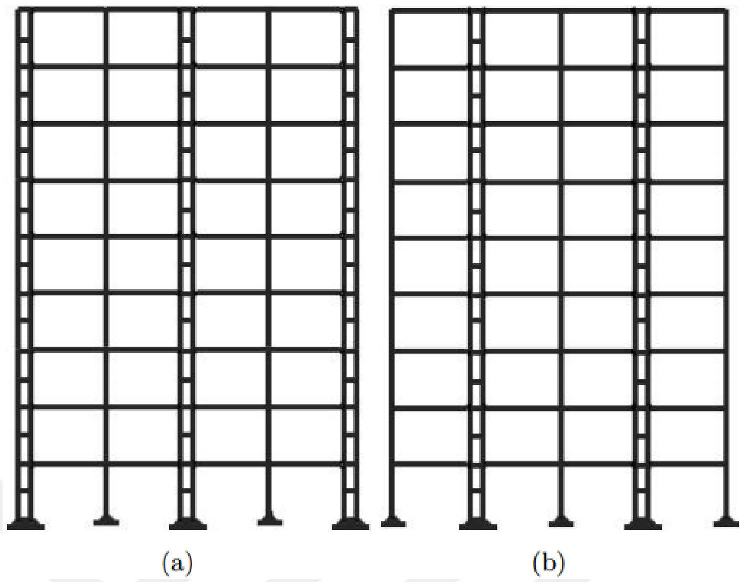

Figure 2.28 Story LCF elevations: (a) LCF with 3 bays of linked columns and (b) LCF with 2 bays of linked columns (Malakoutian et al., 2013)

The seismic response of these systems was investigated for ground motions representing various seismic hazard levels in the study of Malakoutian et al. (2013). Results show that the LCF system not only provides collapse prevention, but also has the capability of limiting economic loss by reducing structural damage and allowing for rapid return to occupancy following earthquakes with shorter return periods. Capacity design resulted in large columns for the 9-story LCF yet the columns remained elastic in almost all of the 2% in 50-year ground motions. Despite the elastic column response, larger story drifts, link rotations, and beam rotations were observed in the lower stories of the 6-story and 9-story LCFs for the 2% in 50-year hazard level. Adding more links at lower stories, using built-up link sections or using built-up or concrete filled tube columns may be options to add stiffness at the lower stories and improve the behavior. The results of nonlinear response history analysis of LCFs for the Seattle location with 40 ground motions show the same results as before: no repair is needed after a 50% in 50-year event as only minor link yielding was observed, rapid repair by replacing the damaged link is applicable after a 10% in 50 hazard level as only link yield, and collapse prevention for 2% in 50 year hazard level since the story drifts were generally less than 5%.

Lopes et al. (2014) defined the linked column frame (LCF) as a new brace-free lateral structural steel system proposed for rapid return to occupancy performance level. The design resistance of the LCF was based upon a prototype building that is a modified version of the 3-story building SAC configuration (Figure 2.29). LCF is more strong under a design level earthquake than the conformist methods. The focus of this work was exclusive full scale experiment using hybrid testing; a combination of physical test of a critical sub-system tied to a numerical model of the building frame. A LCF system was investigated experimentally via hybrid simulation to validate the response at a system level. The system experiment was a blend of physical test of a critical sub-system tied to a numerical model of the building. Consequently, an ultimate cyclic loading was used to test LCF sub-system up to 5% total drift. For the case considered, the structural layout was suitable for entire frame validation using hybrid simulation, the LCF moment frame remained elastic until rapid return to occupancy performance level was achieved, while links yielded and deformed plastically, shear links shown to be effective in protecting gravity system and contributing well past 4% drift, limited demands on gravity beams could indicate less rigorous detailing connections, LCF-3L specimen presented three regions within the lateral response; elastic, yielding of links and yielding of links as well as moment frame beams. Provided the links are replaceable, these correspond to three distinct performance levels; elastic, rapid return to occupancy and collapse prevention.

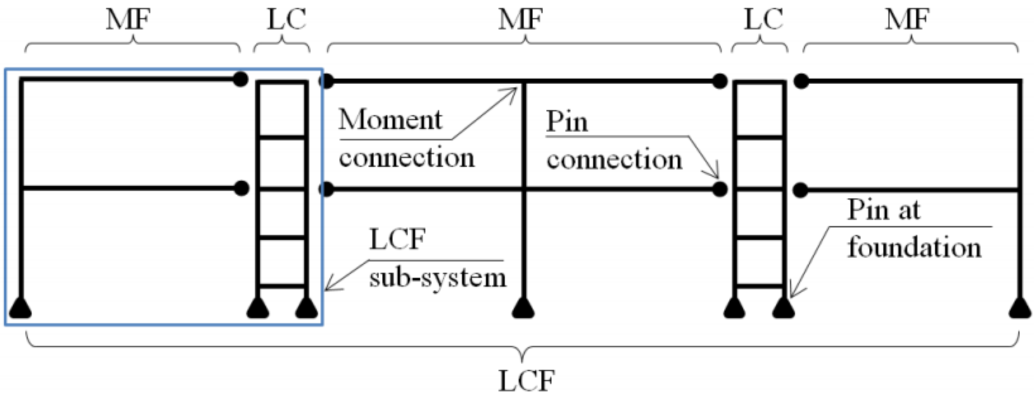

Figure 2.29 LCF layout for a 2-story building (Lopes et al., 2014)

The application of the ground motions exposed arrangement of yielding actions as follows: at base link 1, at first story link 2, at second story link 3, at first story beam 1, and at second story beam 2. the structure displaced up to 1.8% drift and 2.8% when exposed to earthquakes RR1 & RR2 and CP1 & CP2, respectively as displayed in (Figure 2.30 a,c). For all three performance levels the link rotation is presented in (Figure 2.30 b,d).

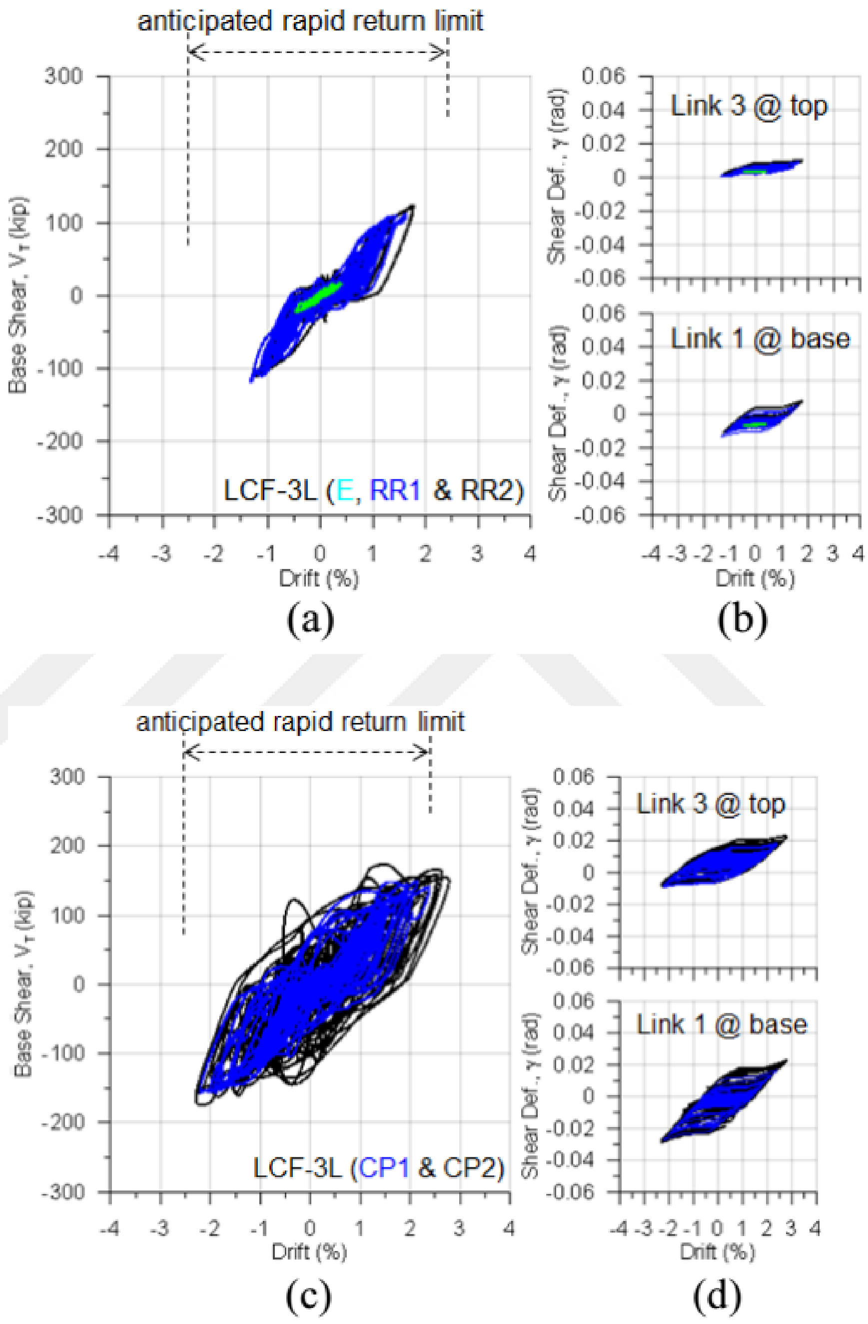

Figure 2.30 Base shear versus drift (a, c) and link shear deformation versus drift (b, d) hysteresis (Lopes et al., 2014)

The link rotation demands in link 3 at second story are smaller than in link 1 at base which concur with the arrangement of yielding events declared above. Whitewash on the links began flaking near mid-span, then circulated toward the end plates as shown in (Figure 2.31). In the collapse prevention performance level, the links have larger inelastic demand and are more possible to require replacement. It should be renowned that under any ground motions used in the hybrid simulation, the links are not failed (Lopes et al., 2014).

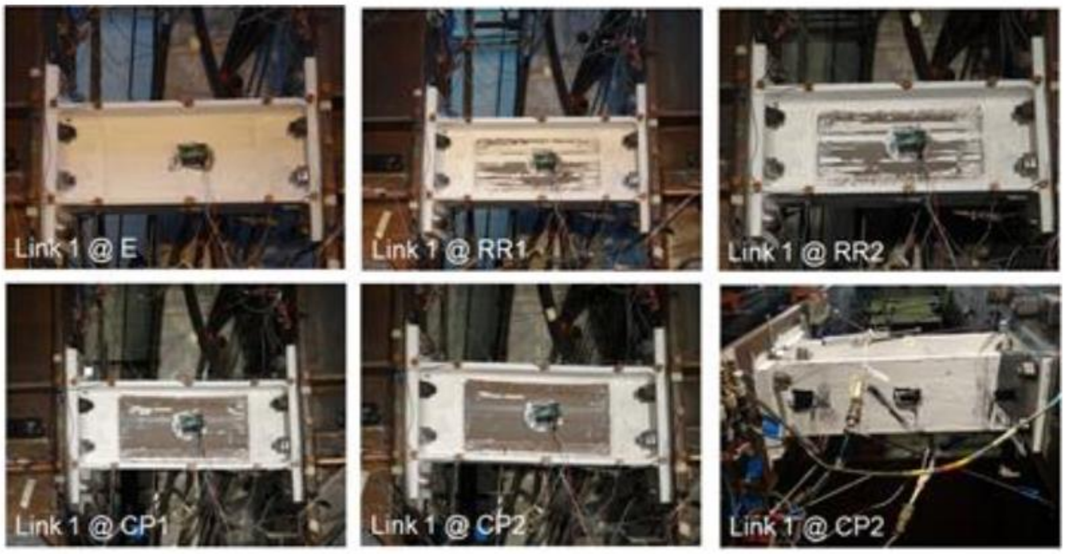

Figure 2.31 Progression of damage in replaceable link 1 (Lopes et al., 2014)

An ultimate cyclic loading was used to test the physical LCF sub-system up to 5% total drift after the hybrid test was finished. FEMA 461 testing procedure was used. (Figure 2.32a) shows the maximum response in terms of hysteresis loop of the physical LCF sub-system. A maximum displacement of 10.8 in. with a 200-kip base shear was achieved by the second story. The link rotation demands in link 1 (γ=0.07 rad.) are bigger than in link 3 (γ=0.05 rad.), in respects to the shear links (Figure 2.32b). Until 4% drift, the web buckling did not start to form in the web of the shear link. With the progression of the cycles, web buckling became more noticeable and a crack taking place at mid-span surveyed by a crack between the top flange and web of the link. Until 5% drift, the cracks kept spreading. The test was stopped when the web began to tear. (Figure 2.33) shows gravity beams 1 and 2 at 5% drift and the performance of links 1, 2 and 3. Shear links shown to be effective in protecting gravity system and participating well past 4% drift and limited damaged presented in the gravity beams.

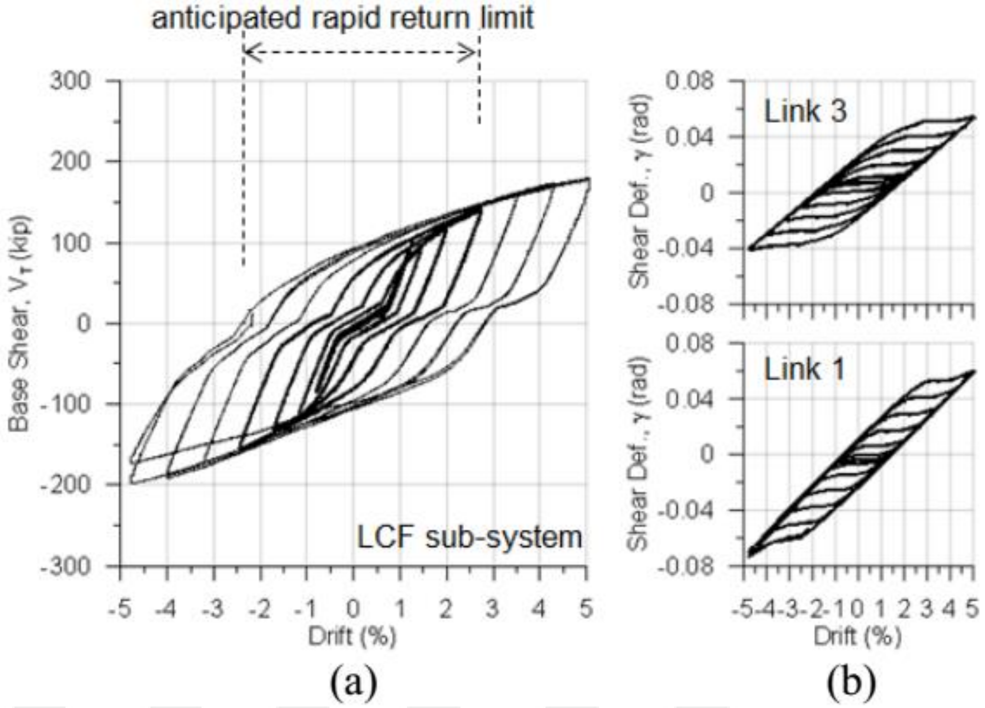

Figure 2.32 Base shear versus drift (a) and link shear deformation versus drift (b) hysteresis (Lopes et al., 2014)

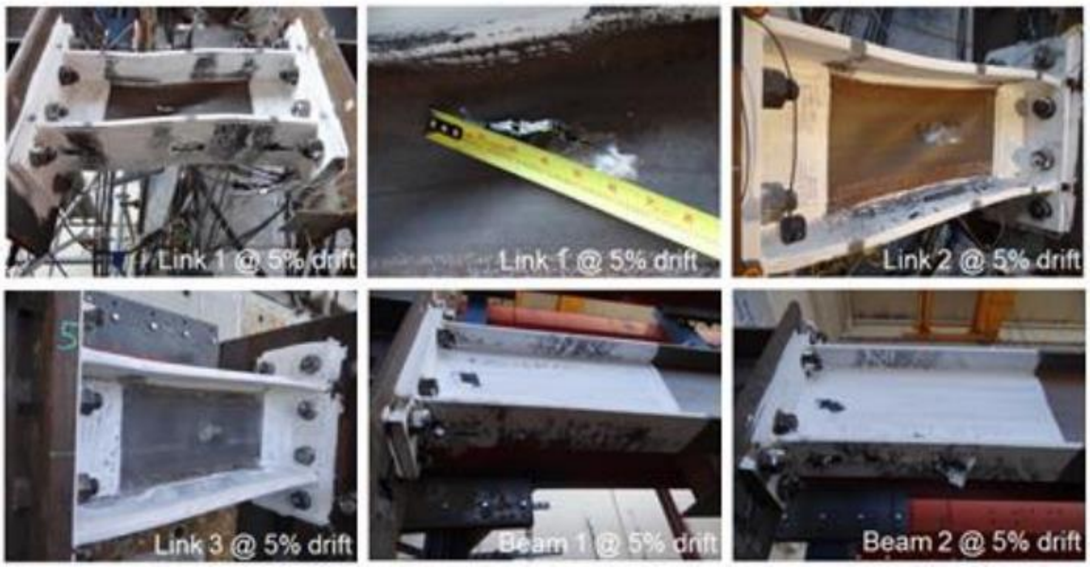

Figure 2.33 Photos of links 1, 2, and 3 and gravity beams 1 and 2 at 5% drift of LCF sub-system (Lopes et al., 2014)

Lydia and Hemalatha (2013) contemplate the linked column frame to concrete structures. By using structural analysis SAP 2000 designed the replaceable link beams as concrete structures connected to the columns concluded bolted joints. To investigate the performance, nonlinear analysis (pushover) was used for a four-story building. The base shear and drift limits were considered. Better load dissipation capabilities shown in the results. The system includes replaceable links placed between closely spaced columns, which the links yield under earthquake lateral loads through a variance movement throughout the height of the structure, the reduction in drift and from the formation of the hinges (Figure 2.34), in addition to the columns such that the structure could rapidly return to occupancy through link replacement, the linked column frame effectively protects the gravity beams, since the cost of construction can be greatly reduced by modeled the replaceable links as reinforced concrete elements. This method can be successfully used as recovery of existing structure not designed to resist seismic forces.

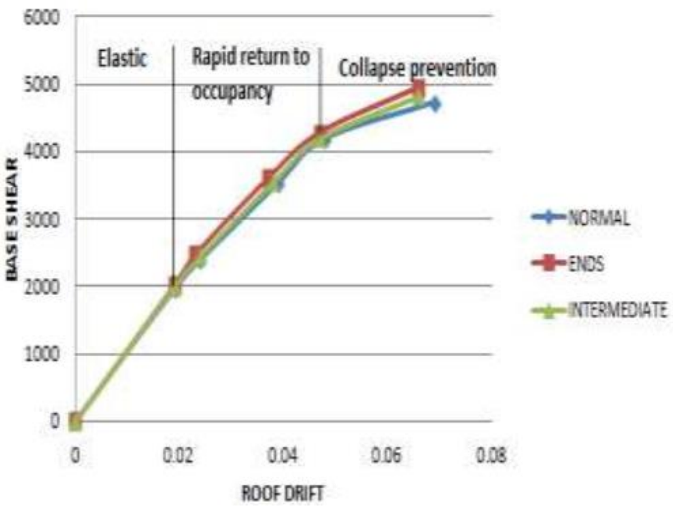

Figure 2.34 Base shear vs roof drift for the models (Lydia and Hemalatha, 2013)

CHAPTER 3

METHODOLOGY

3.1 Analytical Model of Structures

To study the effects of using the linked column frame (LCF) on the structural response, a steel moment resisting frame(MRF) was considered the structural was a three storey office building having a 48 m by 48 m floor plan with a height of 12 m. The frame of the building had 6 bays with equal span length of 8m. Figures 3.1-3.3 show plans three dimensional and elevation views of the case study structure, respectively. The linked column frame models defined as one linked column (LCF1) with three varied length of the link (lc), three linked column (LCF3) with three varied length of the link (lc), five linked column (LCF5) with three varied length of the link (lc) and seven linked column (LCF7) with three varied length of the link (lc) frames were analytically modeled.

The spacing between the linked column (lc) was 1, 2 and 3 m for all models by keeping the total width of the structure as constant value of 48 m by using (L-lc/2) for the beam length that has in one side the linked column and (L-lc) for beam length in both side has linked column; only in case of the model (LCF7), in which the edge beams of the frame (L-1.5lc) were used as shown in Figure 3.4. In the linked column frames by adding the beam link or replaceable link in the mid of height of column the section of the linked column was reduced and reserved for all LCFs as shown in Table 3.1. Thus, 13 different frame models including the MRF and 12 LCFs were investigated. The inter storey height was 4.0 m for all levels and slabs thickness was 15 cm. The details about the profiles of the structural members are given in Table 3.1. The elevation view of the LCF models of LCF1, LCF3, LCF5, and LCF7 are shown in Figures 3.5-3.8 respectively. The analytical models of the frames were developed by using the structural analysis program of SAP 2000.

Table 3.1 Profile details for the frame models

Model	Structural Member	Story No.		
		1st	2nd	3rd
Moment Frame	Column	W14x233	W14x132	W14x120
	Beam	W16x100	W16x77	W16x57
Linked Column System	Column	W14x120	W14x74	W14x30
	Link Beam	W16x100	W16x77	W16x57

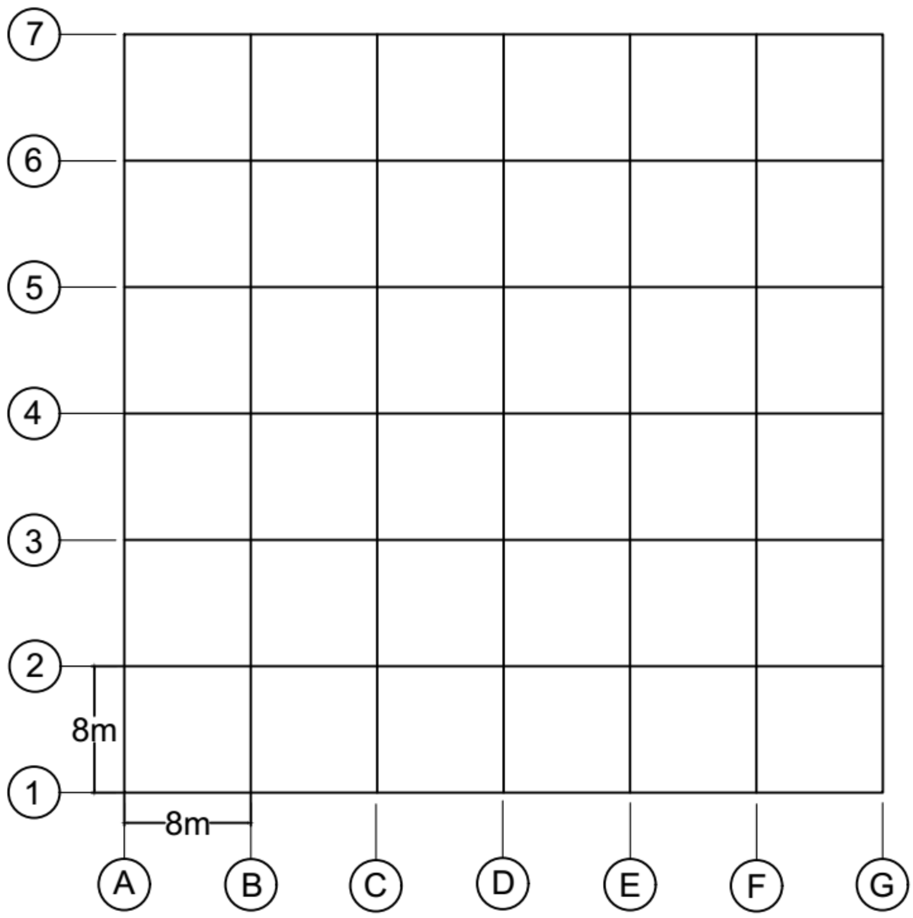

Figure 3.1 Plan view of the MRF

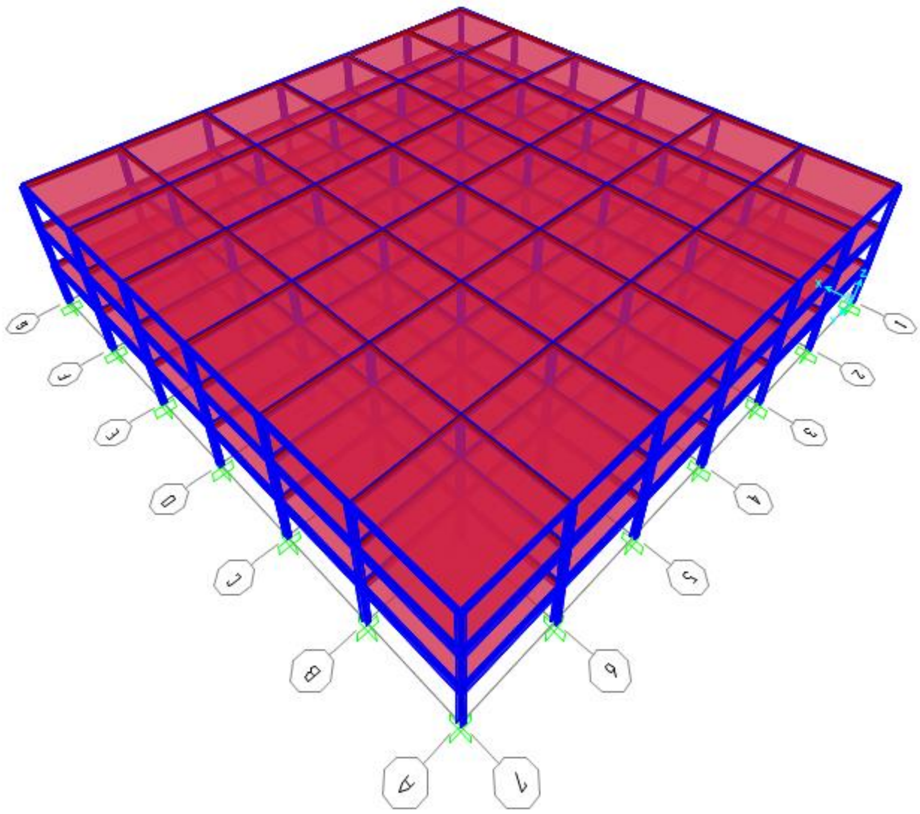

Figure 3.2 Three-dimensional view three storey of the MRF

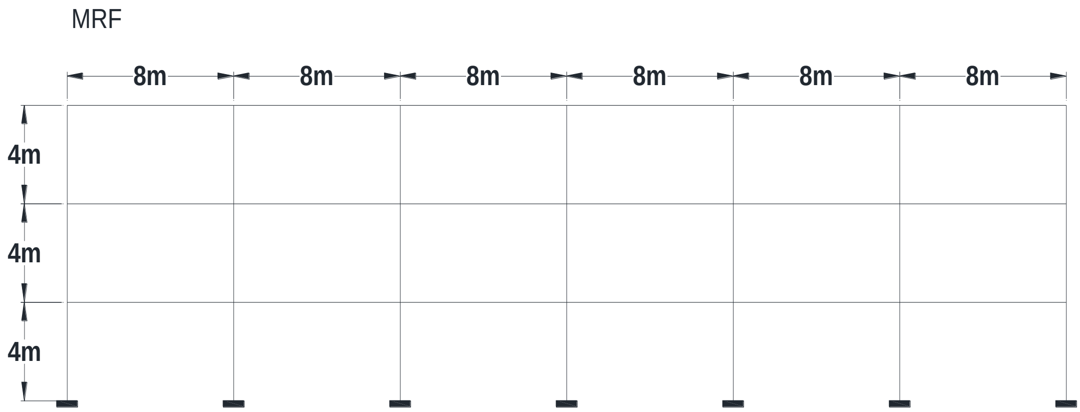

Figure 3.3 Elevation view of the MRF

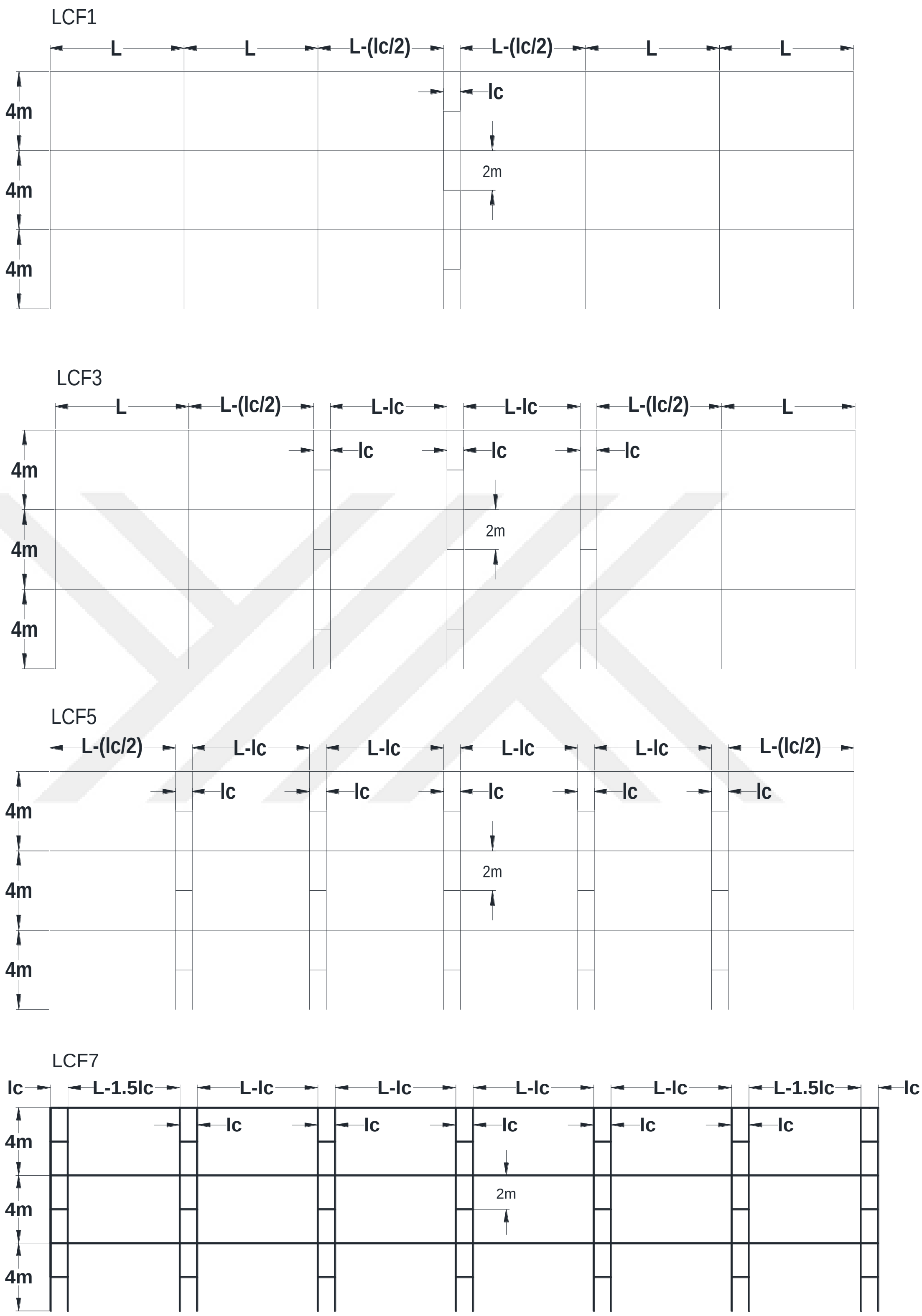

Figure 3.4 Design details of link column and replaceable link element

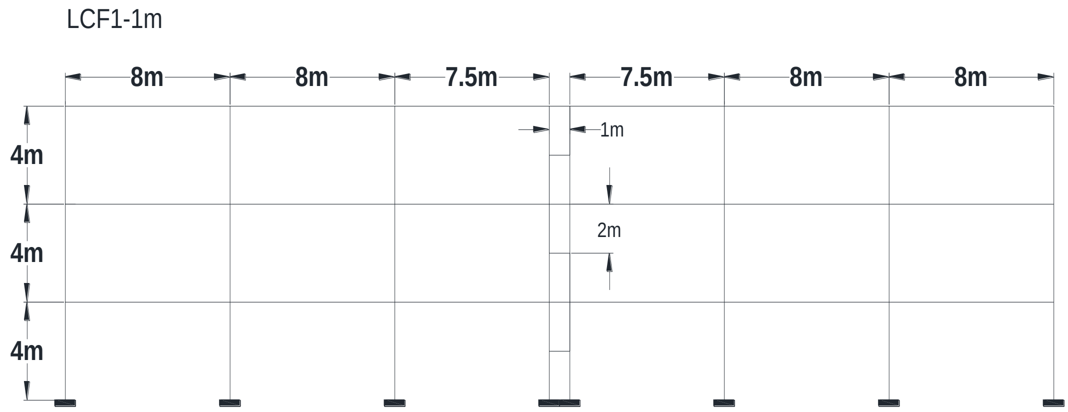

a)

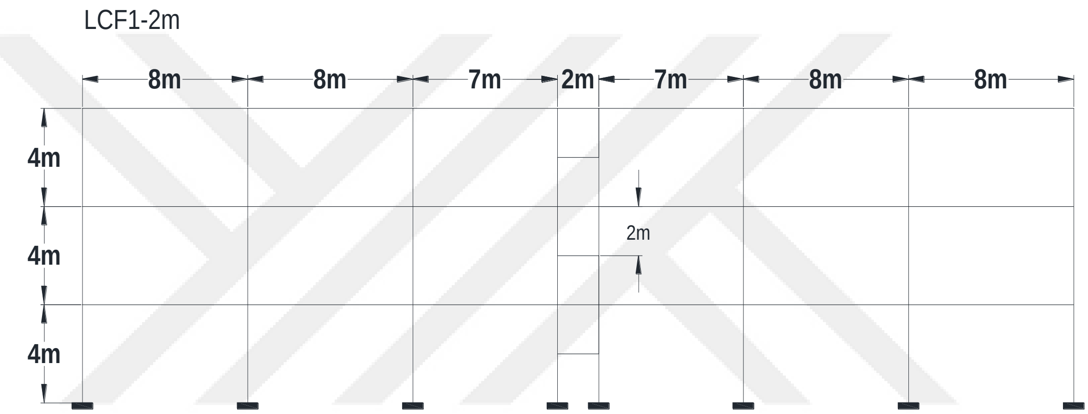

b)

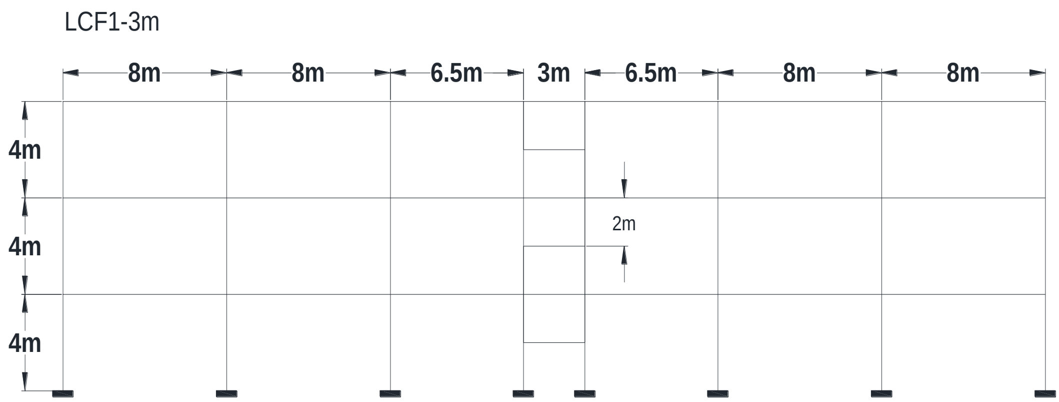

c)

Figure 3.5 LCF1 with different spacing of a) 1 m, b) 2 m, and c) 3 m

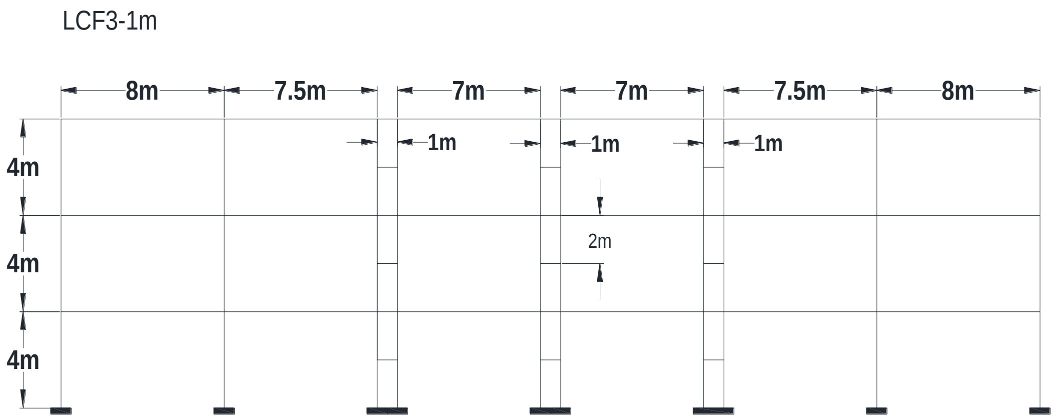

a)

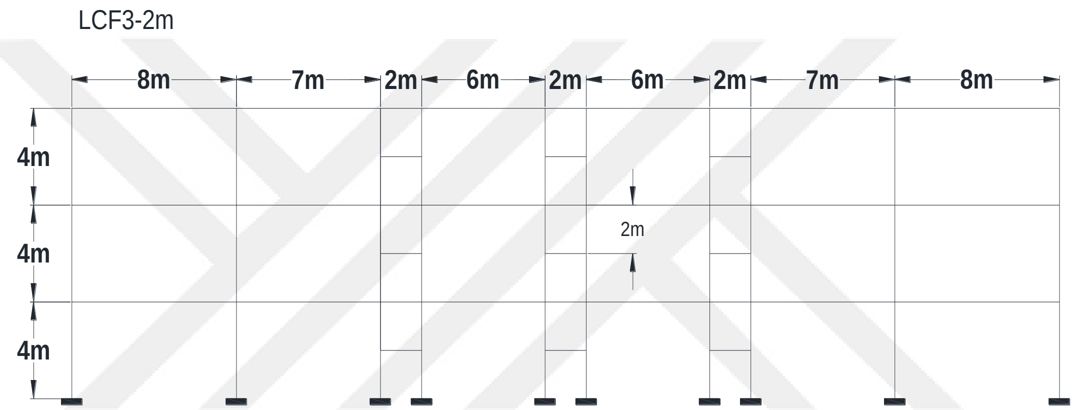

b)

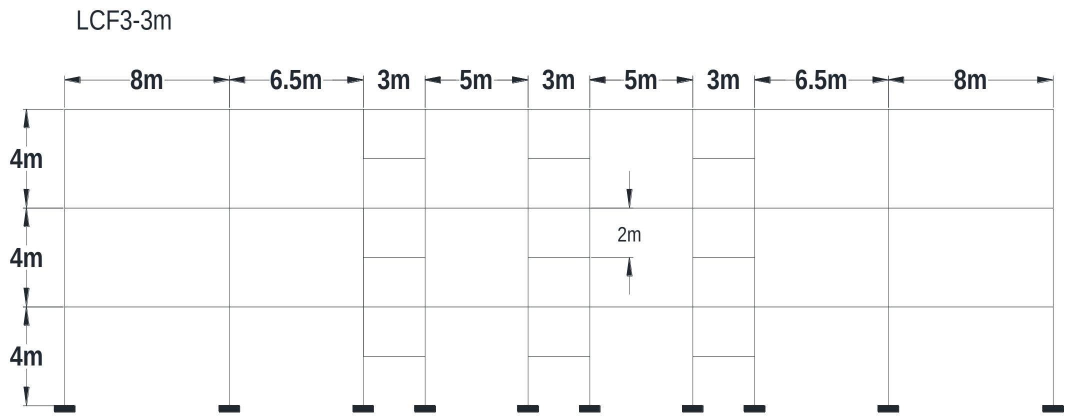

c)

Figure 3.6 LCF3 with different spacing of a) 1 m, b) 2 m, and c) 3 m

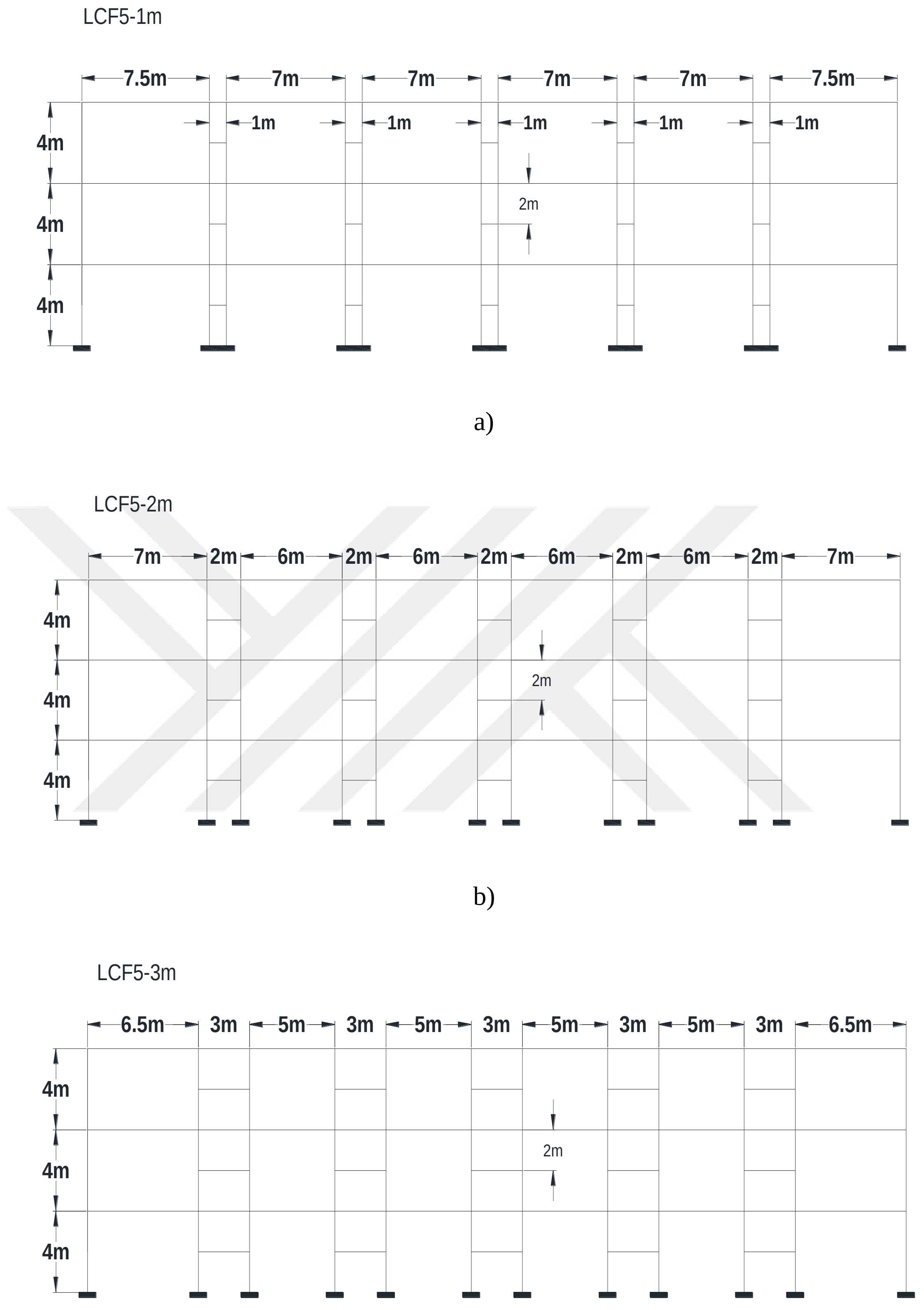

a)

b)

c)

Figure 3.7 LCF5 with different spacing of a) 1 m, b) 2 m, and c) 3 m

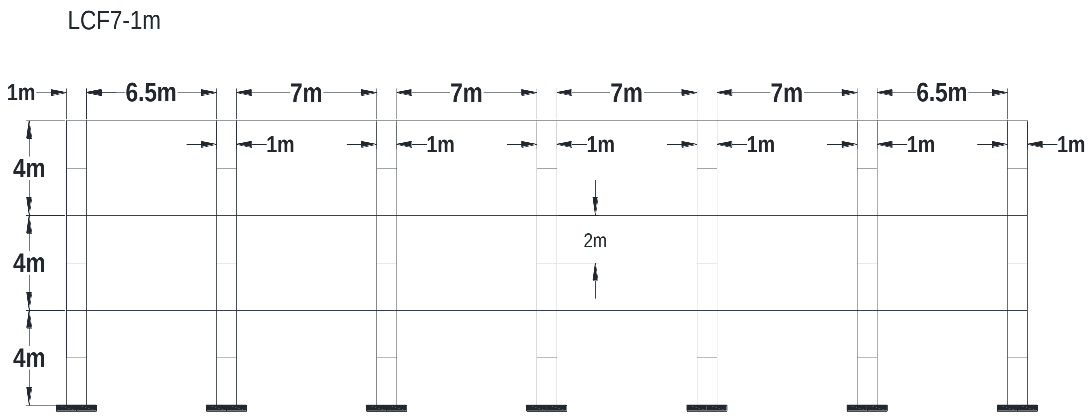

a)

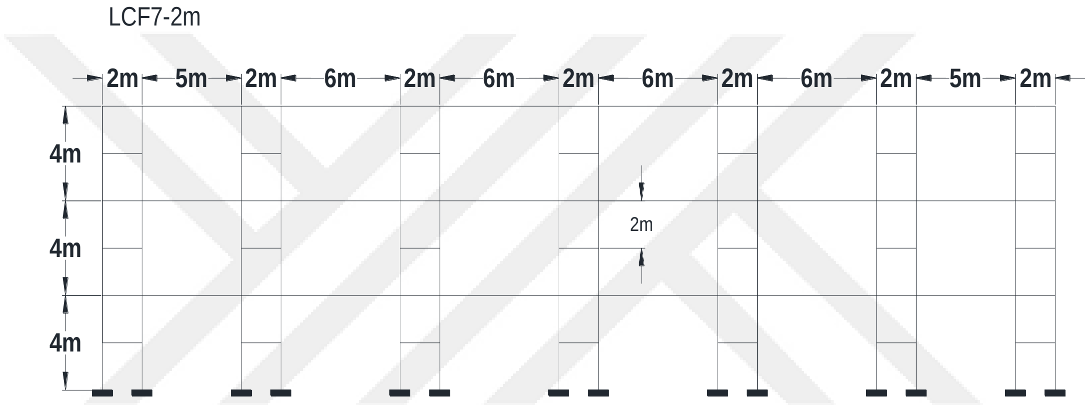

b)

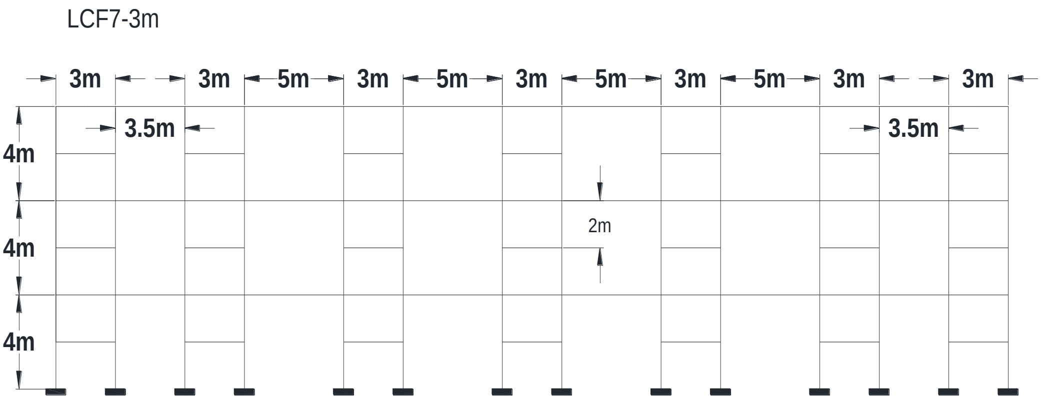

c)

Figure 3.8 LCF7 with different spacing of a) 1 m, b) 2 m, and c) 3 m

3.2 Nonlinear Analysis

For the nonlinear static and time history analysis, SAP 2000 structural analysis program was utilized. For the evaluation of the seismic behavior of the MRF and LCFs, the extensively utilized methods such as nonlinear static (pushover) and nonlinear time history analysis were conducted. In modeling the nonlinear behavior of the structural members, nonlinearity was defined in the concentrated plastic hinge points with the hysteretic nonlinear behavior defined according to (FEMA 356, 2000). The possible plastic hinge formation points were defined as the both ends of the member for the beams and columns. For the column members, axial force and flexural moment hinges, for the beams, flexural moment hinges and for beam links the flexural moment and shear hinges were considered. For the nonlinear pushover analysis, uniform lateral load distribution was considered.

In this analysis, the uniform lateral loads which increased incrementally were applied and at each load increment, the strength and stiffness properties of structural members were altered. A plot of the total base shear vs. displacement in a structure was formed by static (pushover) analysis that would expose any previous failure. The analysis was increasing lateral forces until a specified displacement was reached, therefore it was possible to require yielding point of the system. With the purpose of further examining the effects of link columns on the response of the frames, the behavior of the frames were examined under earthquake accelerations through nonlinear time history analysis.

In the nonlinear time history analysis, the buildings were imperiled to real ground motion record. The MRF and LCFs were examined under different earthquake ground accelerations. In the nonlinear time history analysis, analytical models consisting the nonlinear behavior of the structural members were subjected to earthquake ground accelerations. In the nonlinear time history analysis, as earthquake accelerations, Newhall, Holliste, and Petrolia earthquake records were considered as shown in Figure 3.9. In the analysis, as gravity loading, the total dead load and 30% of the live load were applied on the frames.

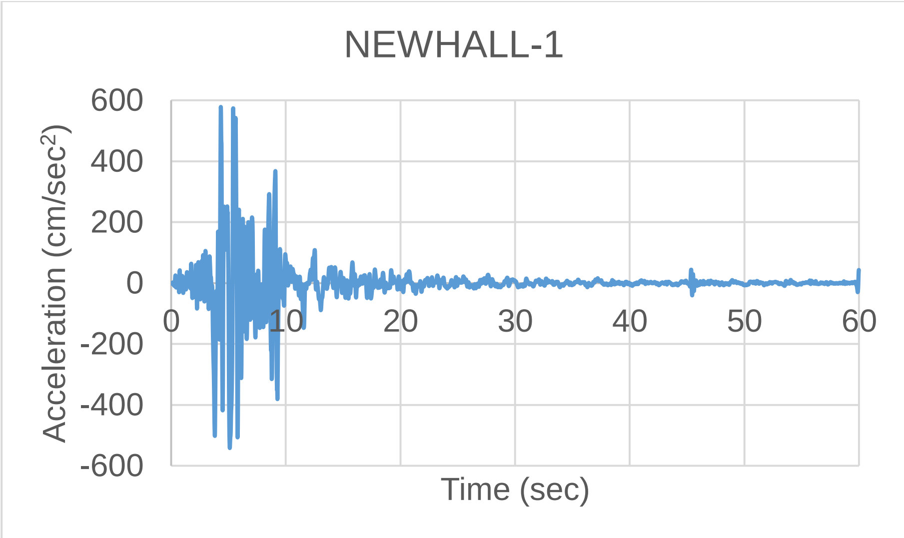

a)

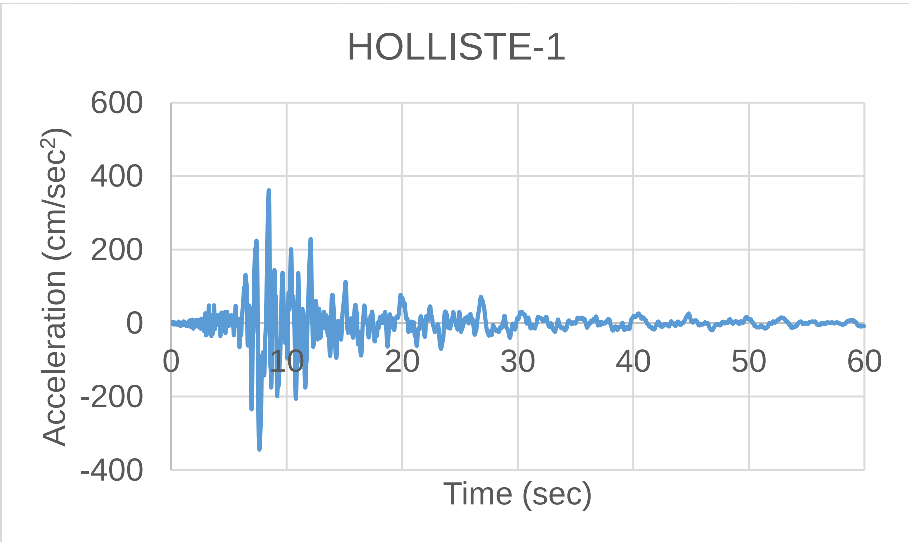

b)

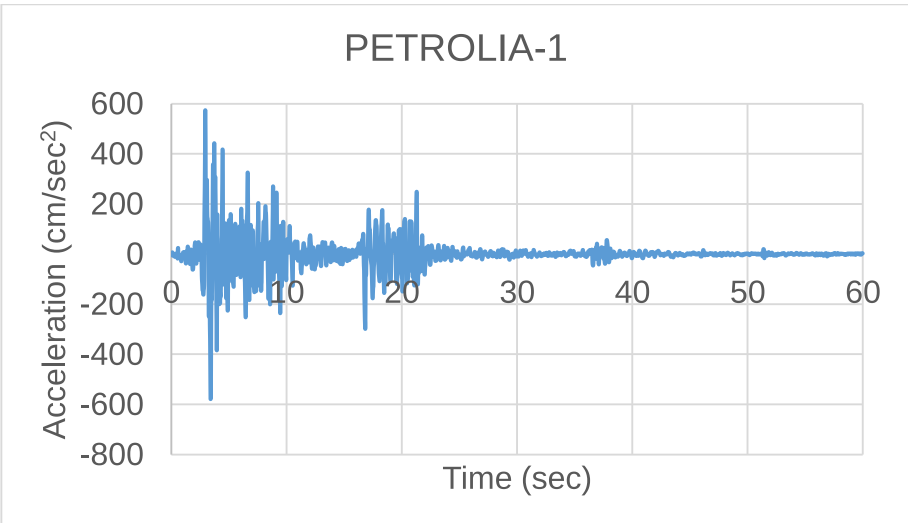

c)

Figure 3.9 Earthquake accelerations: a) Newhall b) Holliste and c) Petrolia

CHAPTER 4

RESULTS AND DISCUSSION

4.1 Nonlinear Pushover Analysis

From the nonlinear pushover analysis, the capacity curves in terms of base shear vs. roof displacement were obtained for the MRF and LCFs as given in Figure 4.1, 2, 3 and 4 As seen from the figure, increase in the number of link column systems caused changing in the curves which shows increasing in the strength and initial stiffness of the frame. For instance, for the LCF1 having link beam length of 1, 2 and 3 m base shear was obtained as 1.06, 1.11, 1.13 times the base shear capacity of the MRF, the LCF3 having link beam length of 1,2 and 3 m base shear was obtained as 1.22, 1.33, 1.39 times the base shear capacity of the MRF, the LCF5 having link beam length of 1, 2 and 3 m base shear was obtained as 1.41, 1.58, 1.67 times the base shear capacity of the MRF and the LCF7 having link beam length of 1, 2 and 3 m base shear was obtained as 1.54, 1.81, 1.94 times the base shear capacity of the MRF.

When the effect of the link beam length in these LCFs were examined, it was observed that with the increase in the number of link column systems, the effect of the link beam length was more pronounced. For example, by altering the link beam length from 1 to 3 m, for the LCF1, the change in the maximum base shear capacity with respect to MRF became 1.06 to 1.13 times; on the other hand, for LCF7, the increase was observed as 1.54 to 1.94 times.

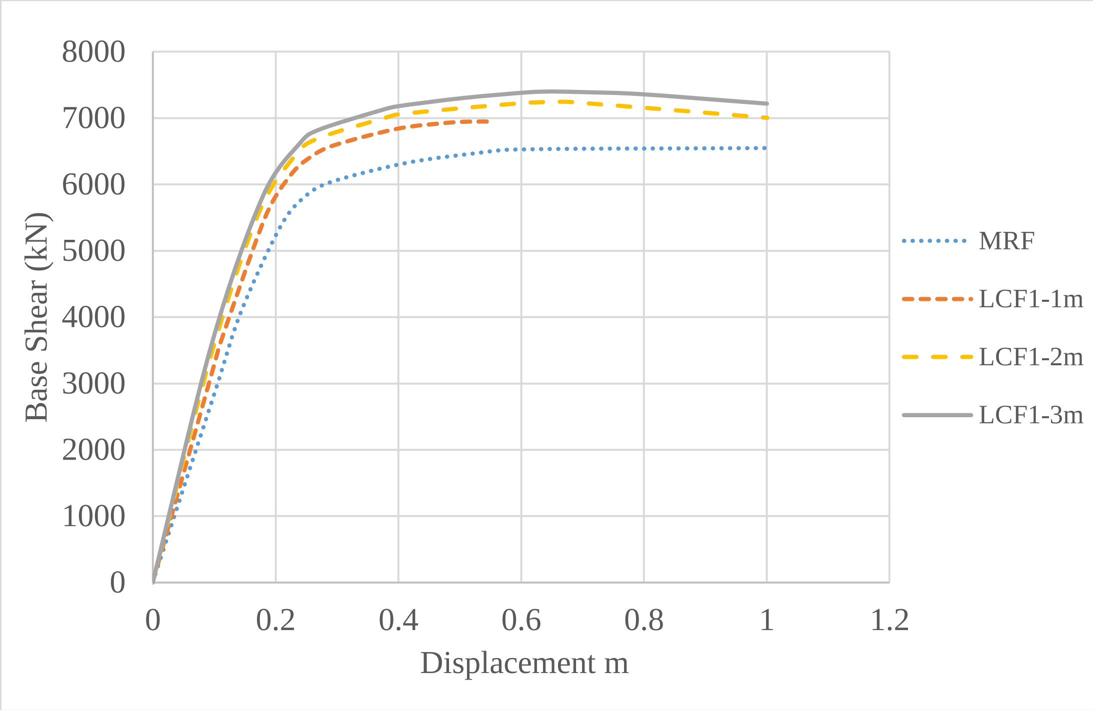

Figure 4.1 Capacity curves obtained for the MRF and LCF1 with column spacing of 1, 2 and 3 m

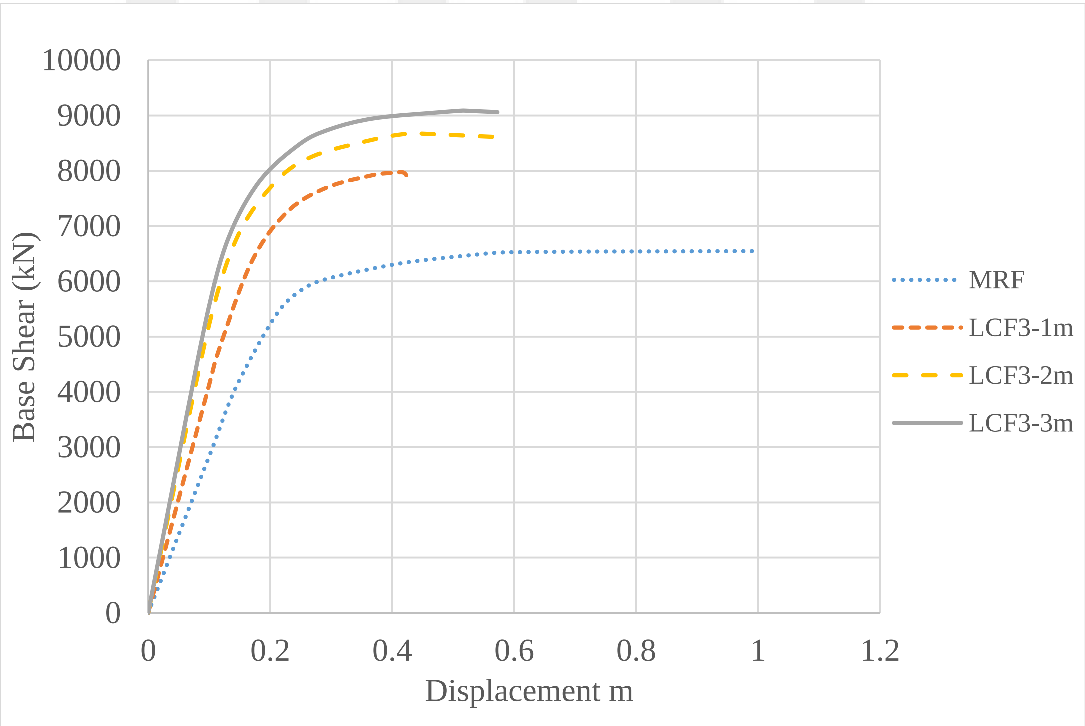

Figure 4.2 Capacity curves obtained for the MRF and LCF3 with column spacing of 1, 2 and 3 m

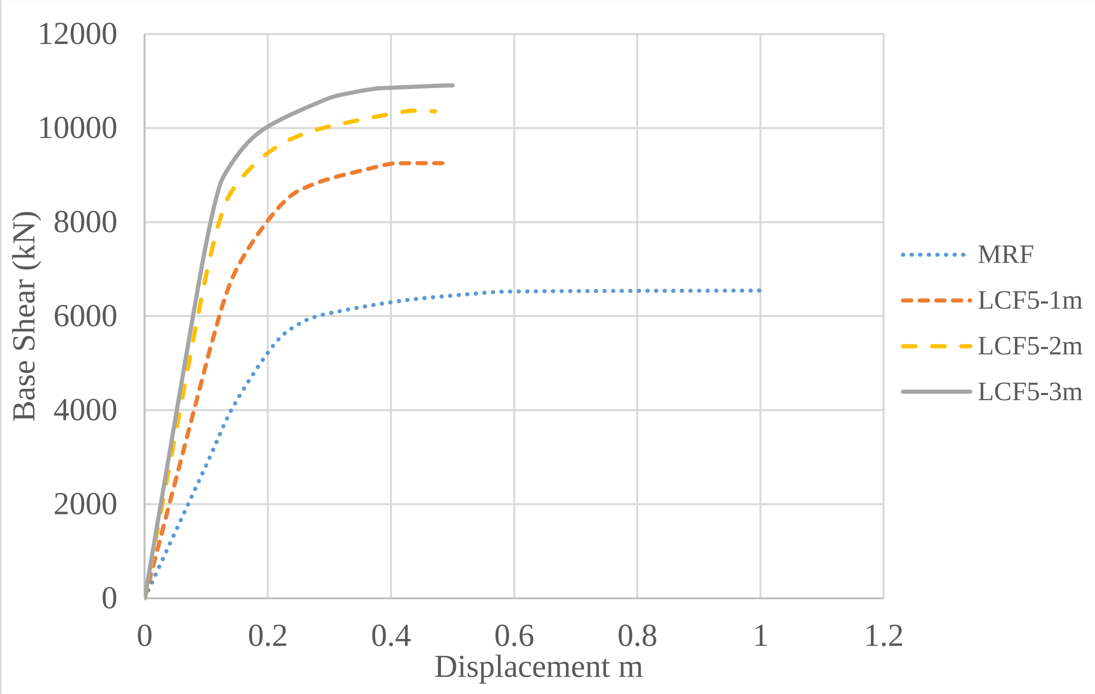

Figure 4.3 Capacity curves obtained for the MRF and LCF5 with column spacing of 1, 2 and 3 m

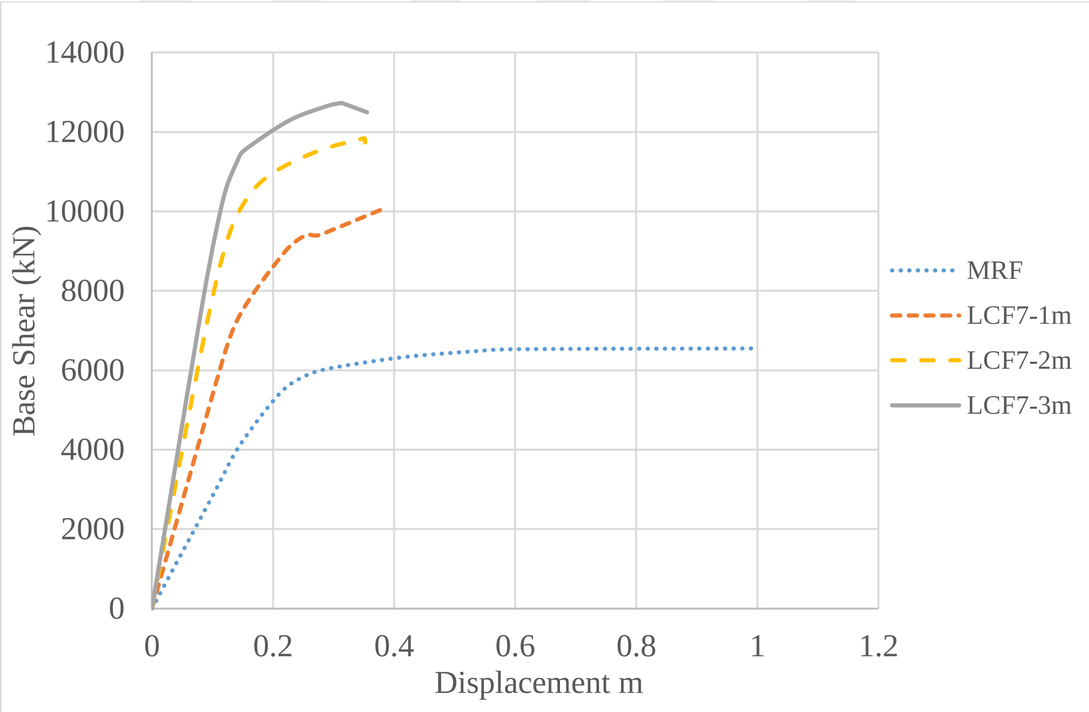

Figure 4.4 Capacity curves obtained for the MRF and LCF7 with column spacing of 1, 2 and 3 m

The plastic hinge formations of all structure are given in Figure 4.5 to 4.17 for example according to the results as shown in Figures 4.5 and 4.6 the by adding linked column the collapse from columns in ground level moved to the linked column and beam links, and increased rapid return to occupancy in LCFs.

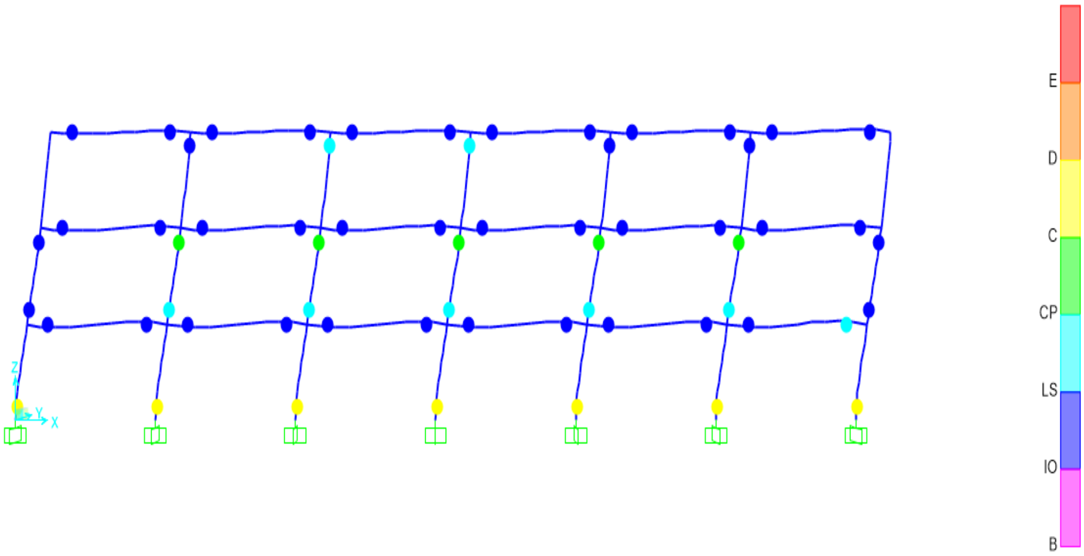

Figure 4.5 Plastic hinge distribution at the final stage of MRF under effect of pushover

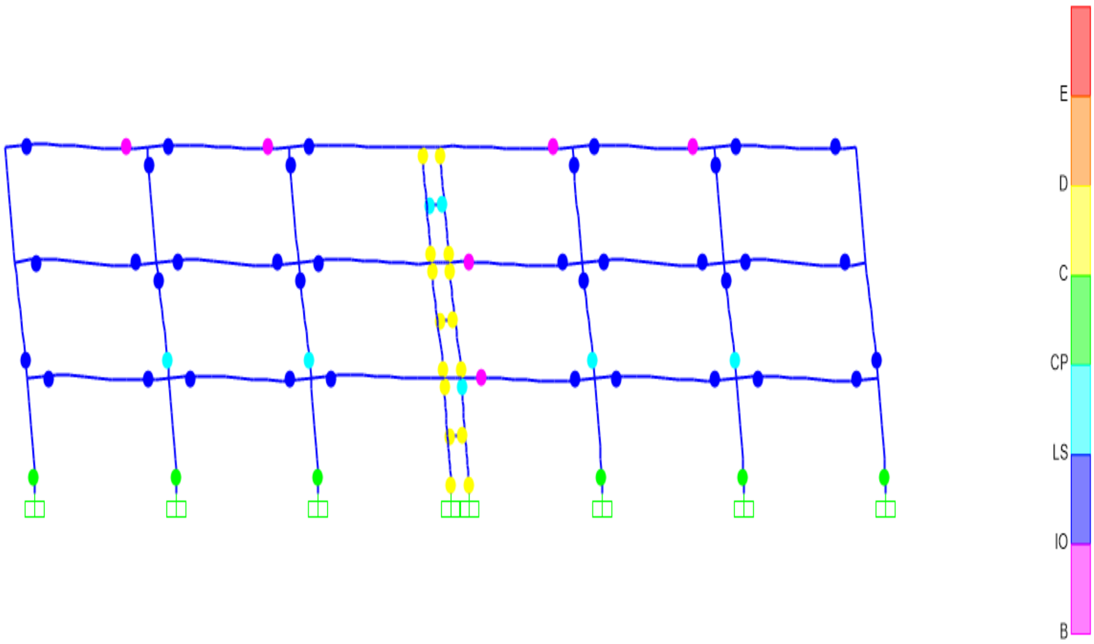

Figure 4.6 Plastic hinge distribution at the final stage of LCF1-1m under effect of pushover

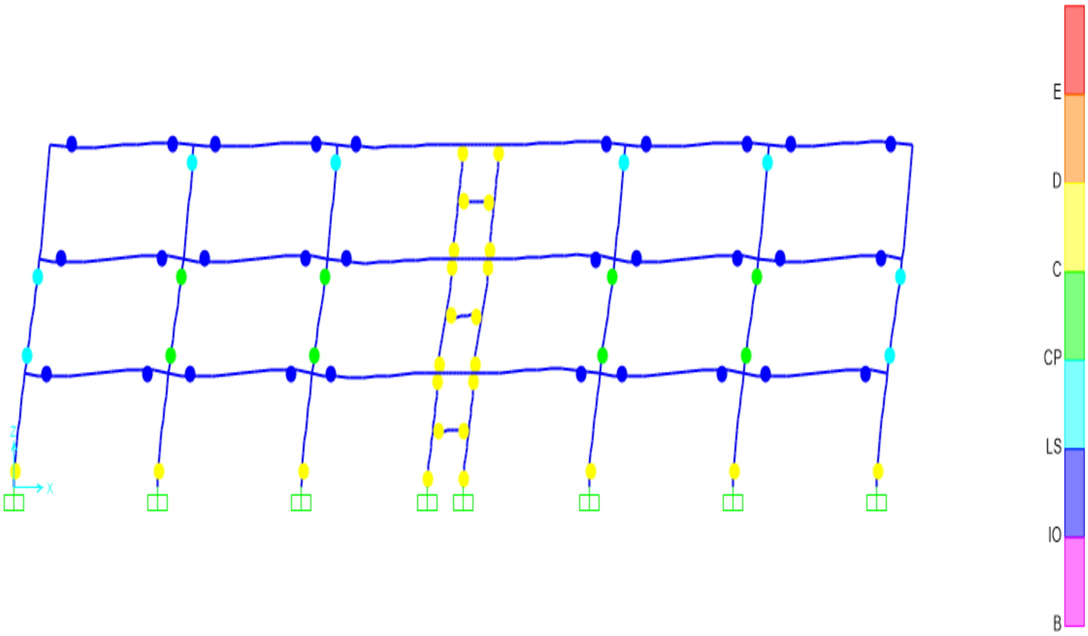

Figure 4.7 Plastic hinge distribution at the final stage of LCF1-2m under effect of pushover

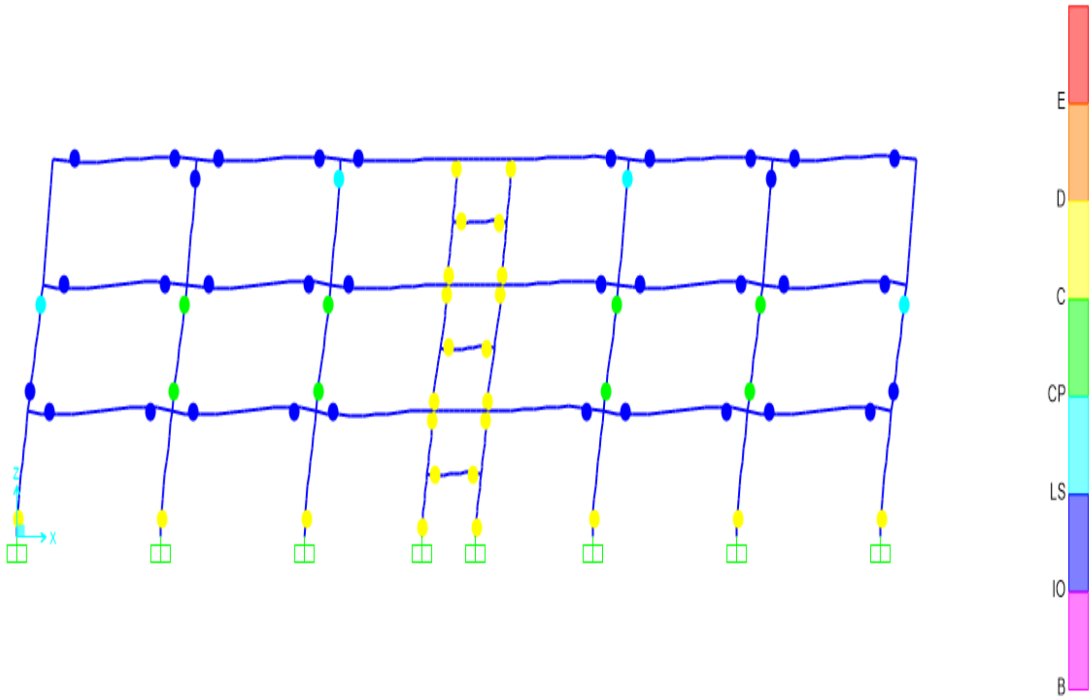

Figure 4.8 Plastic hinge distribution at the final stage of LCF1-3m under effect of pushover

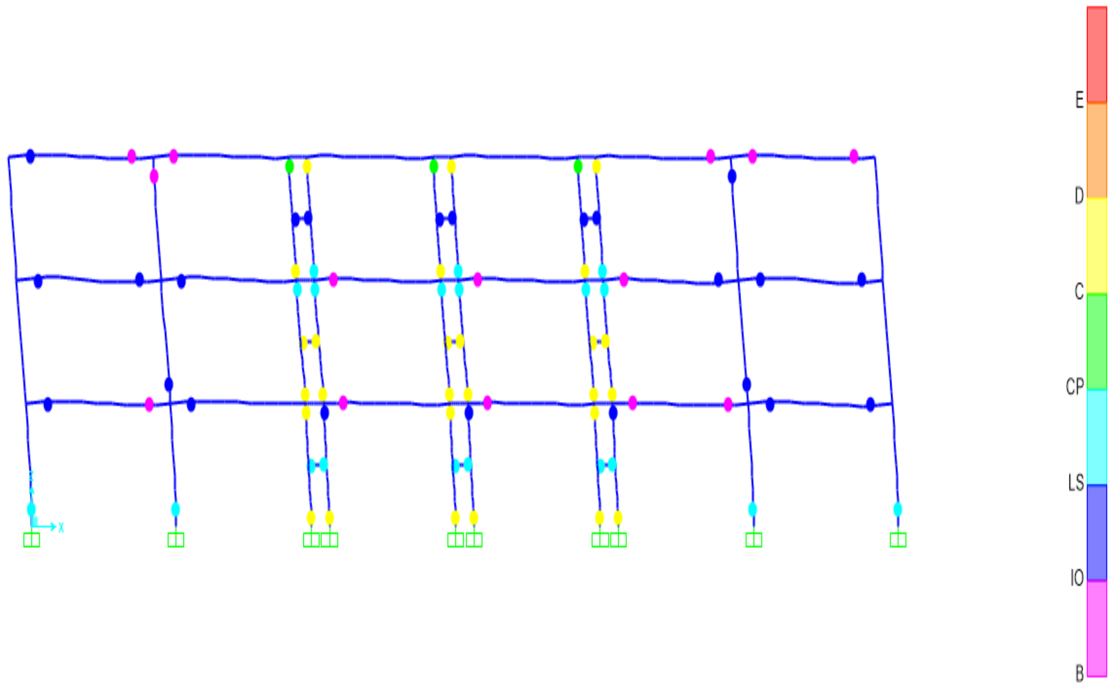

Figure 4.9 Plastic hinge distribution at the final stage of LCF3-1m under effect of pushover

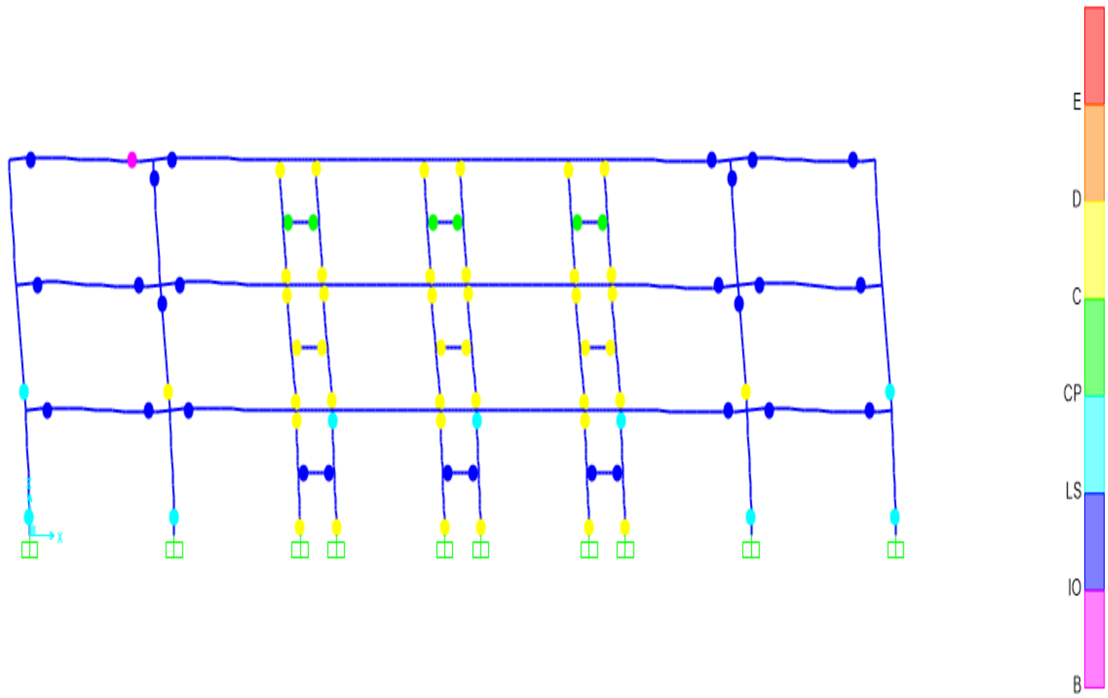

Figure 4.10 Plastic hinge distribution at the final stage of LCF3-2m under effect of pushover

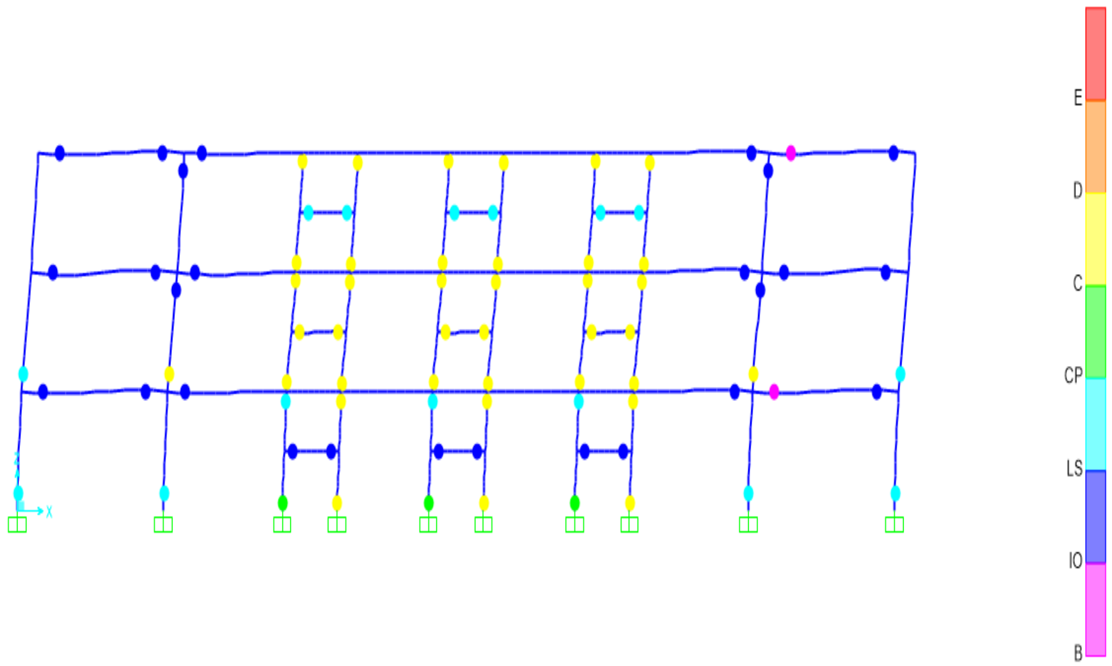

Figure 4.11 Plastic hinge distribution at the final stage of LCF3-3m under effect of pushover

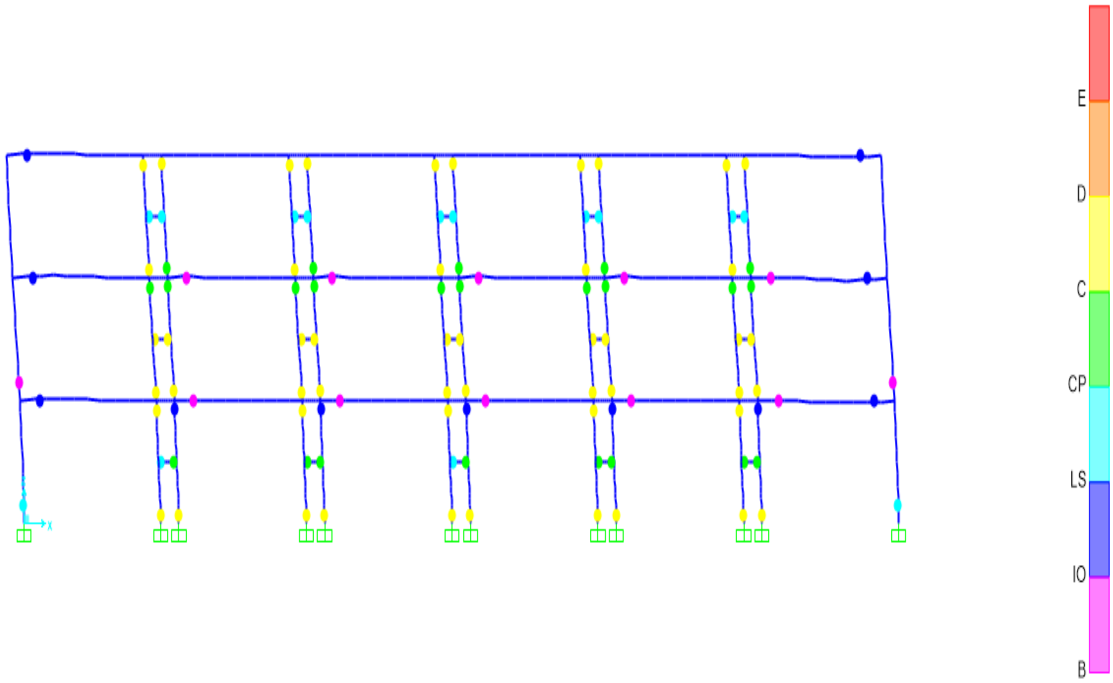

Figure 4.12 Plastic hinge distribution at the final stage of LCF5-1m under effect of pushover

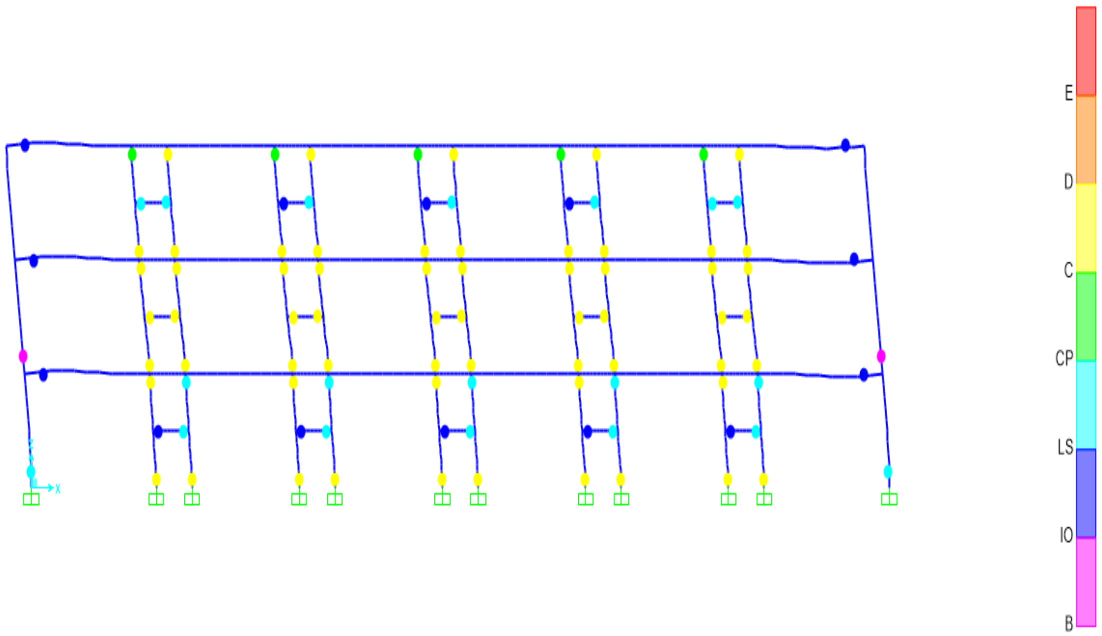

Figure 4.13 Plastic hinge distribution at the final stage of LCF5-2m under effect of pushover

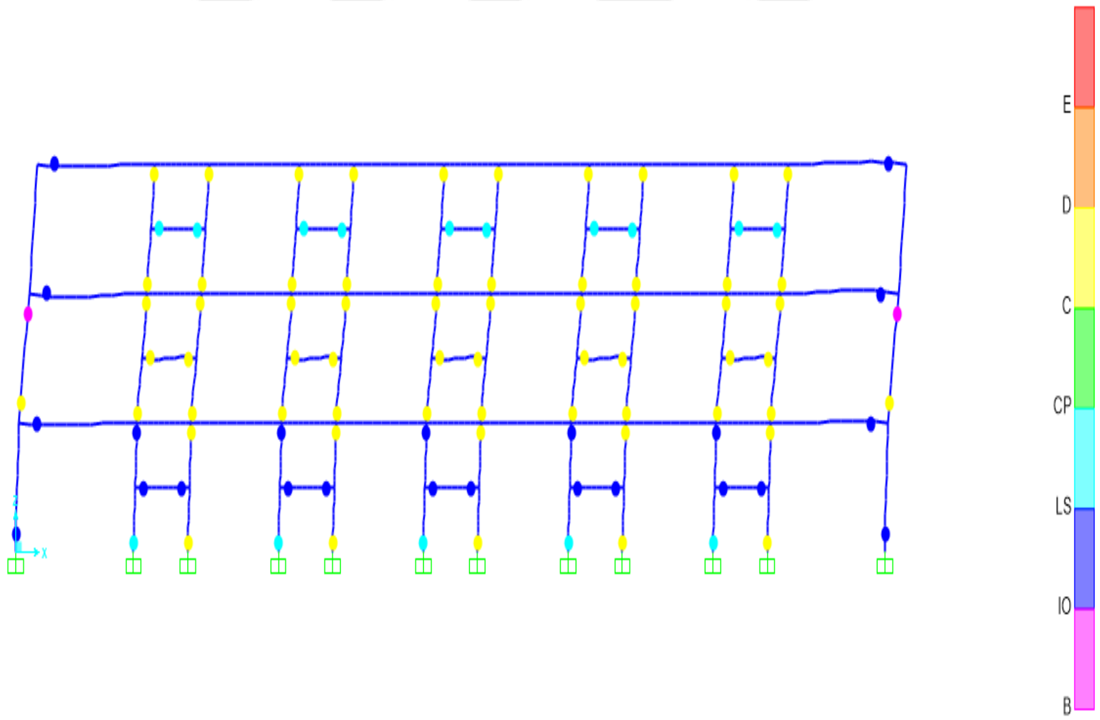

Figure 4.14 Plastic hinge distribution at the final stage of LCF5-3m under effect of pushover

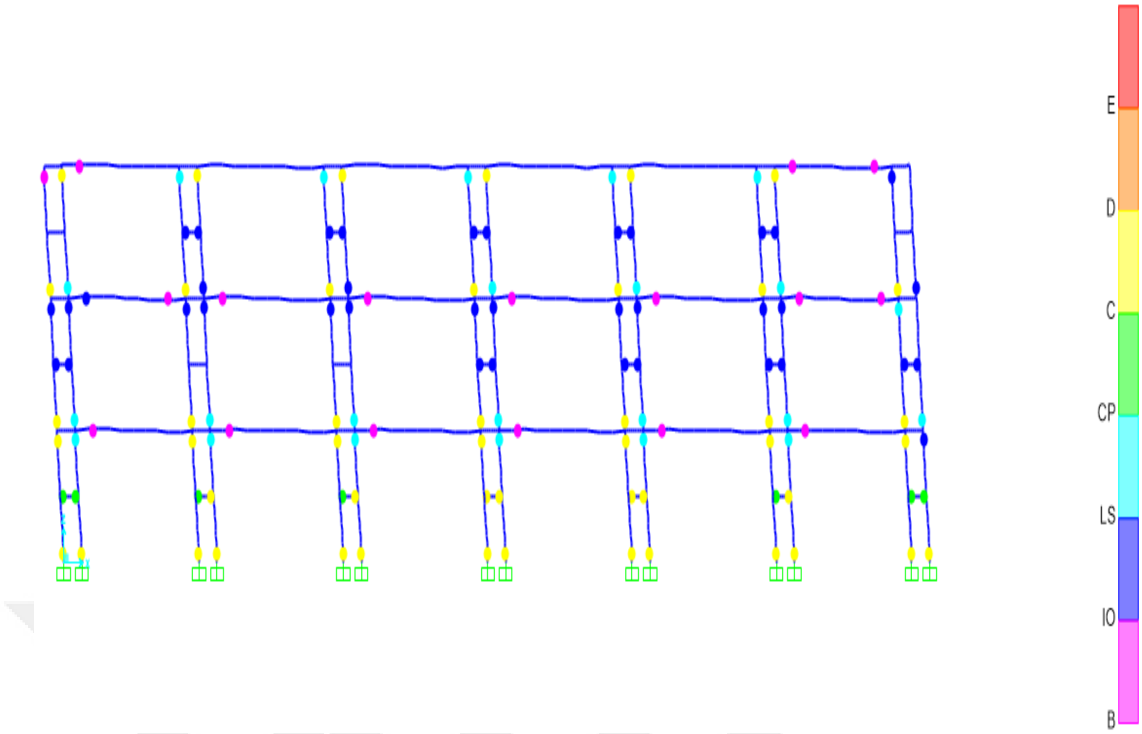

Figure 4.15 Plastic hinge distribution at the final stage of LCF7-1m under effect of pushover

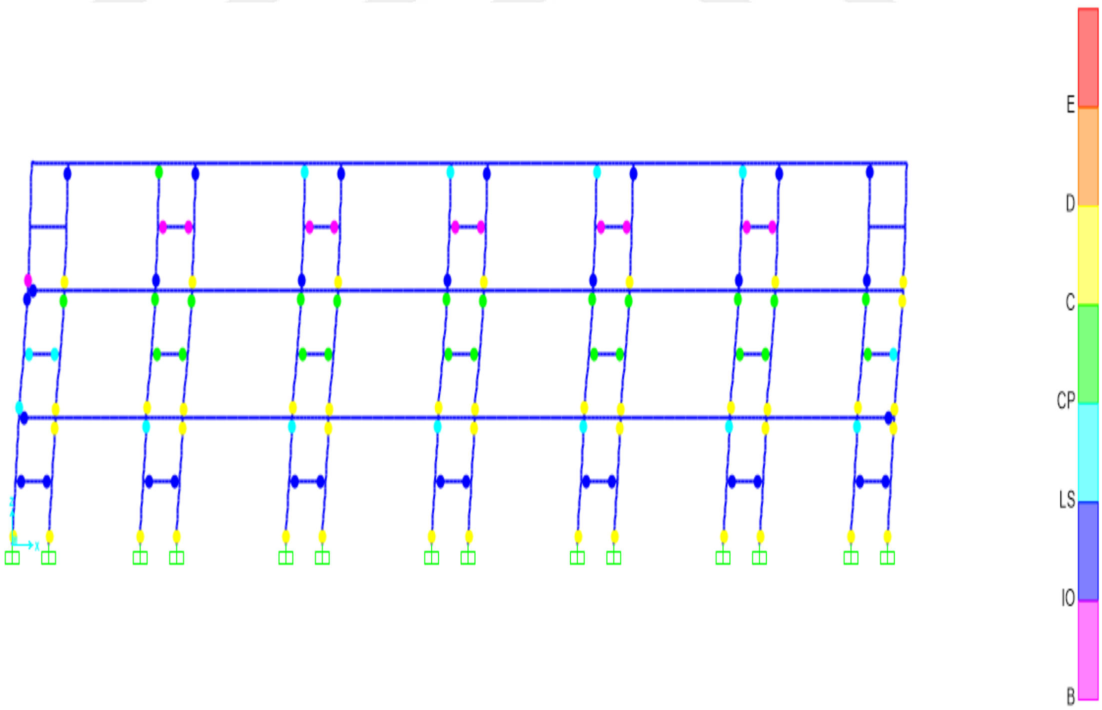

Figure 4.16 Plastic hinge distribution at the final stage of LCF7-2m under effect of pushover

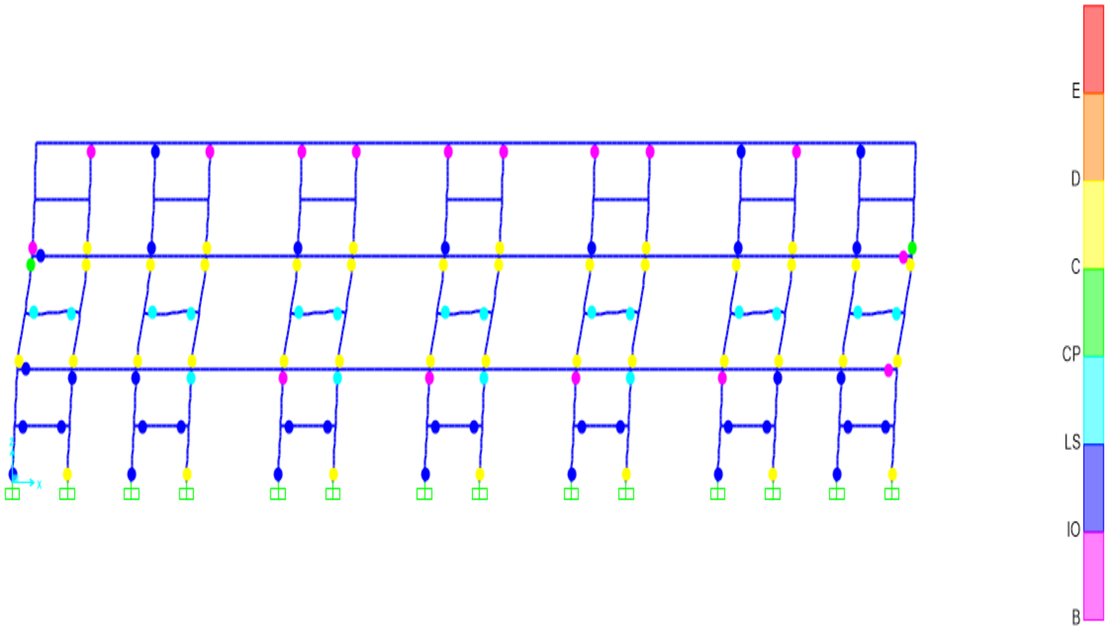

Figure 4.17 Plastic hinge distribution at the final stage of LCF7-3m under effect of pushover

4.2 Nonlinear Time History Analysis

By conducting nonlinear time history analysis, the history response of the frames such as lateral roof displacement variation with time was obtained under the effect of Newhall, Petrolia and Holliste earthquake accelerations as illustrated from Figures 4.18 to 4.29 With the link column systems in the frame, the maximum roof displacement of the frame was decreased.

For instance, under Newhall earthquake ground motion as shown from Figures 4.18,19,20, and 21, the obtained maximum roof displacements for the MRF, LCF1, LCF3, LCF5 and LCF7 with a link beam length of 1 m were 0.99, 0.68, 0.40, 0.28, and 0.21 m, respectively. From Figures 4.22-4.25 under Petrolia earthquake ground motion, the obtained maximum roof displacements for the MRF, LCF1, LCF3, LCF5 and LCF7 with a link beam length of 1 m were 0.37, 0.30, 0.24, 0.20, and 0.17 m, respectively. Similarly, when the frames were subjected to Holliste ground motion acceleration, the maximum roof displacements for the MRF, LCF1, LCF3, LCF5 and LCF7 with a link beam length of 1 m were gathered as 0.38, 0.30, 0.20, 0.16 and 0.13 m, respectively as shown from Figures 4.26-4.29.

In addition, the change in the roof displacement demand of the LCF (especially LCF1 and LCF3) with the variation in the link beam length was so small, such that under Petrolia earthquake ground motion, the maximum roof displacement demand observed for LCF1 with 1 m, 2 m and 3 m length of link beam was 0.68, 0.60 and 0.62 m, respectively.

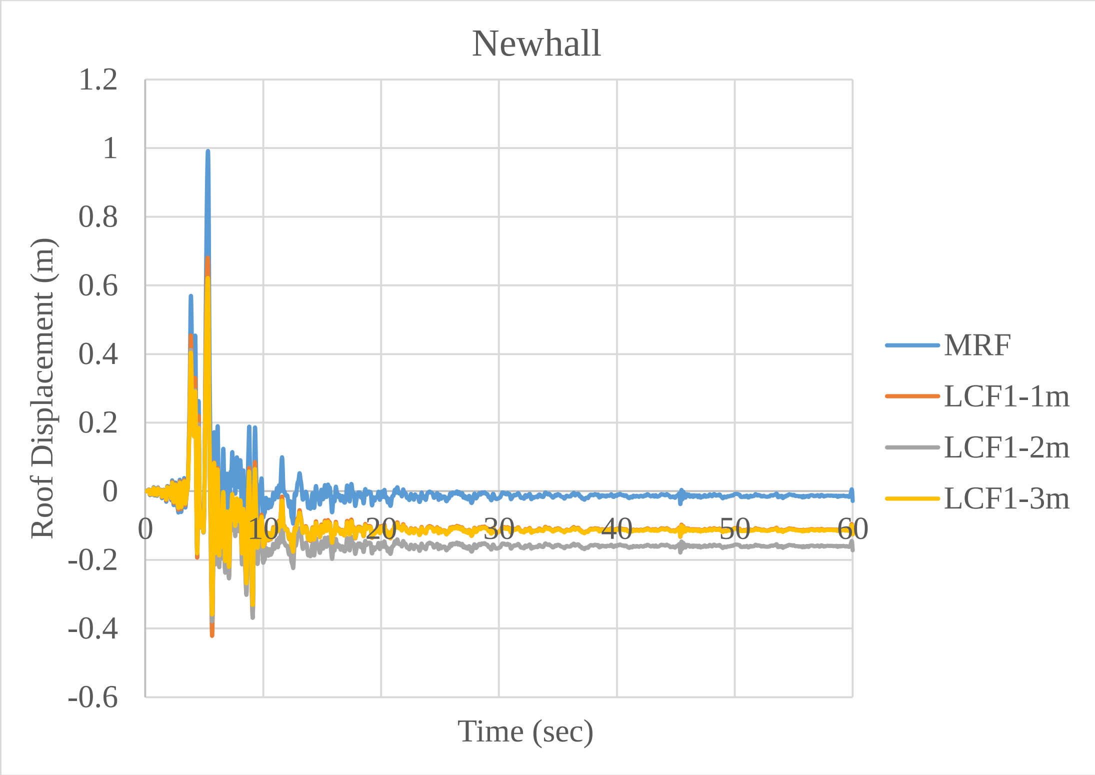

Figure 4.18 Roof displacement time history of MRF and LCF1 with column spacing of 1, 2, and 3 m under Newhall earthquake

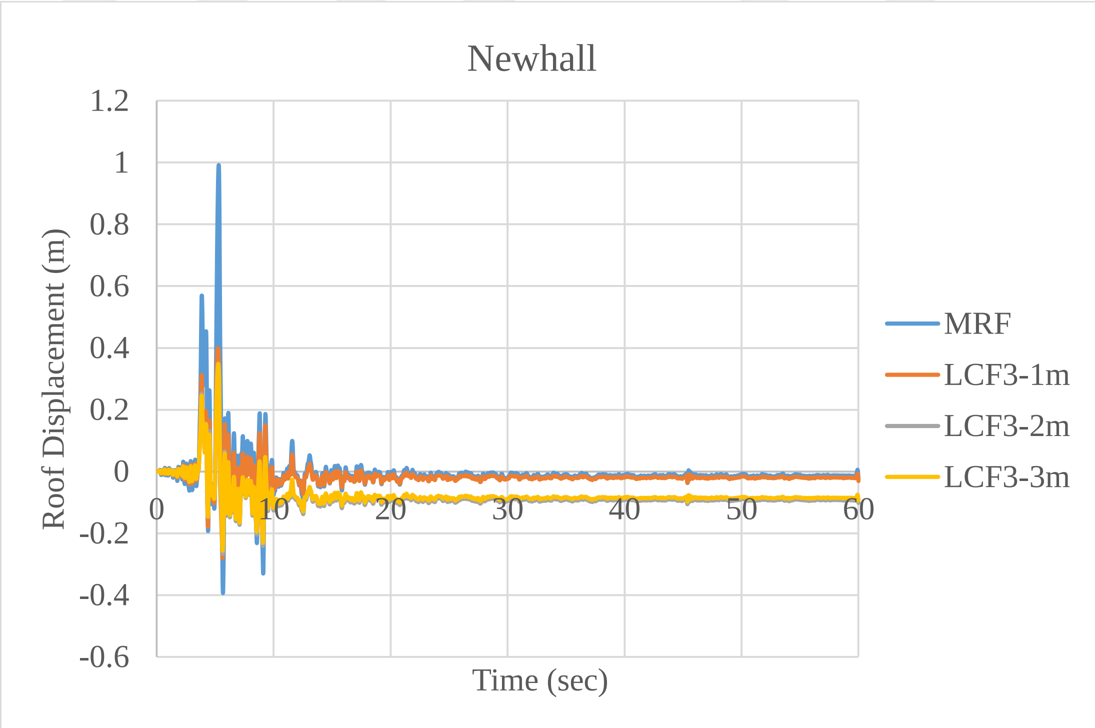

Figure 4.19 Roof displacement time history of MRF and LCF3 with column spacing of 1, 2, and 3 m under Newhall earthquake

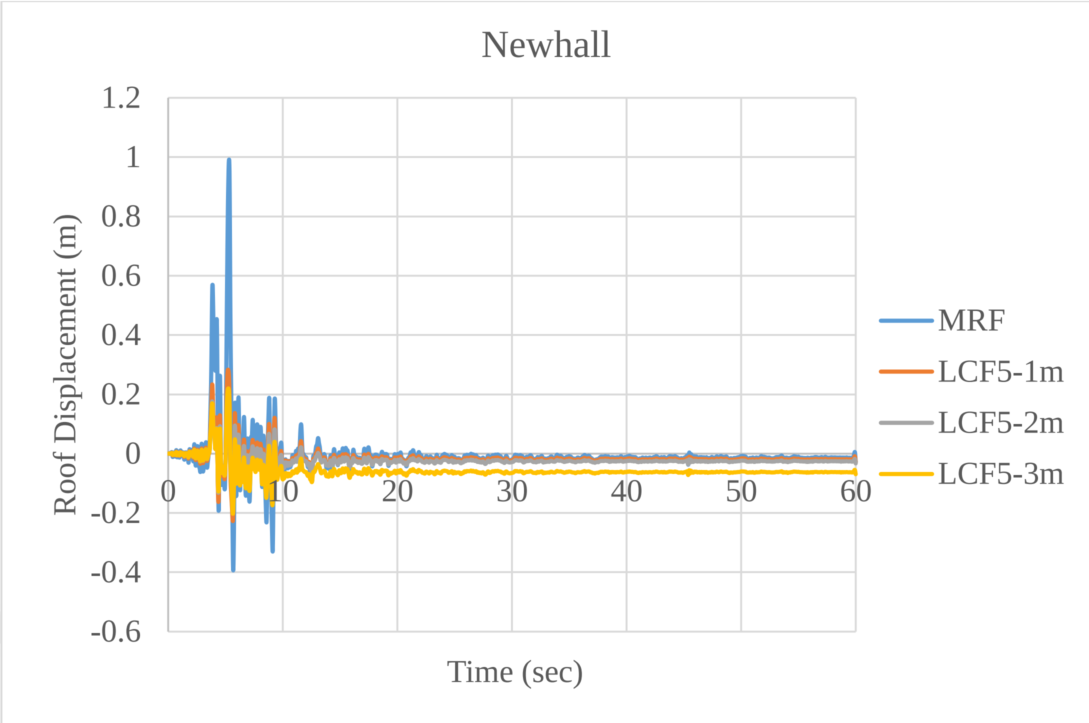

Figure 4.20 Roof displacement time history of MRF and LCF5 with column spacing of 1, 2, and 3 m under Newhall earthquake

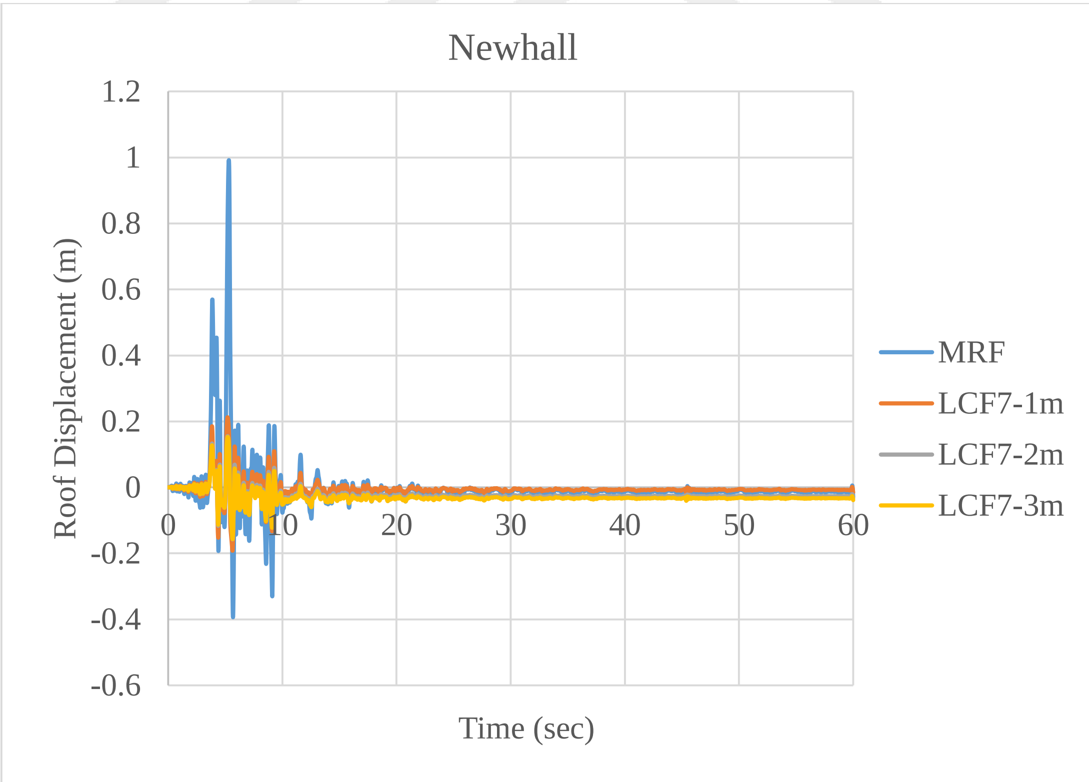

Figure 4.21 Roof displacement time history of MRF and LCF7 with column spacing of 1, 2, and 3 m under Newhall earthquake

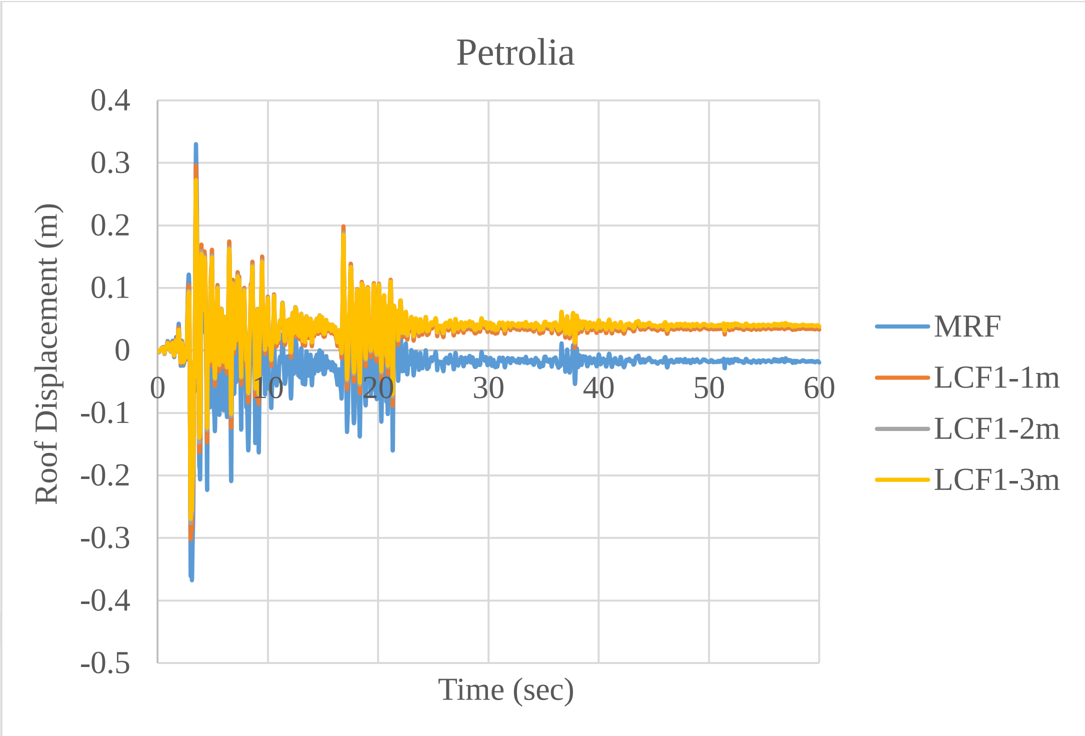

Figure 4.22 Roof displacement time history of MRF and LCF1 with column spacing of 1, 2, and 3 m under Petrolia earthquake

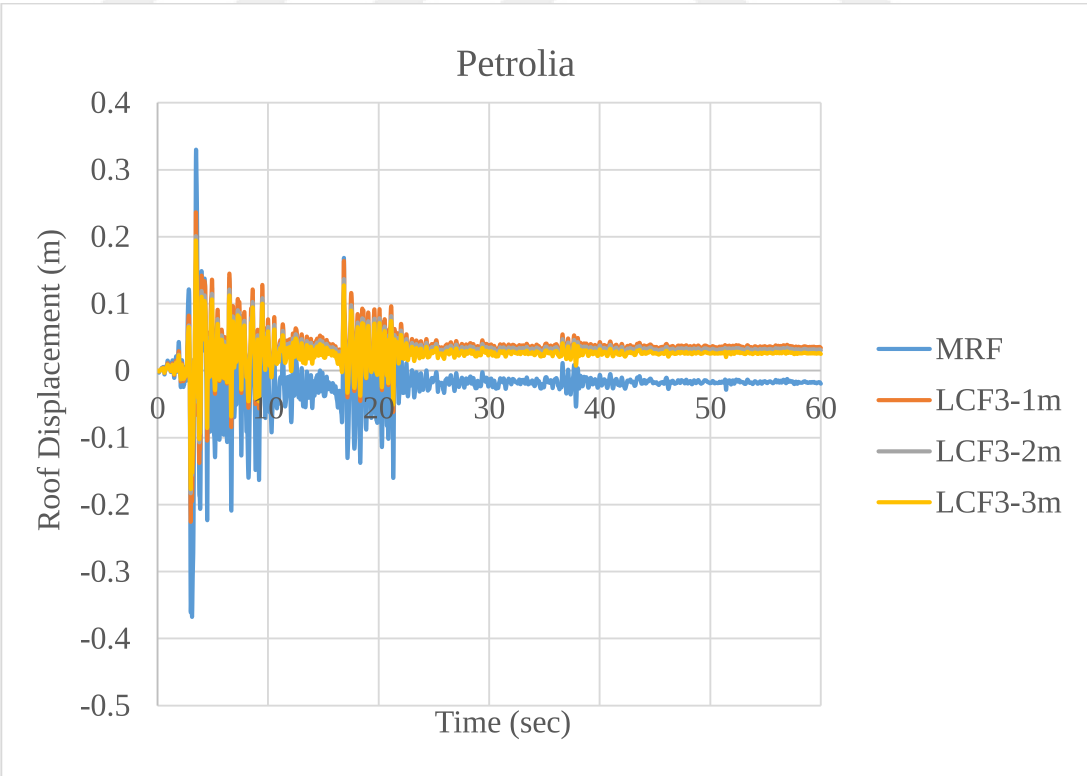

Figure 4.23 Roof displacement time history of MRF and LCF3 with column spacing of 1, 2, and 3 m under Petrolia earthquake

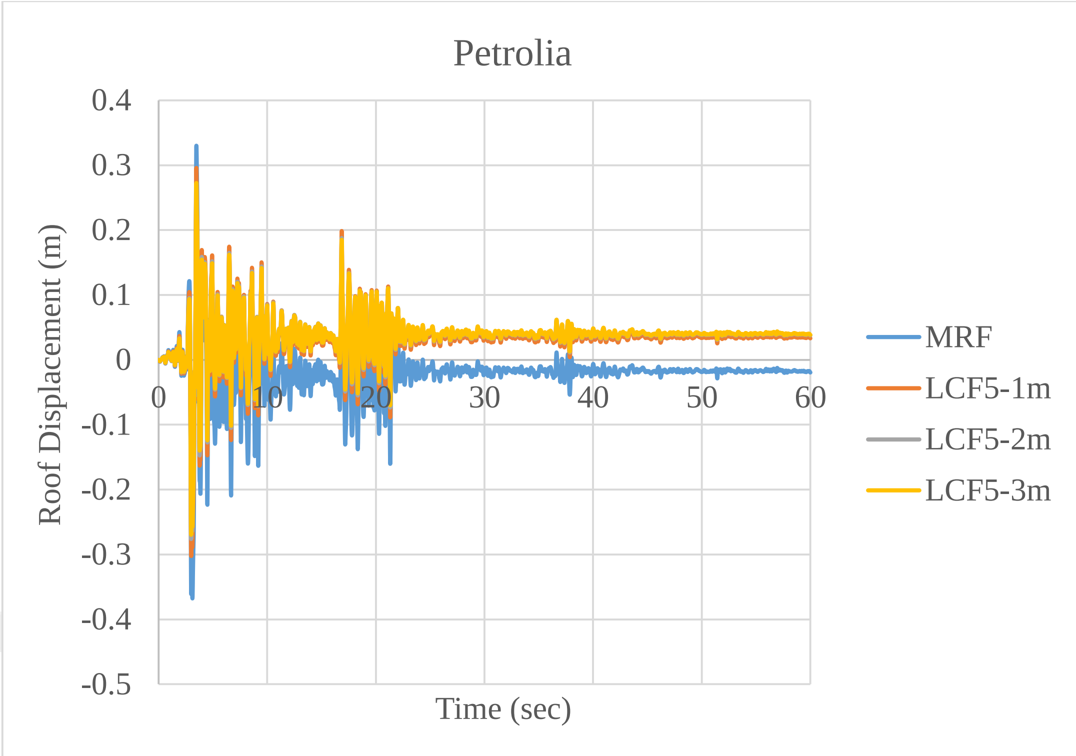

Figure 4.24 Roof displacement time history of MRF and LCF5 with column spacing of 1, 2, and 3 m under Petrolia earthquake

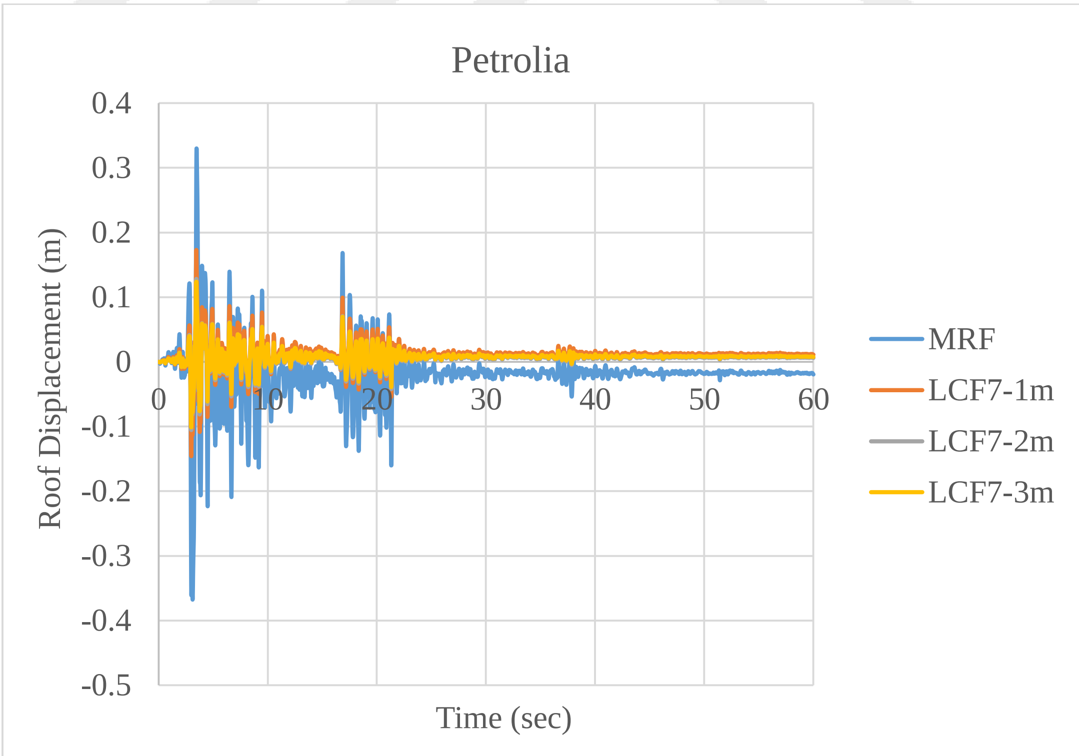

Figure 4.25 Roof displacement time history of MRF and LCF7 with column spacing of 1, 2, and 3 m under Petrolia earthquake

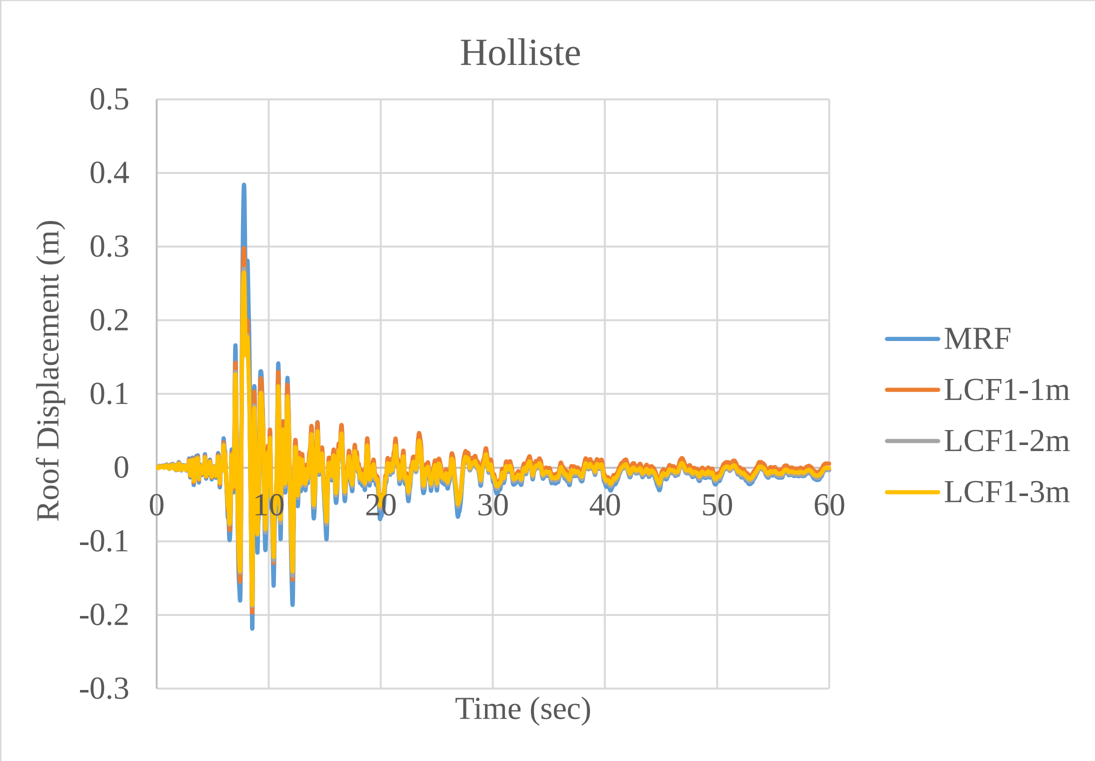

Figure 4.26 Roof displacement time history of MRF and LCF1 with column spacing of 1, 2, and 3 m under Holliste earthquake

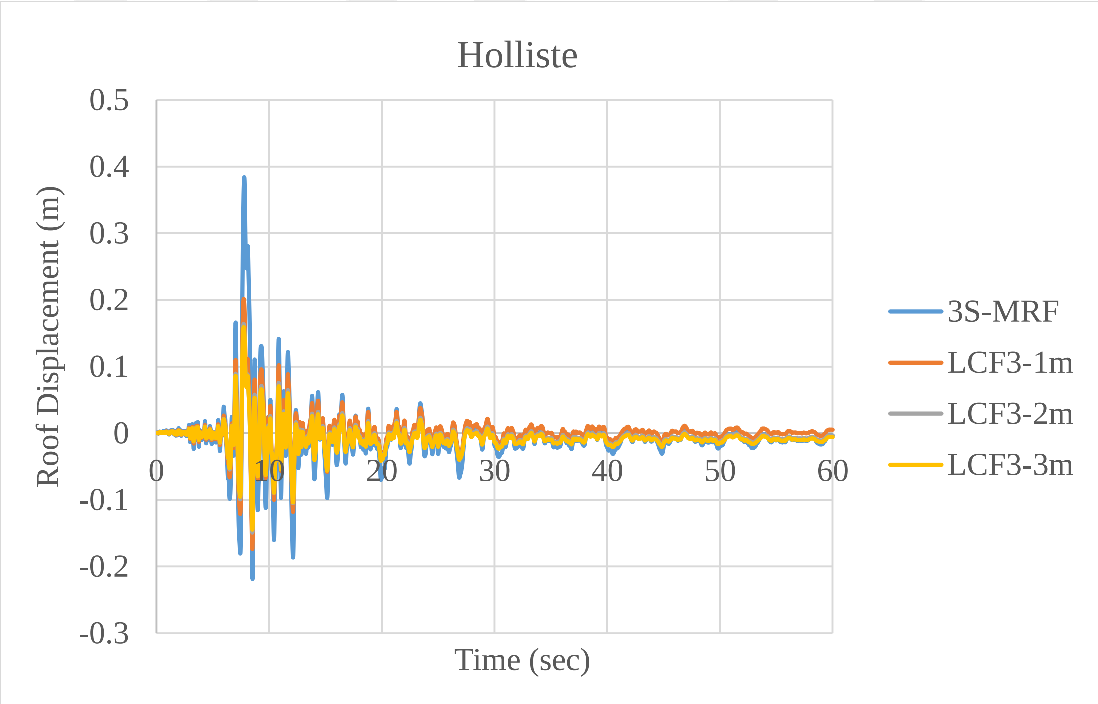

Figure 4.27 Roof displacement time history of MRF and LCF3 with column spacing of 1, 2, and 3 m under Holliste earthquake

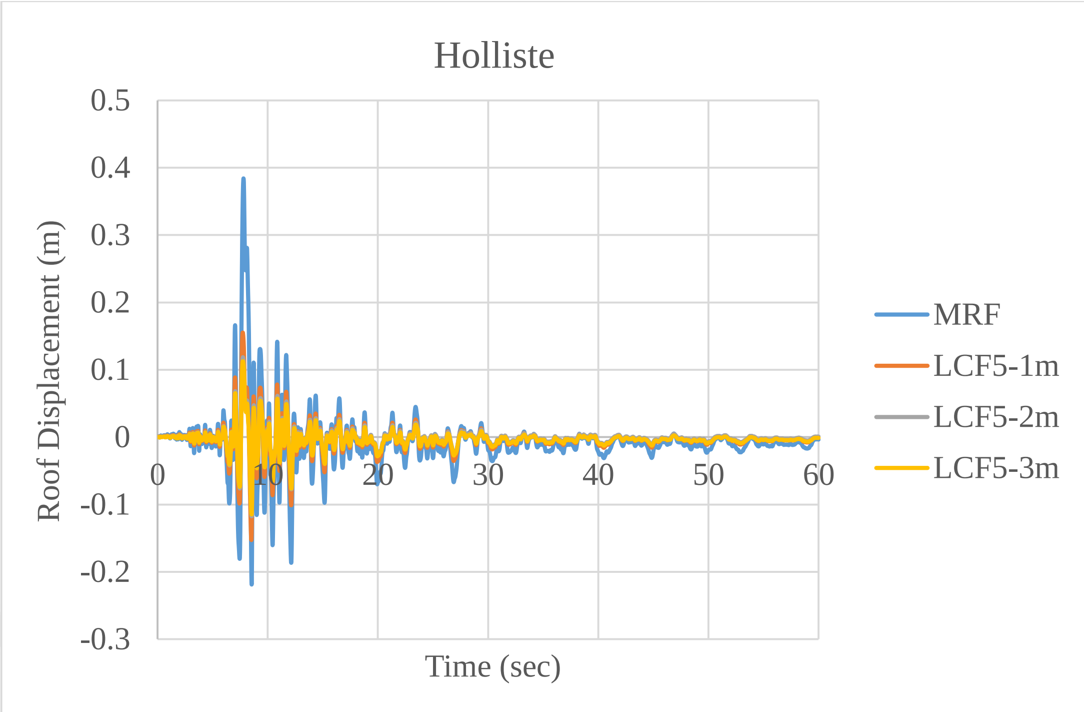

Figure 4.28 Roof displacement time history of MRF and LCF5 with column spacing of 1, 2, and 3 m under Holliste earthquake

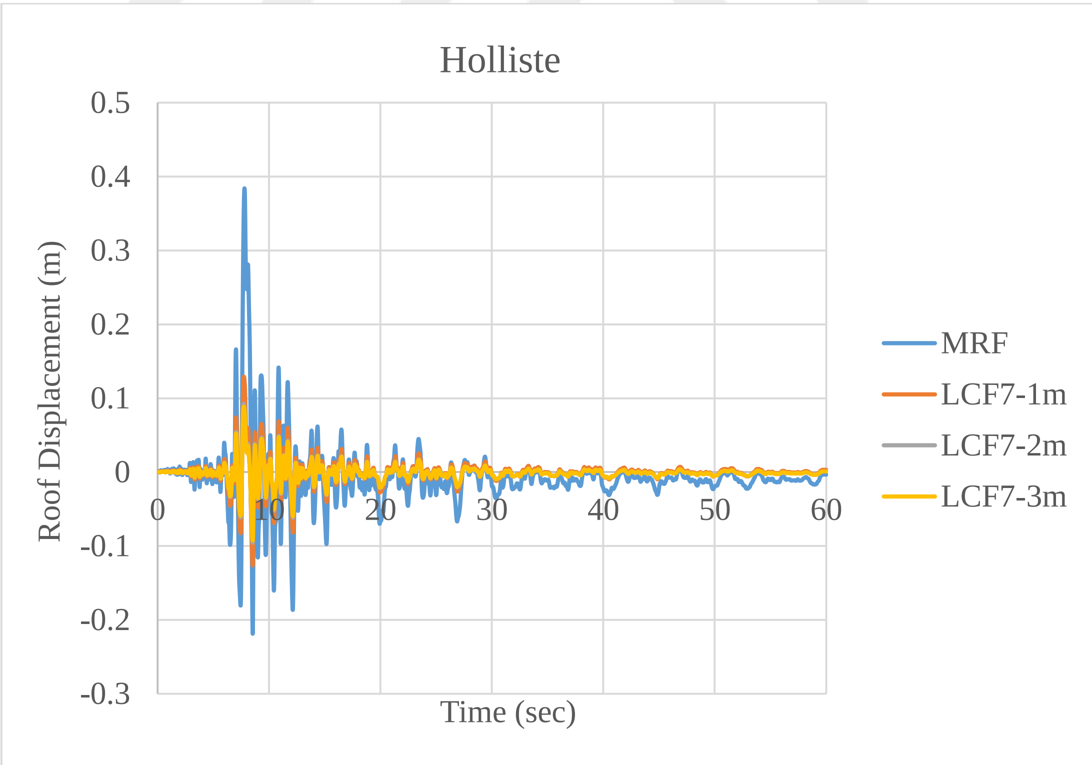

Figure 4.29 Roof displacement time history of MRF and LCF7 with column spacing of 1, 2, and 3 m under Holliste earthquake

Furthermore, in order to examine the response of the frames in detailed, the maximum values of the displacement of each story in the positive or negative lateral direction was recorded and the maximum story displacement demand at each story was plotted as given from Figures 4.30 to 4.41. The general trend is similar to the previous findings that the displacement demand at each story decreased with the increase in the number of link column systems.

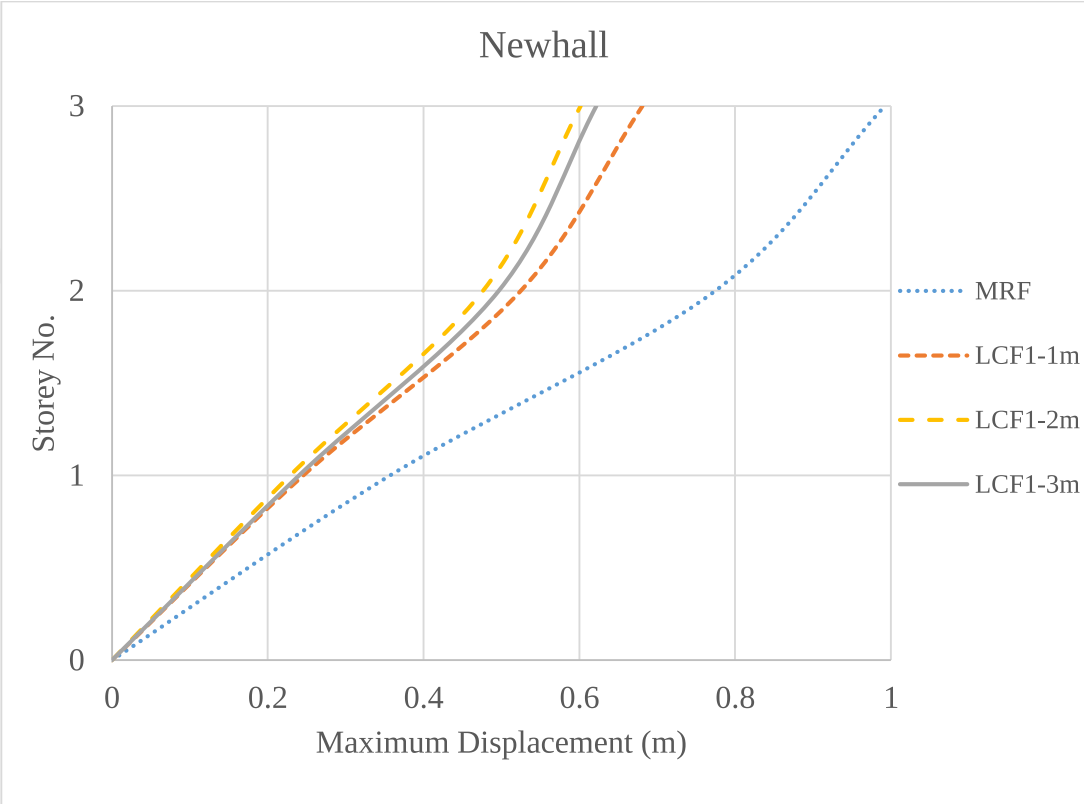

Figure 4.30 Maximum displacement demand for MRF and LCF1 with column spacing of 1, 2, and 3 m under Newhall earthquake

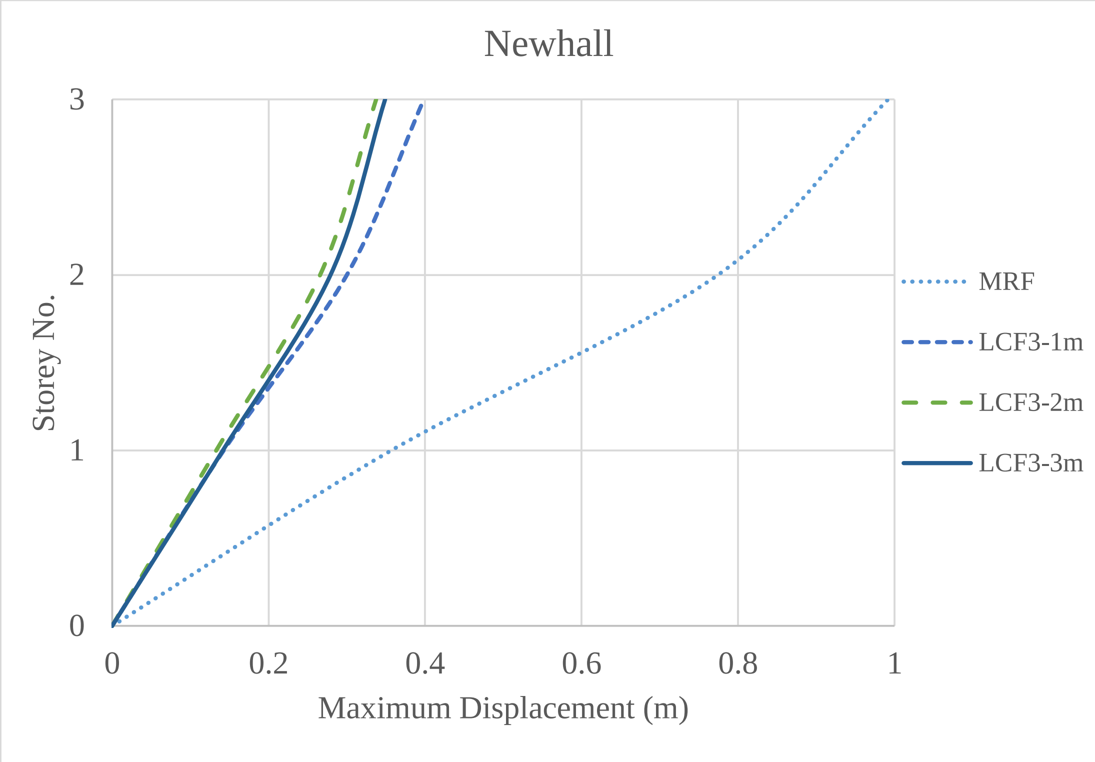

Figure 4.31 Maximum displacement demand for MRF and LCF3 with column spacing of 1, 2, and 3 m under Newhall earthquake

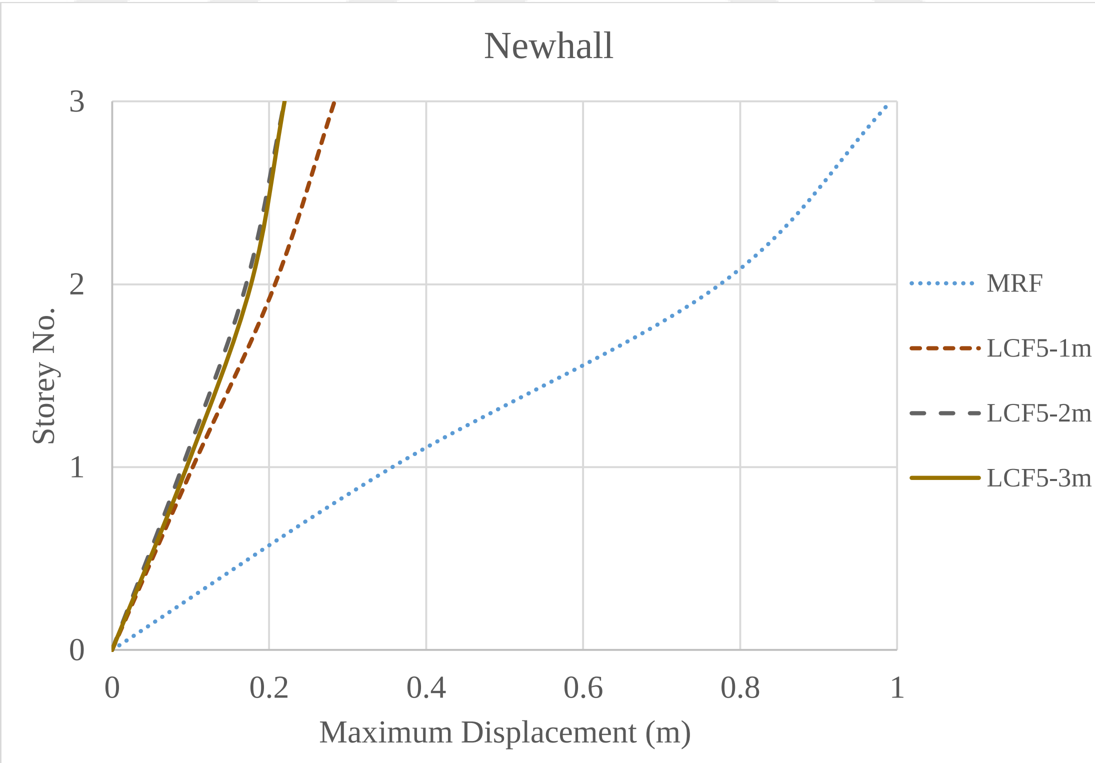

Figure 4.32 Maximum displacement demand for MRF and LCF5 with column spacing of 1, 2, and 3 m under Newhall earthquake

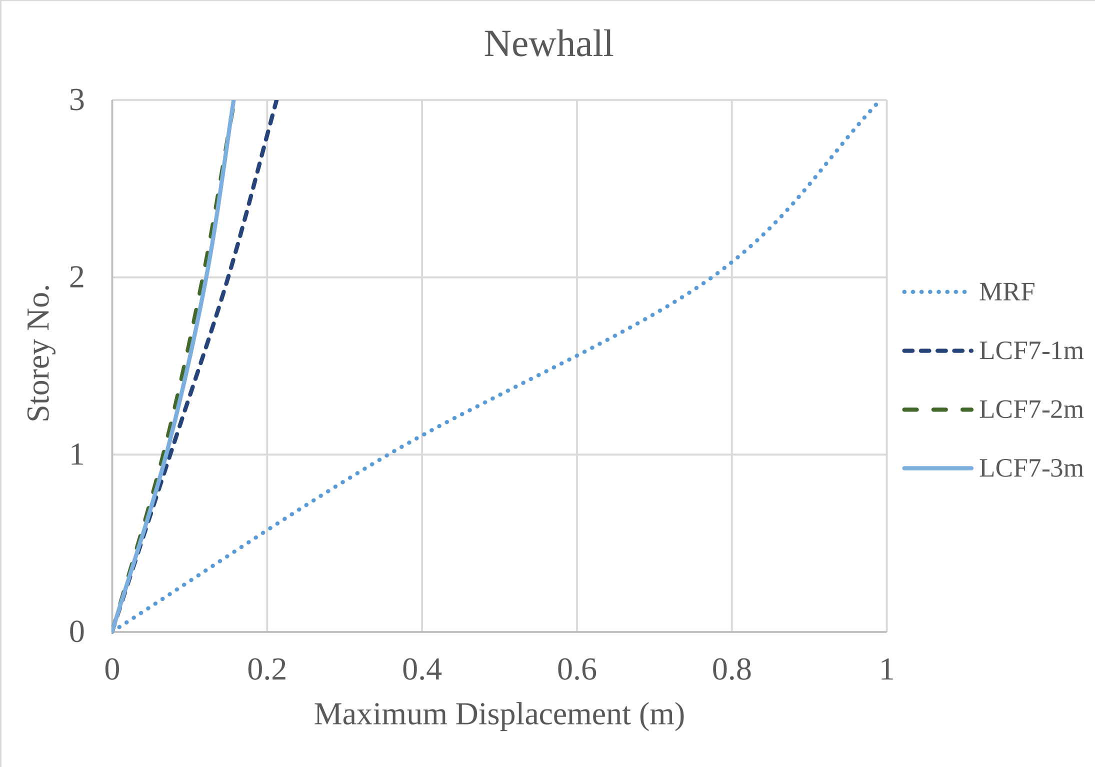

Figure 4.33 Maximum displacement demand for MRF and LCF7 with column spacing of 1, 2, and 3 m under Newhall earthquake

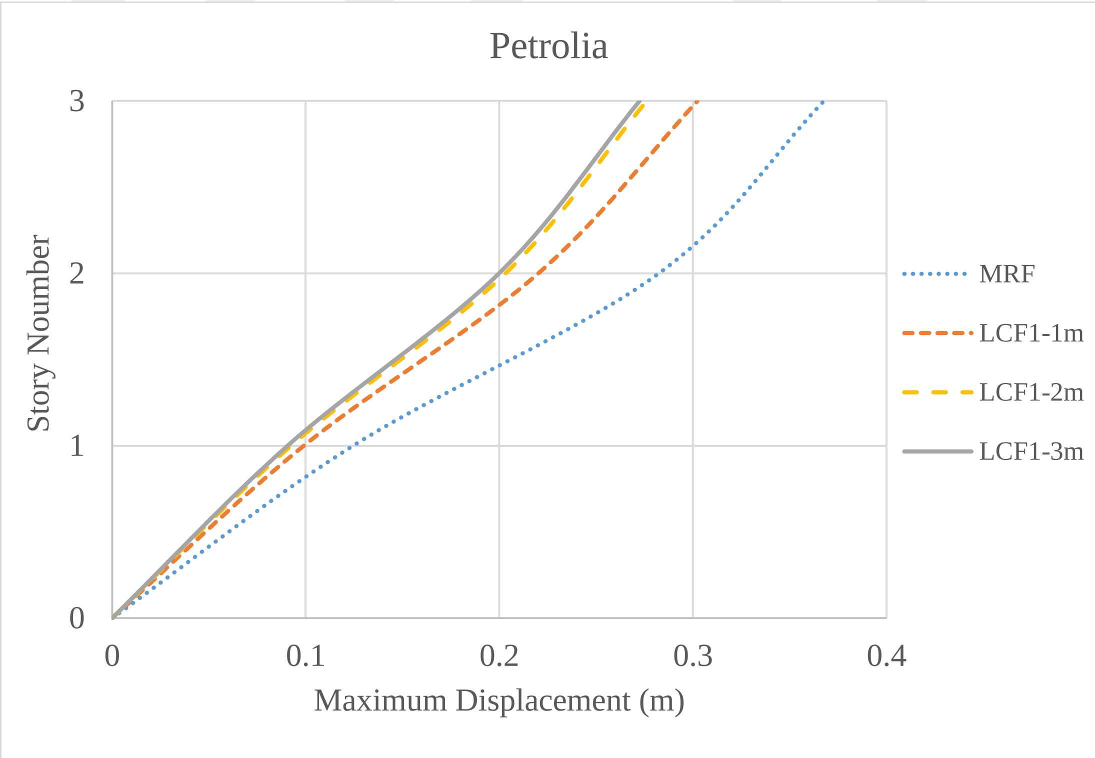

Figure 4.34 Maximum displacement demand for MRF and LCF1 with column spacing of 1, 2, and 3 m under Petrolia earthquake

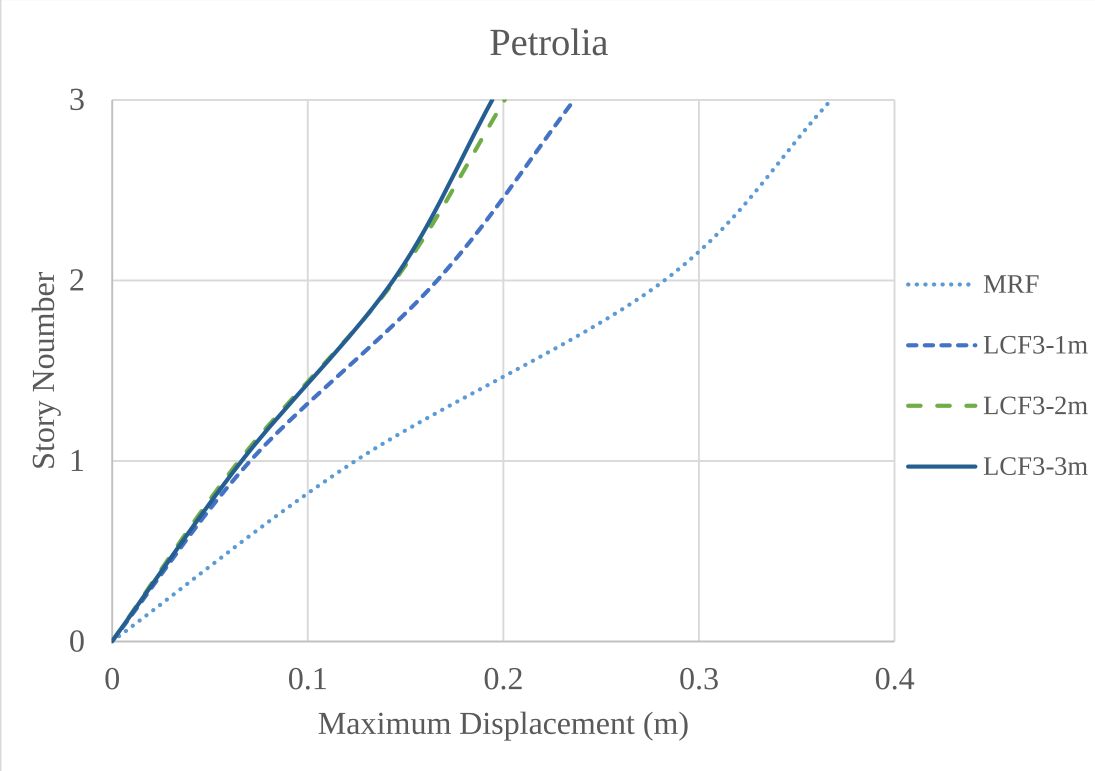

Figure 4.35 Maximum displacement demand for MRF and LCF3 with column spacing of 1, 2, and 3 m under Petrolia earthquake

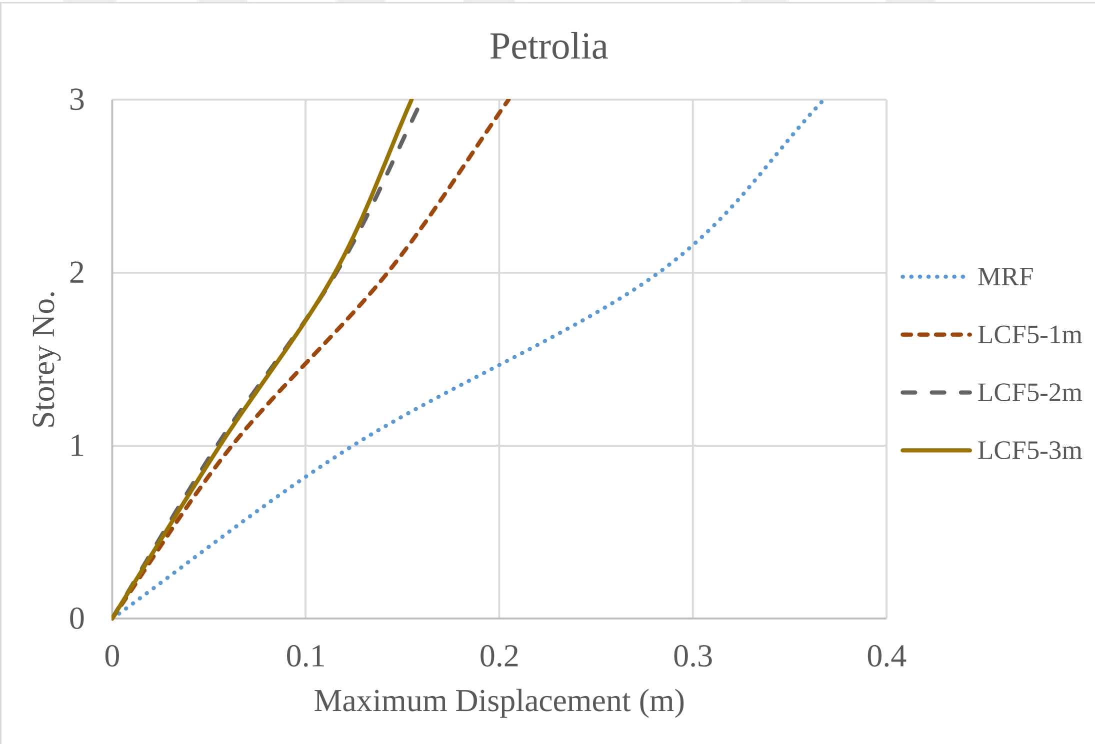

Figure 4.36 Maximum displacement demand for MRF and LCF5 with column spacing of 1, 2, and 3 m under Petrolia earthquake

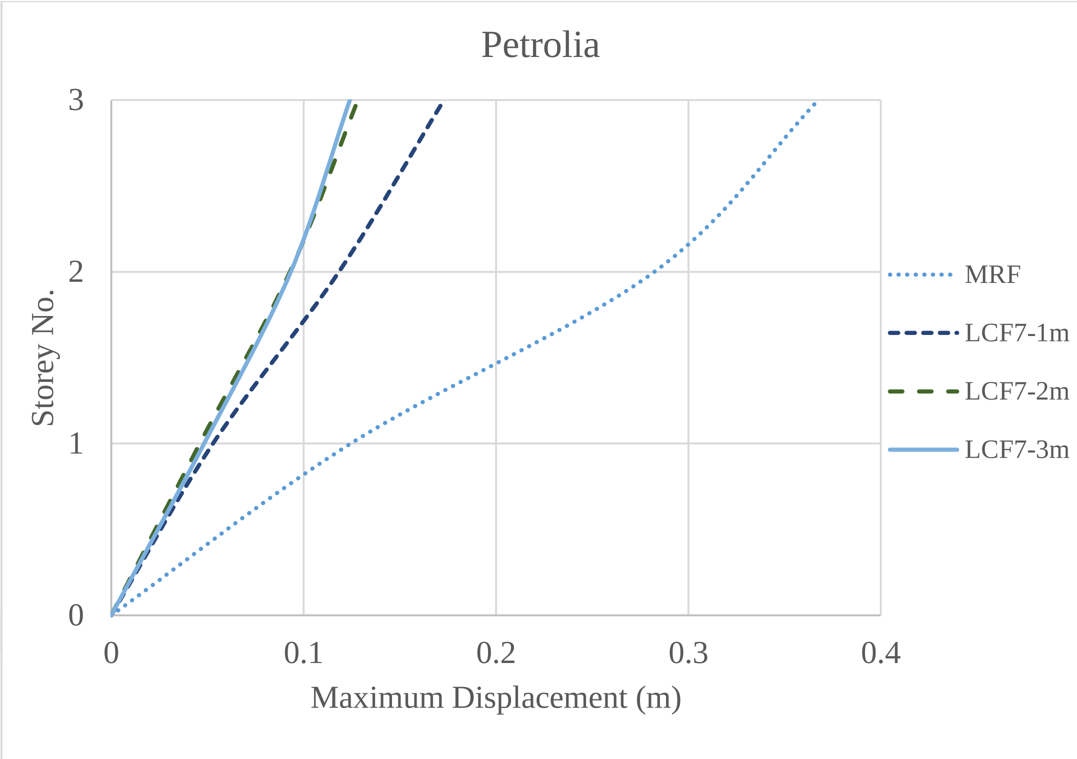

Figure 4.37 Maximum displacement demand for MRF and LCF7 with column spacing of 1, 2, and 3 m under Petrolia earthquake

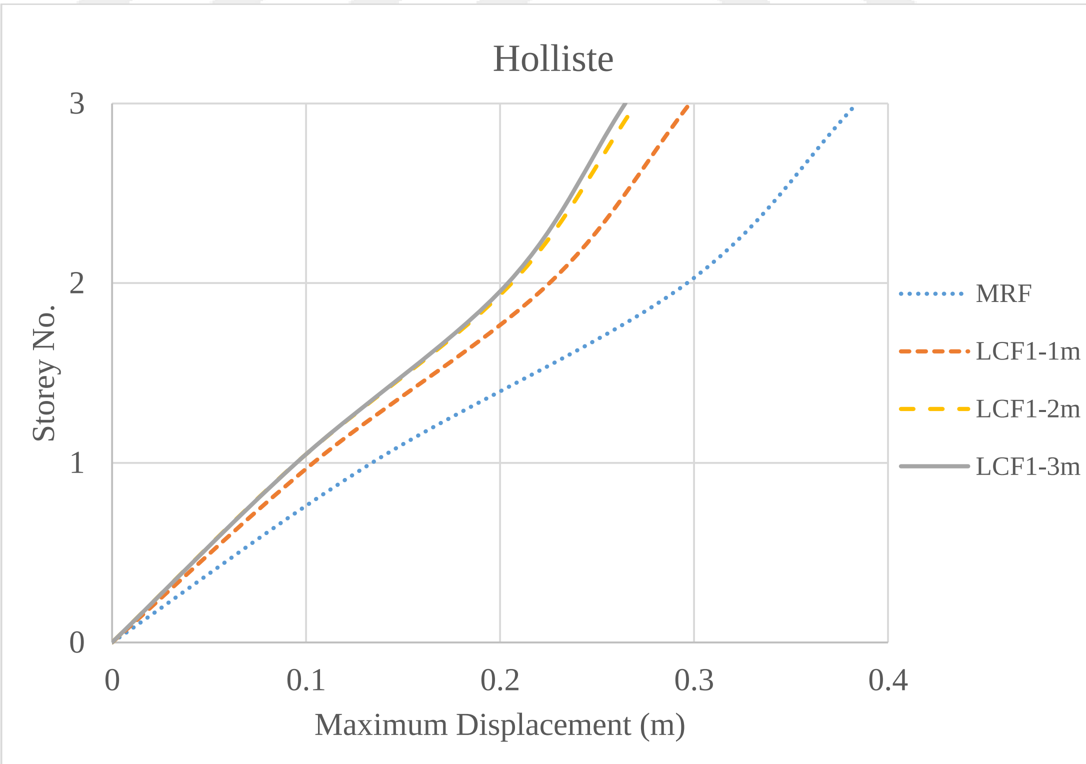

Figure 4.38 Maximum displacement demand for MRF and LCF1 with column spacing of 1, 2, and 3 m under Holliste earthquake

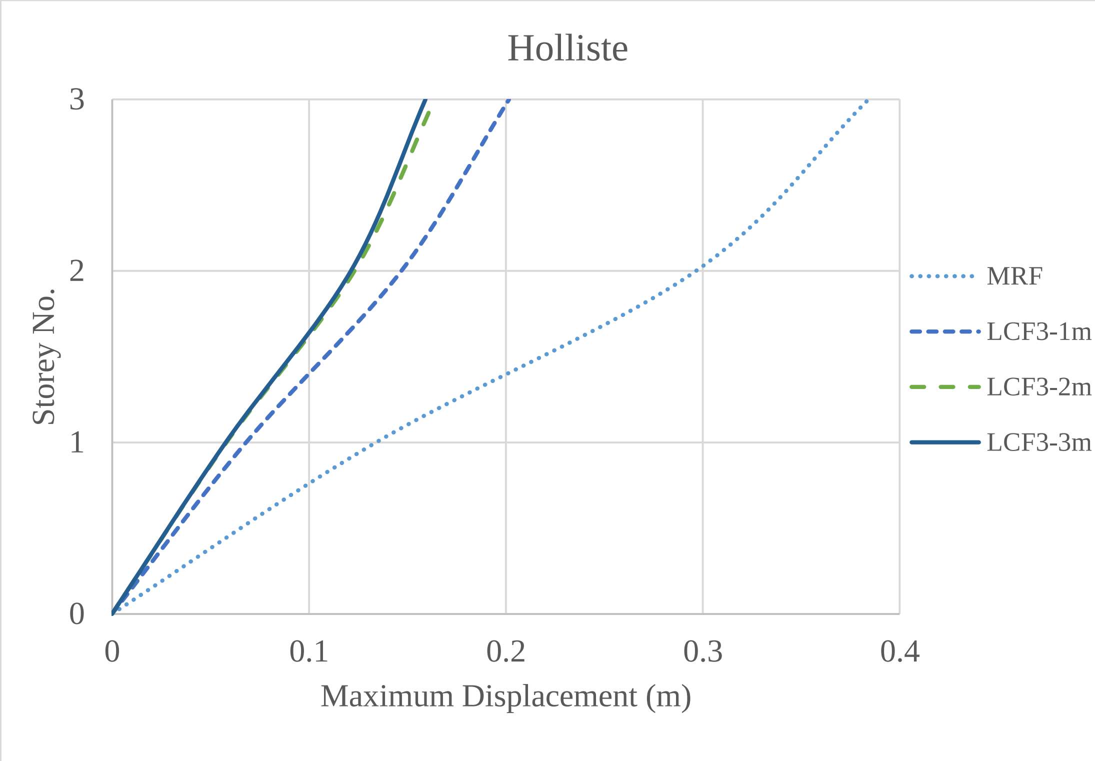

Figure 4.39 Maximum displacement demand for MRF and LCF3 with column spacing of 1, 2, and 3 m under Holliste earthquake

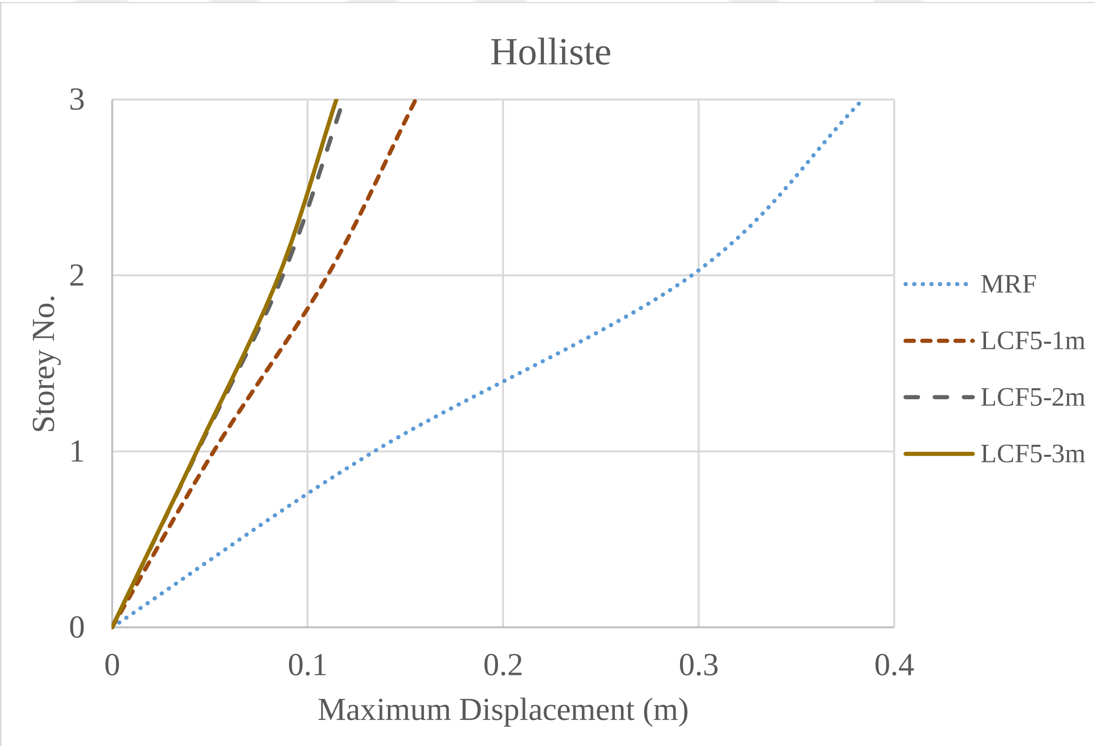

Figure 4.40 Maximum displacement demand for MRF and LCF5 with column spacing of 1, 2, and 3 m under Holliste earthquake

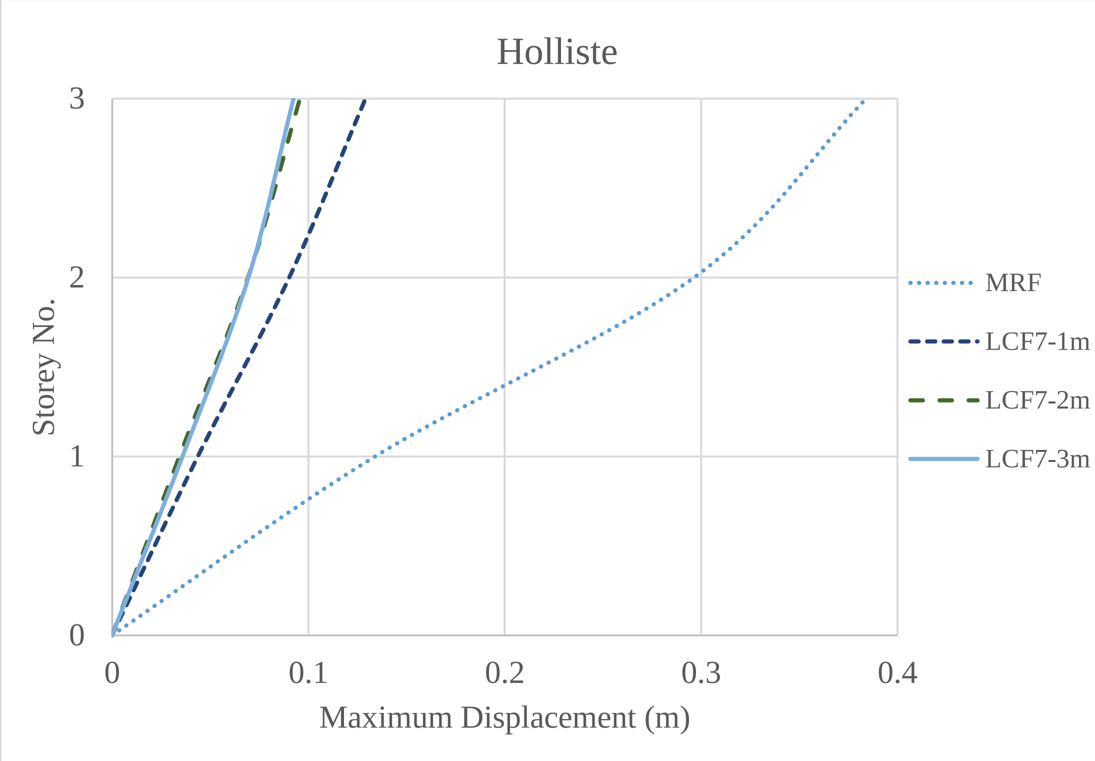

Figure 4.41 Maximum displacement demand for MRF and LCF7 with column spacing of 1, 2, and 3 m under Holliste earthquake

As an indication of the damage that can be observed in the structures, the variation of the maximum inter-story drift demand when subjected to these two earthquake accelerations were evaluated. The obtained results are given from Figure 4.42 to 4.53 in terms of the variation of maximum inter-story drift demand through the frame height. As seen from the figures, with the addition of link column frame systems, the inter-story drift demand in the frames was reduced for these earthquake accelerations. When the variation in the link beam length were considered, as observed from the graphs, the difference of the maximum inter-story drift of the LCFs having link beam length of 2 and 3 m was negligible. For instance, under the Petrolia earthquake acceleration, the LCF3 with the link beam length of 2 and 3 m had maximum inter-story drift demand of 1.99 and 1.94%, respectively. Figure 4.54 to 4.92 also show the plastic hinge formation of the structure under all earthquakes.

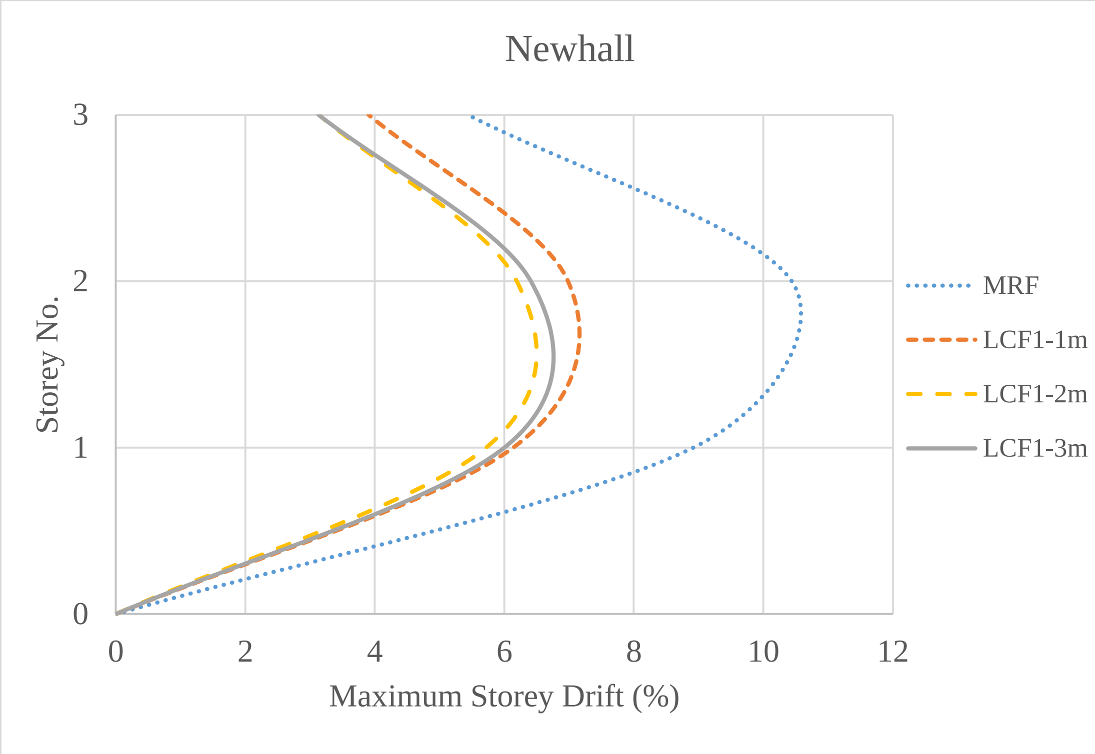

Figure 4.42 Maximum inter-story drift for MRF and LCF1 with column spacing of 1, 2, and 3 m under Newhall earthquake

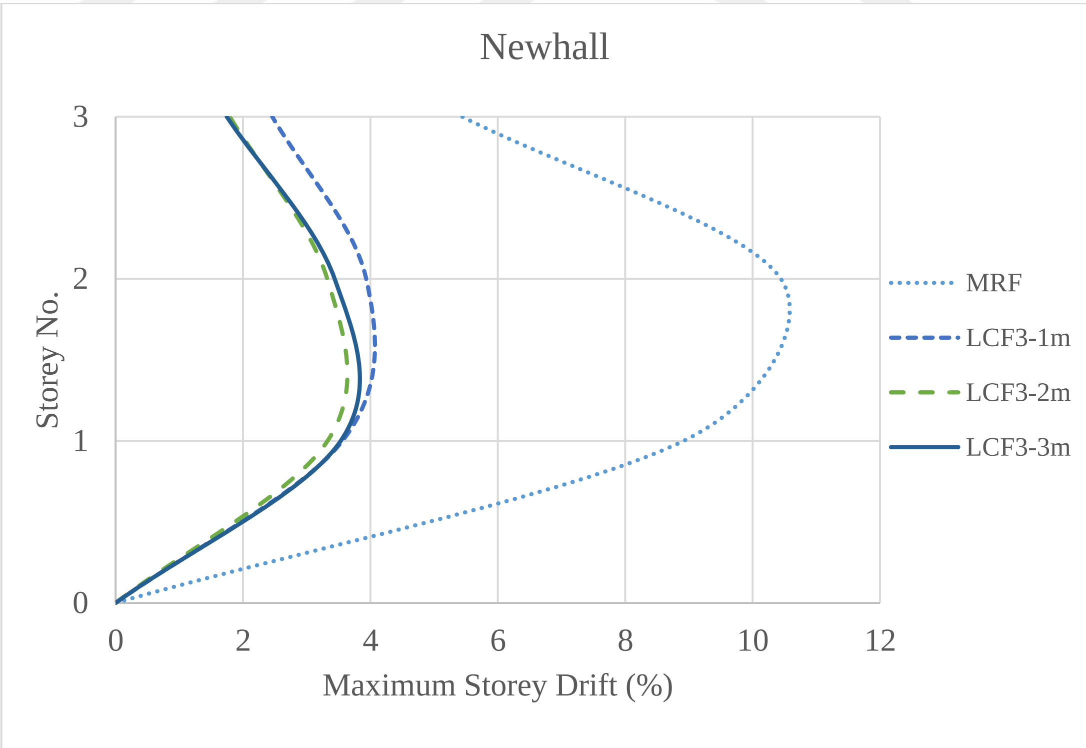

Figure 4.43 Maximum inter-story drift for MRF and LCF3 with column spacing of 1, 2, and 3 m under Newhall earthquake

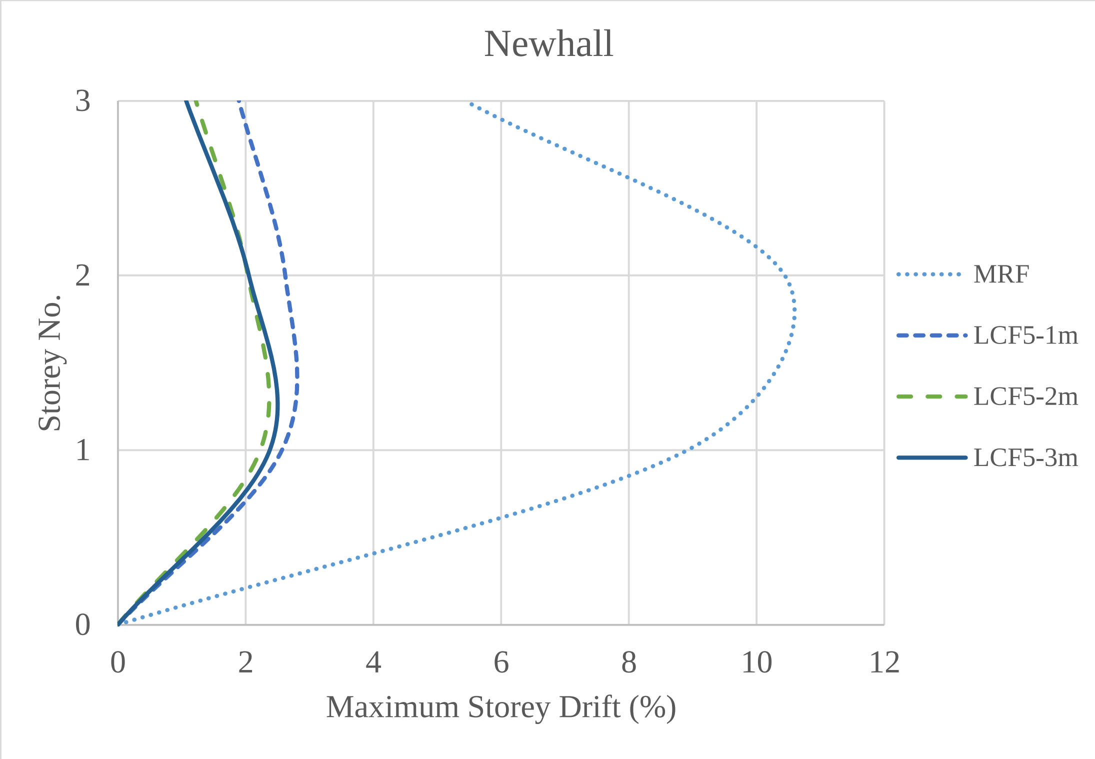

Figure 4.44 Maximum inter-story drift for MRF and LCF5 with column spacing of 1, 2, and 3 m under Newhall earthquake

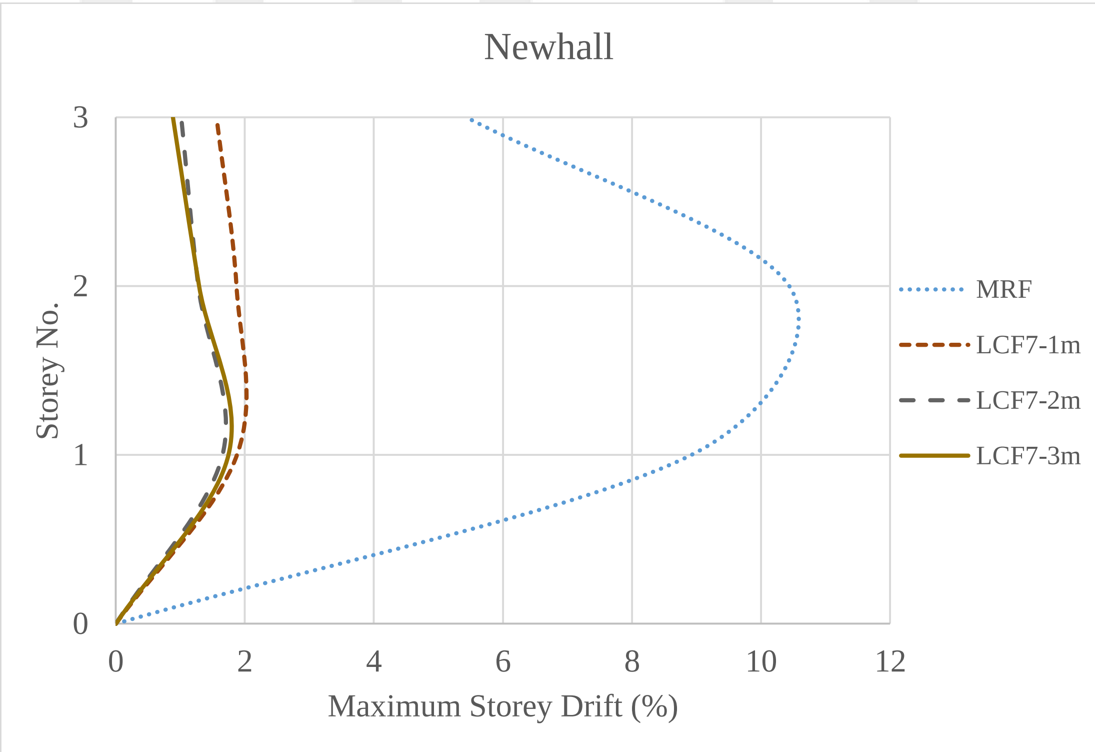

Figure 4.45 Maximum inter-story drift for MRF and LCF7 with column spacing of 1, 2, and 3 m under Newhall earthquake

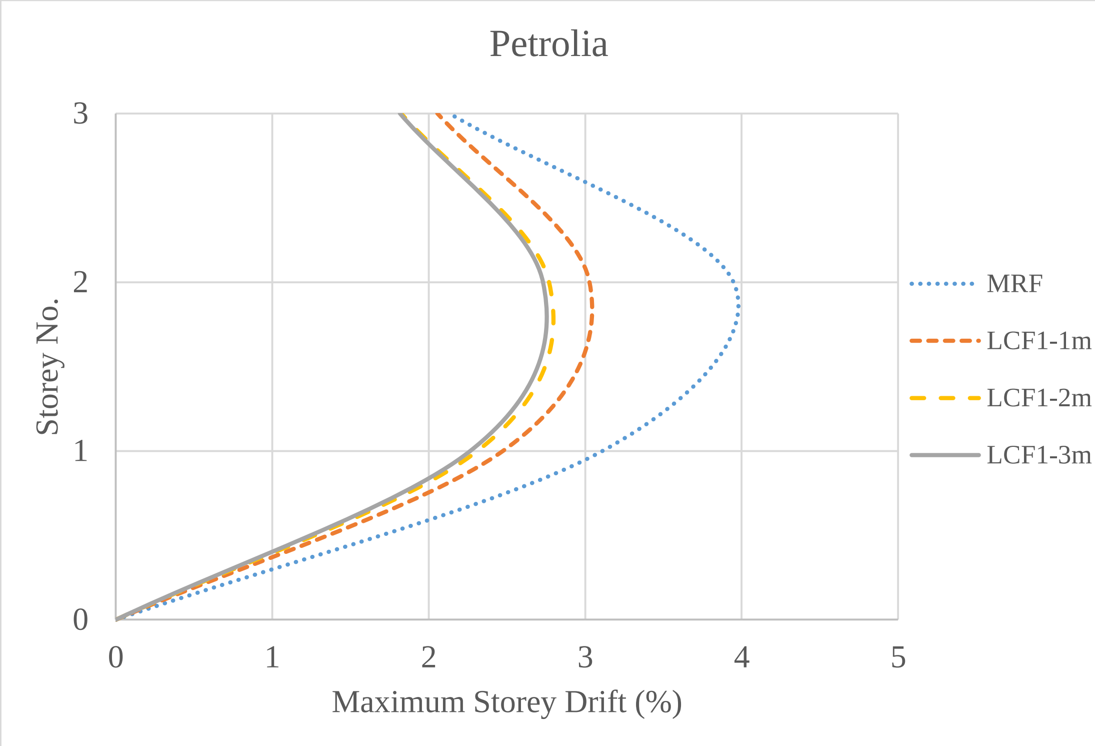

Figure 4.46 Maximum inter-story drift for MRF and LCF1 with column spacing of 1, 2, and 3 m under Petrolia earthquake

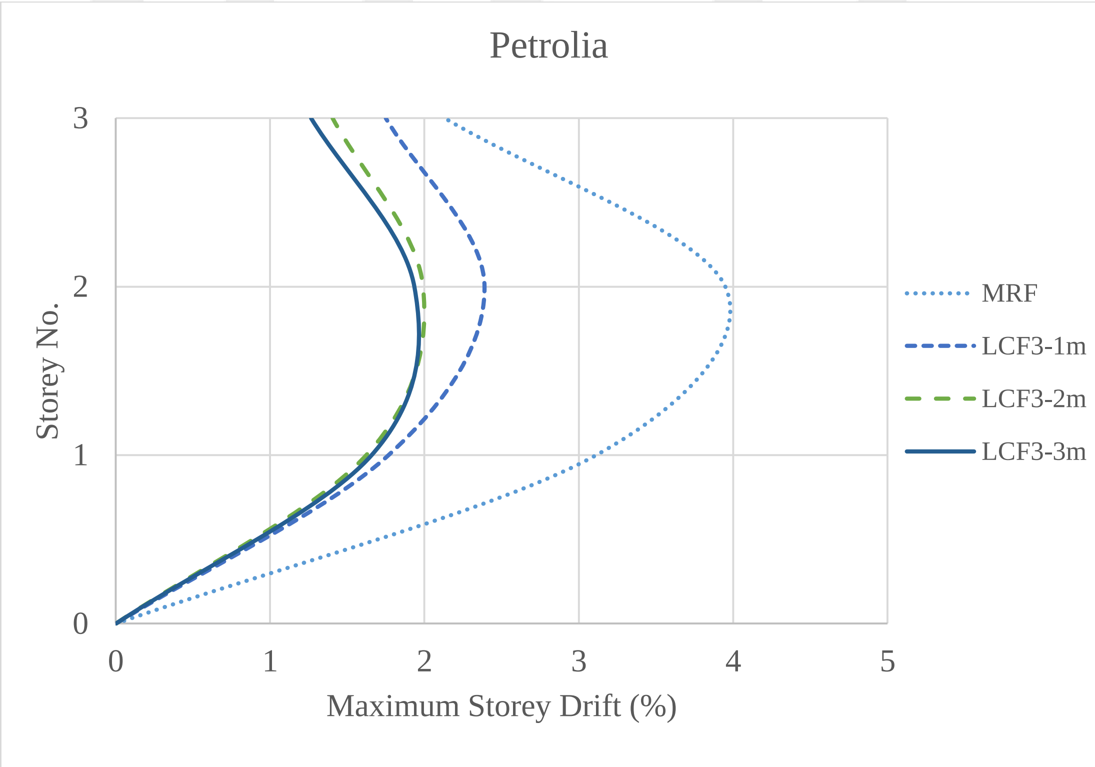

Figure 4.47 Maximum inter-story drift for MRF and LCF3 with column spacing of 1, 2, and 3 m under Petrolia earthquake

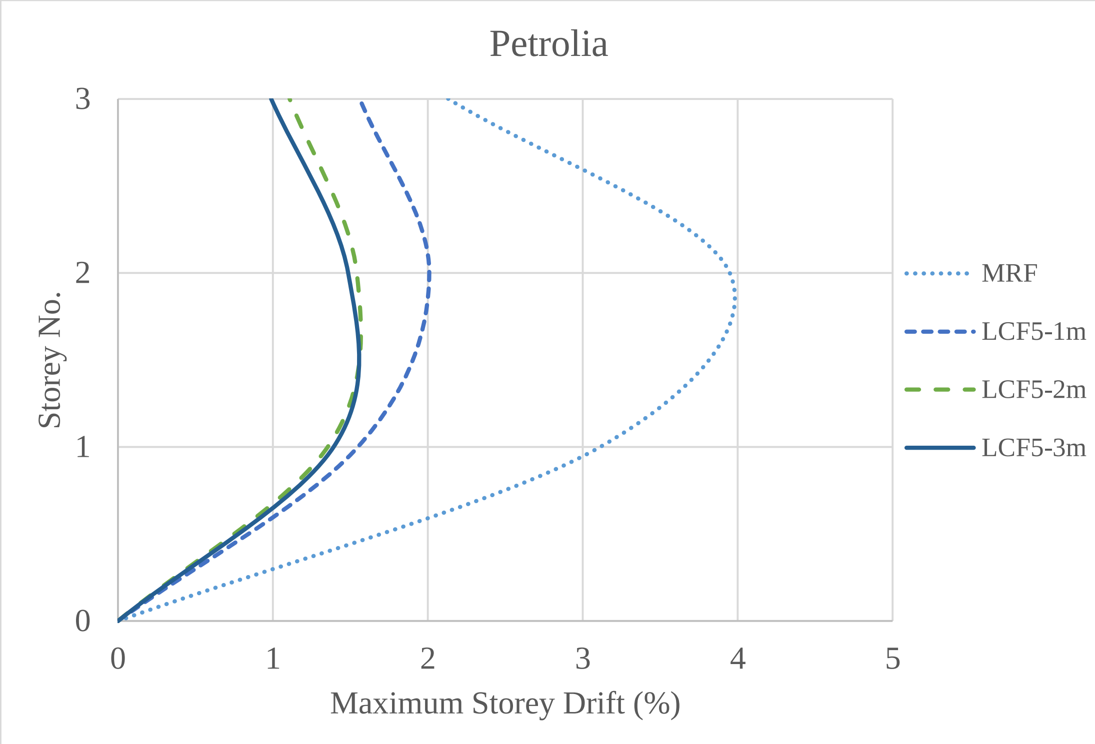

Figure 4.48 Maximum inter-story drift for MRF and LCF5 with column spacing of 1, 2, and 3 m under Petrolia earthquake

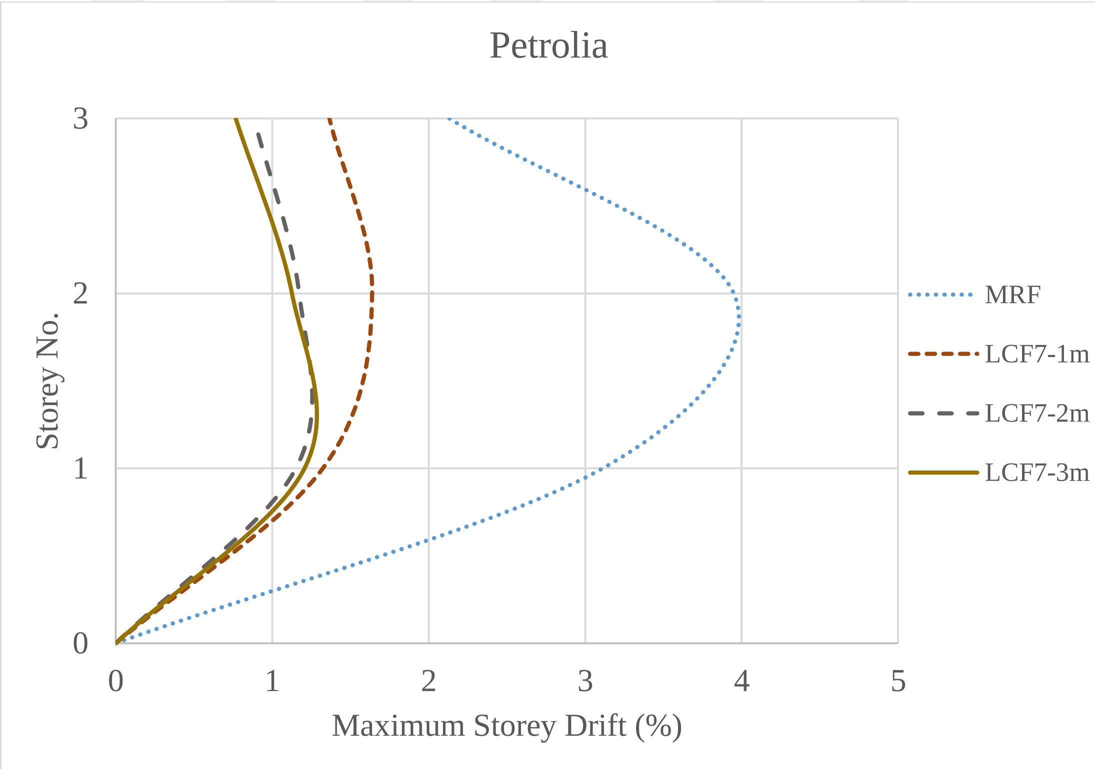

Figure 4.49 Maximum inter-story drift for MRF and LCF7 with column spacing of 1, 2, and 3 m under Petrolia earthquake

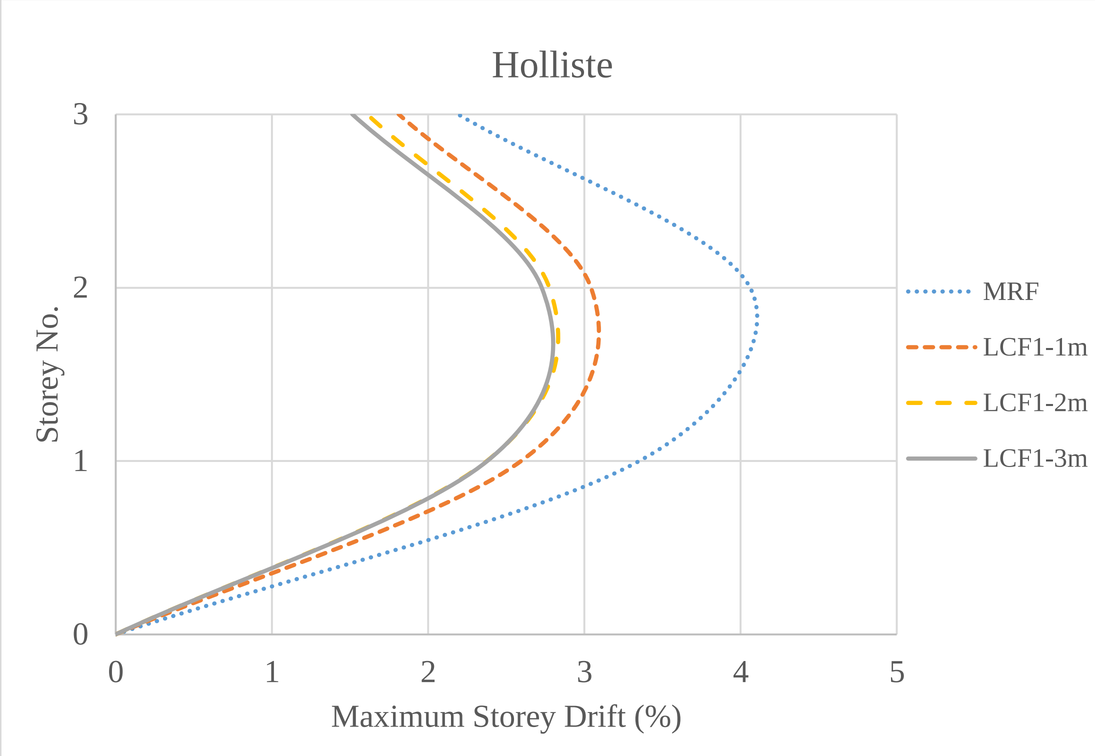

Figure 4.50 Maximum inter-story drift for MRF and LCF1 with column spacing of 1, 2, and 3 m under Holliste earthquake

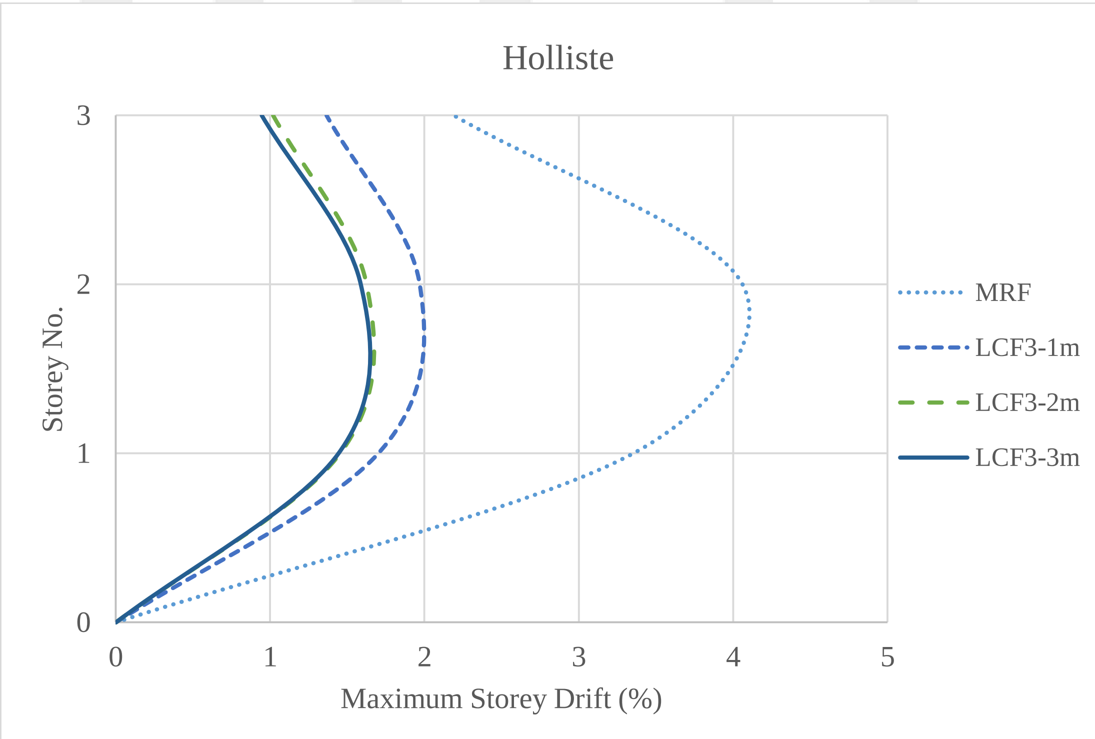

Figure 4.51 Maximum inter-story drift for MRF and LCF3 with column spacing of 1, 2, and 3 m under Holliste earthquake

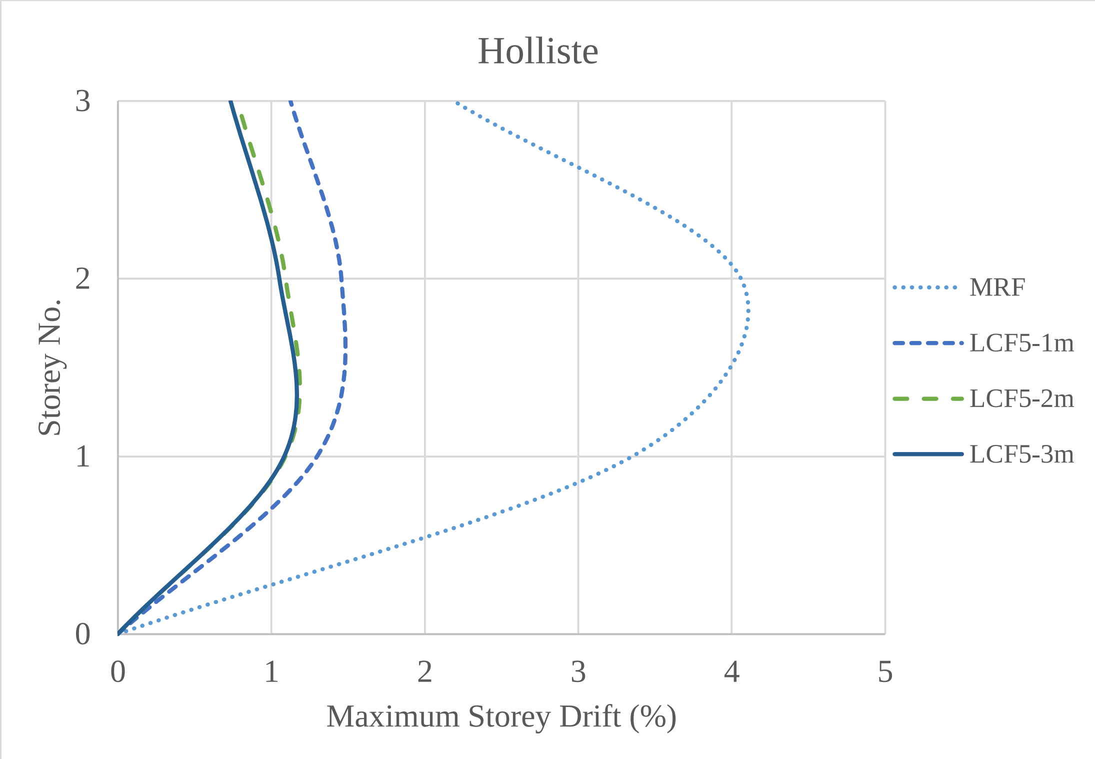

Figure 4.52 Maximum inter-story drift for MRF and LCF5 with column spacing of 1, 2, and 3 m under Holliste earthquake

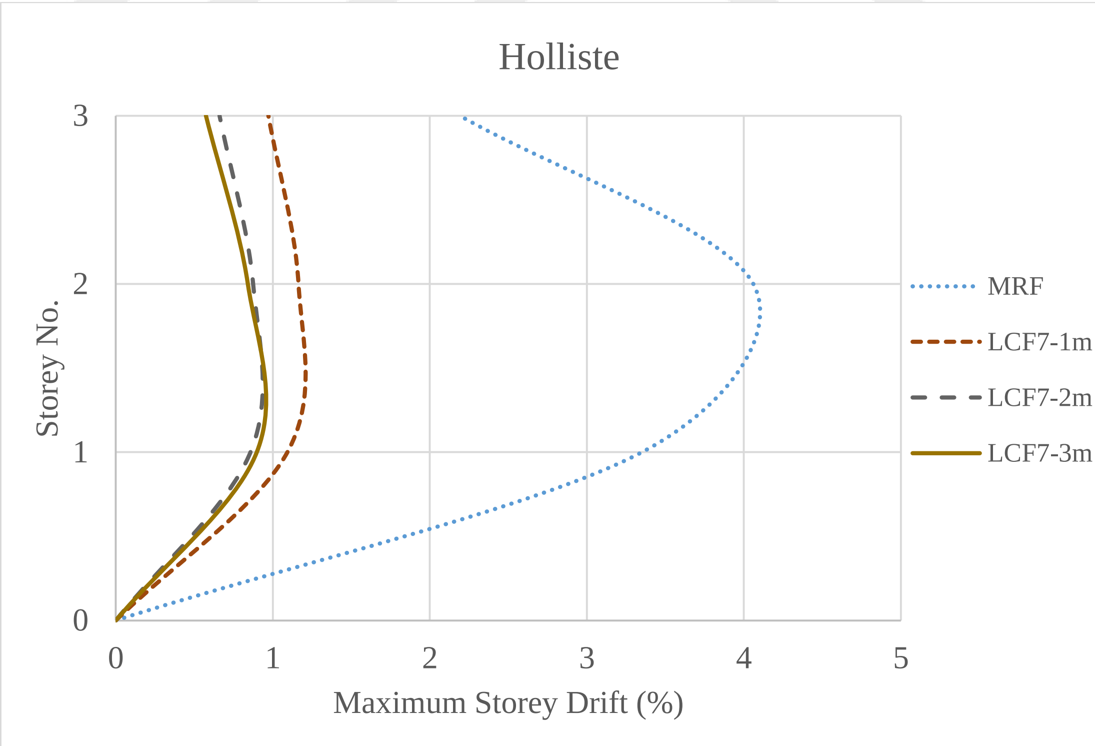

Figure 4.53 Maximum inter-story drift for MRF and LCF7 with column spacing of 1, 2, and 3 m under Holliste earthquake

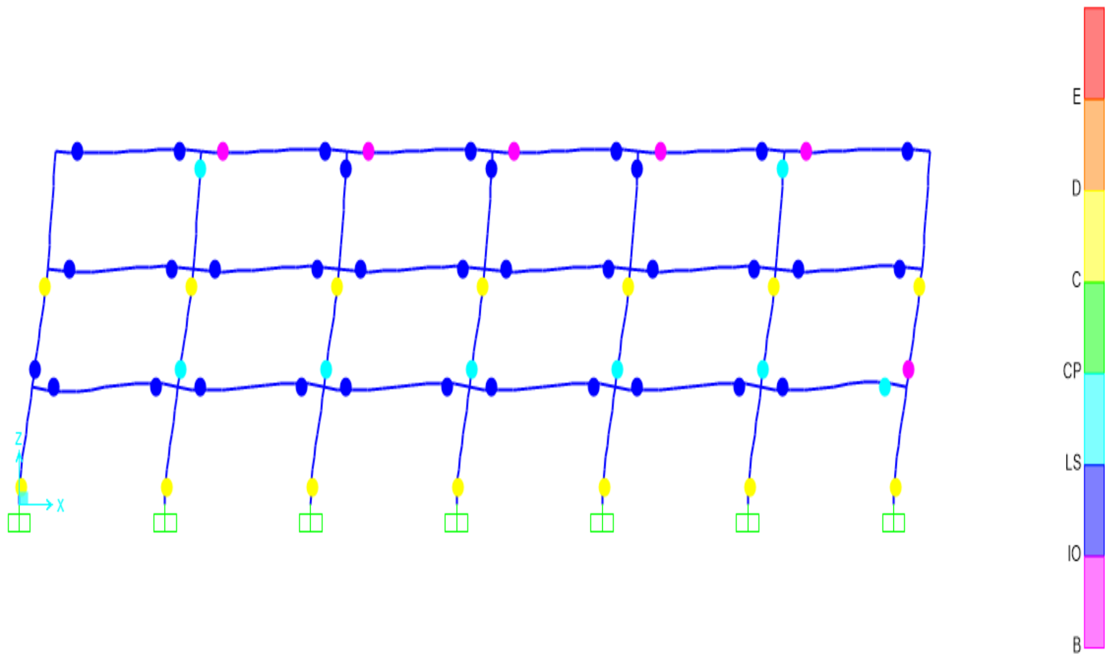

Figure 4.54 Plastic hinge distribution at the final stage of MRF under effect of Newhall earthquake

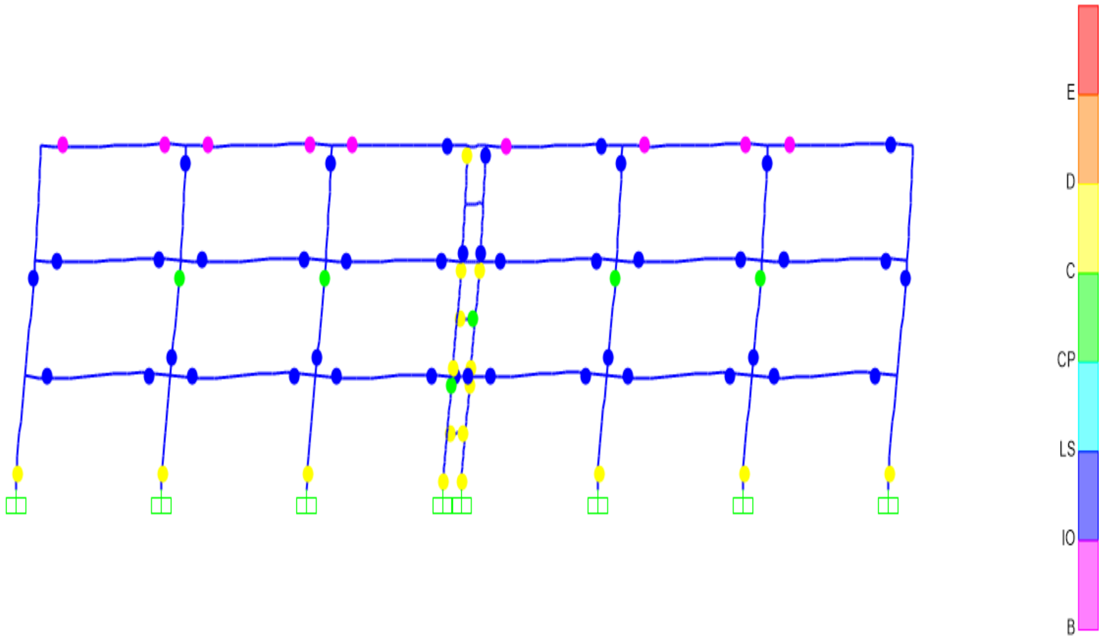

Figure 4.55 Plastic hinge distribution at the final stage of LCF1-1m under effect of Newhall earthquake

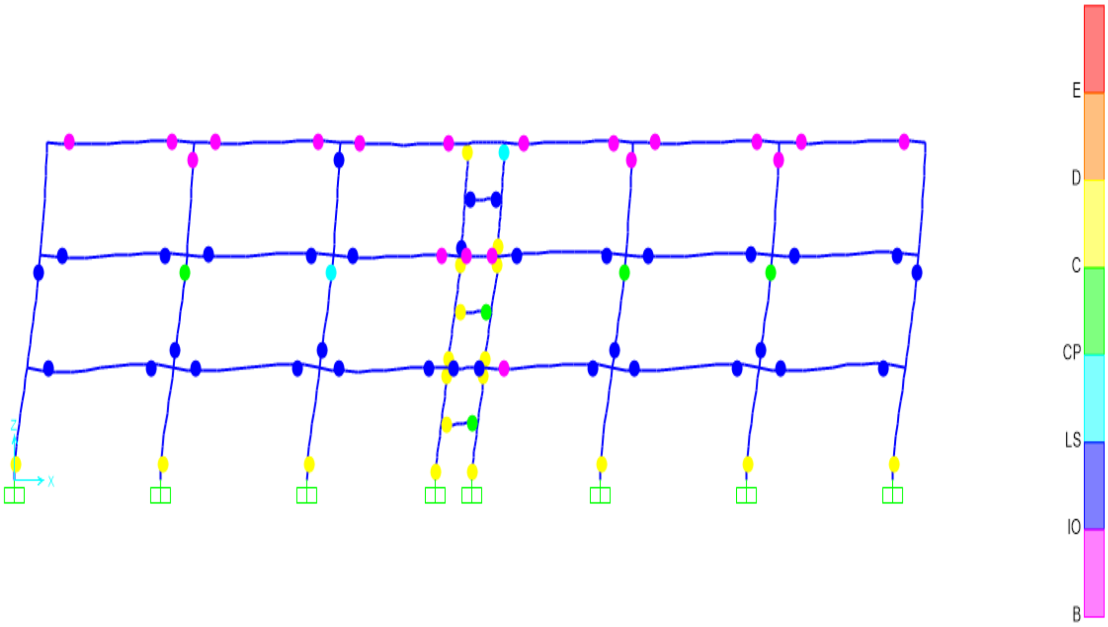

Figure 4.56 Plastic hinge distribution at the final stage of LCF1-2m under effect of Newhall earthquake

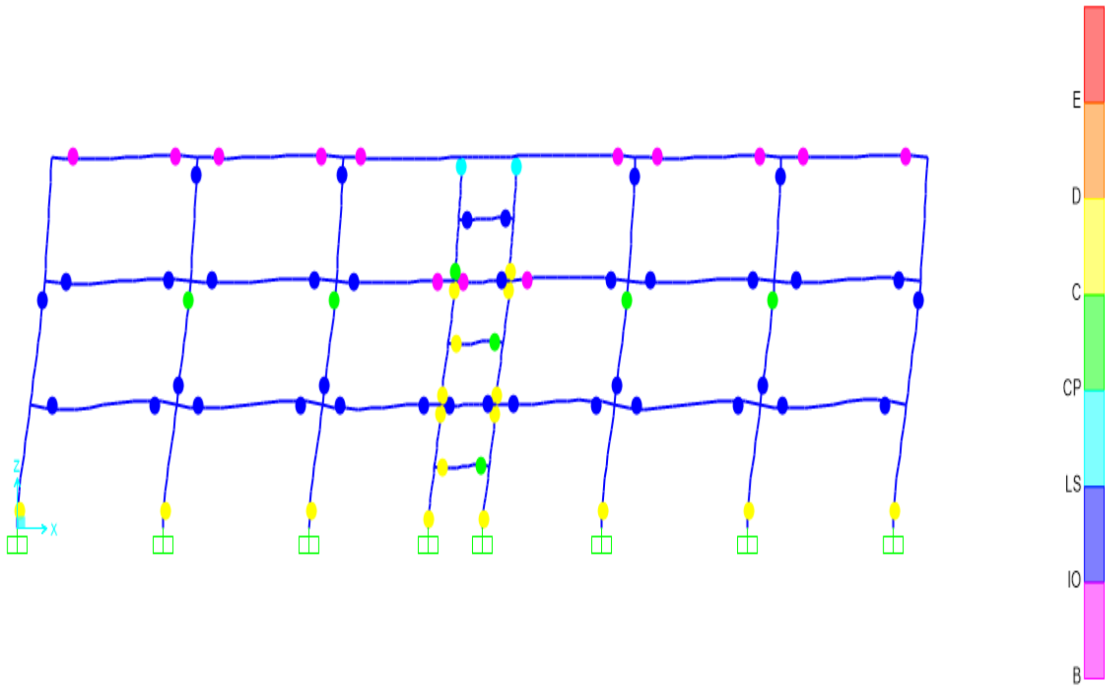

Figure 4.57 Plastic hinge distribution at the final stage of LCF1-3m under effect of Newhall earthquake

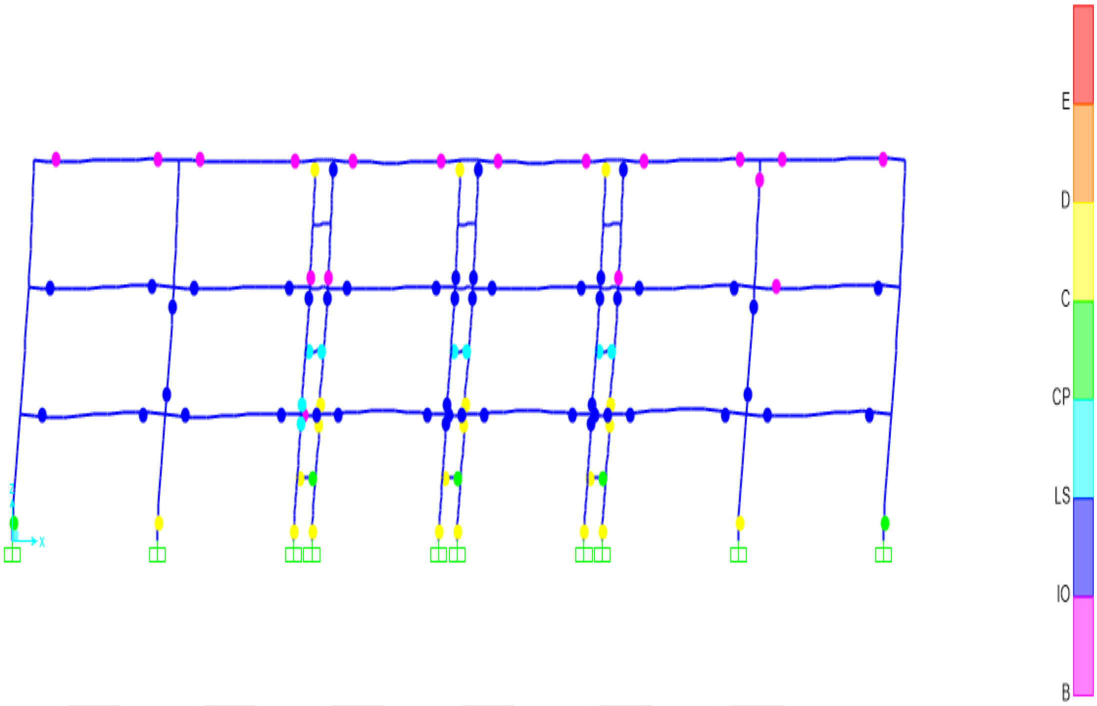

Figure 4.58 Plastic hinge distribution at the final stage of LCF3-1m under effect of Newhall earthquake

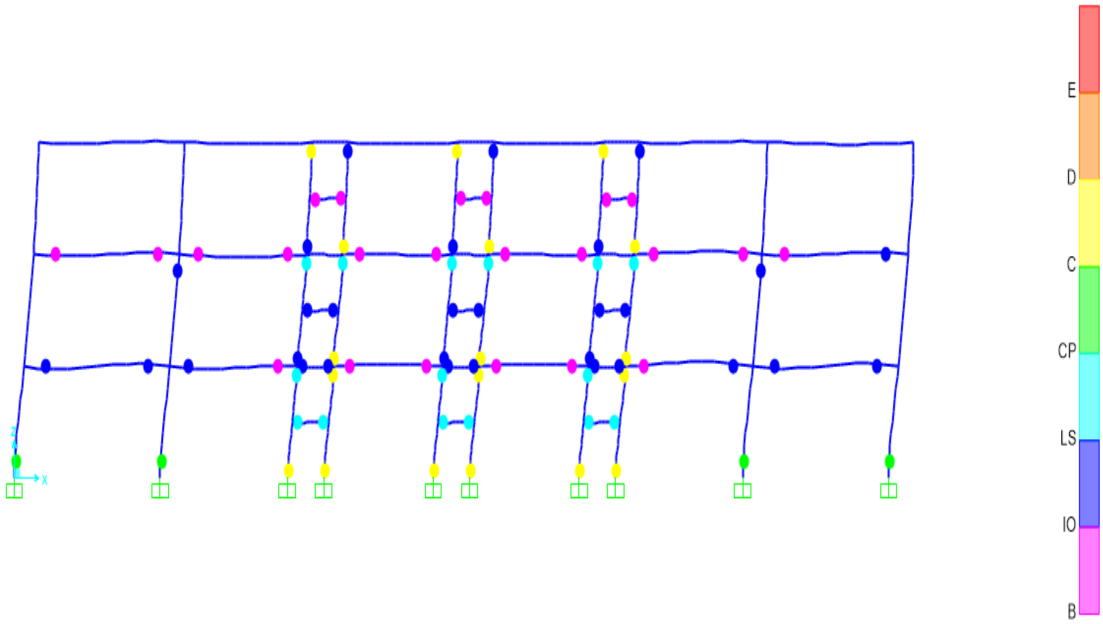

Figure 4.59 Plastic hinge distribution at the final stage of LCF3-2m under effect of Newhall earthquake

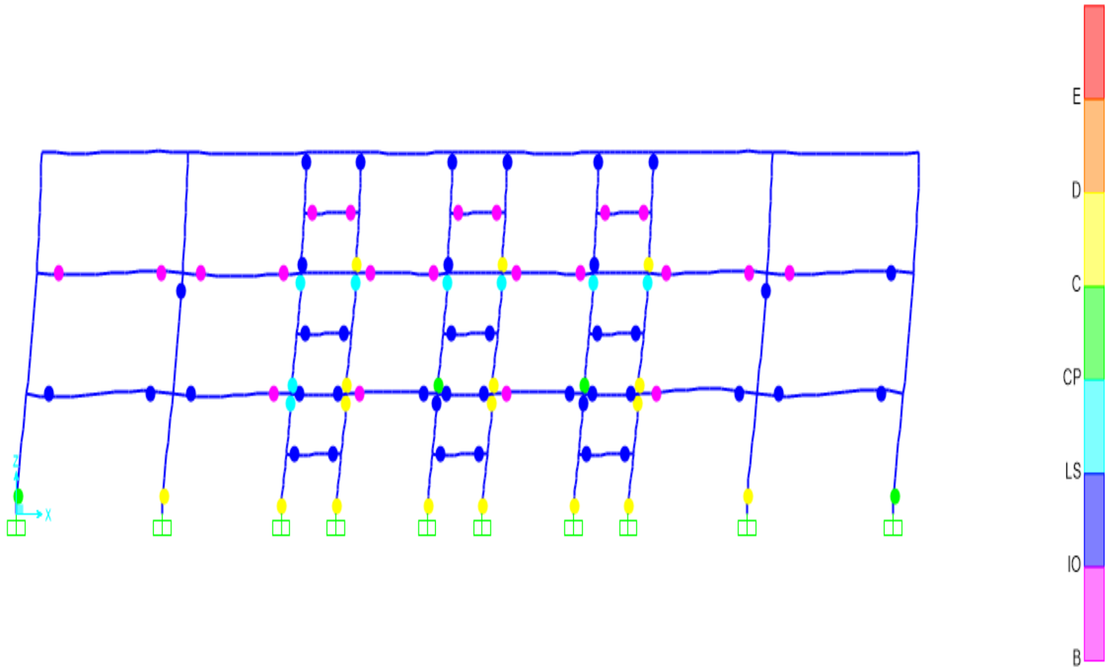

Figure 4.60 Plastic hinge distribution at the final stage of LCF3-3m under effect of Newhall earthquake

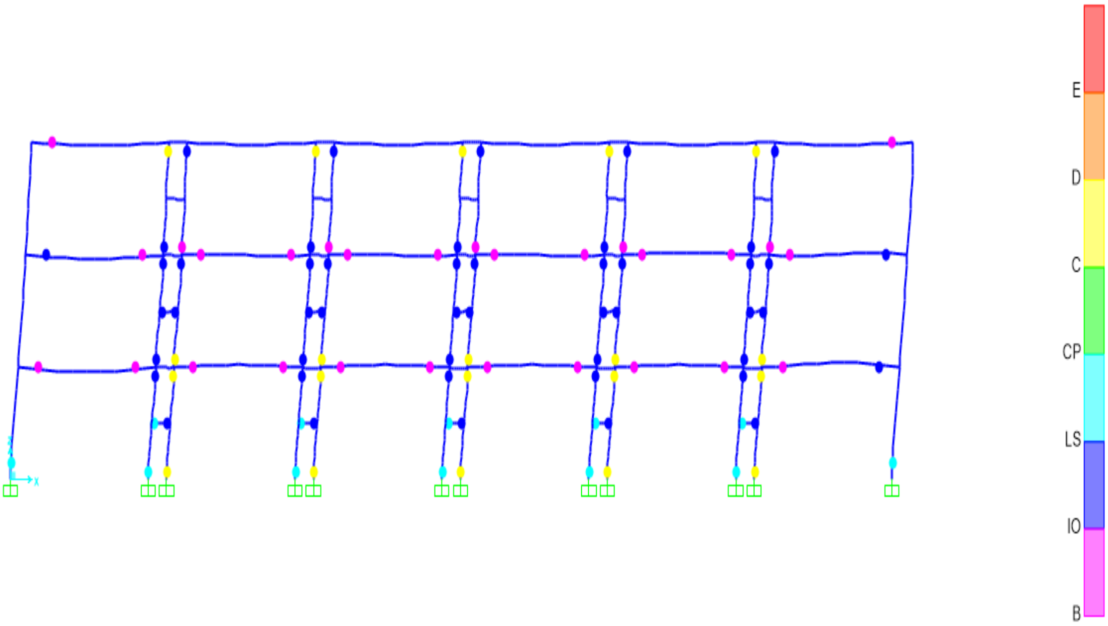

Figure 4.61 Plastic hinge distribution at the final stage of LCF5-1m under effect of Newhall earthquake

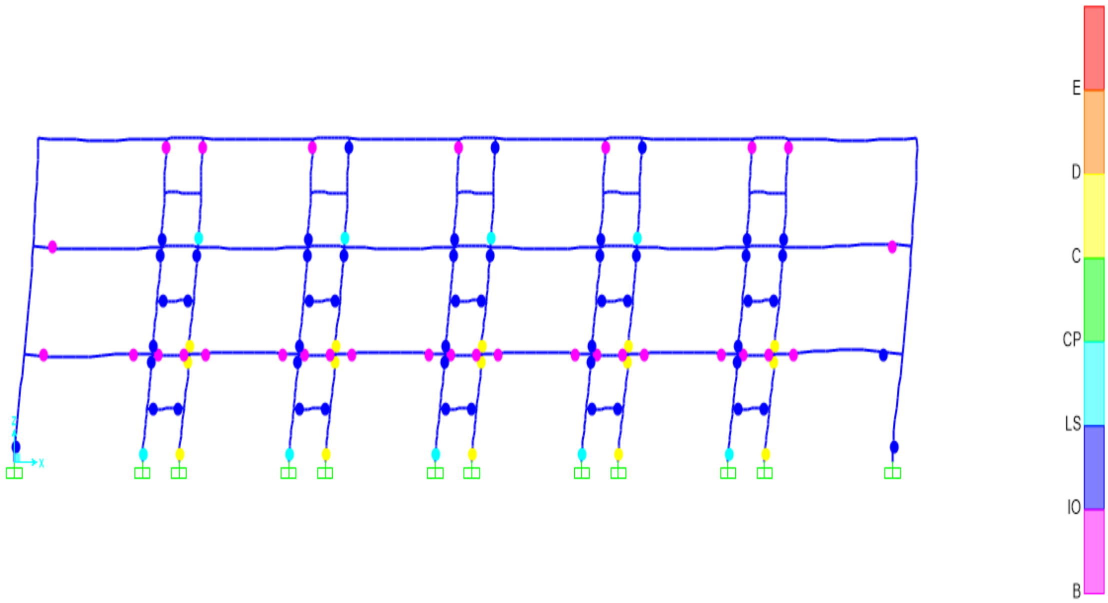

Figure 4.62 Plastic hinge distribution at the final stage of LCF5-2m under effect of Newhall earthquake

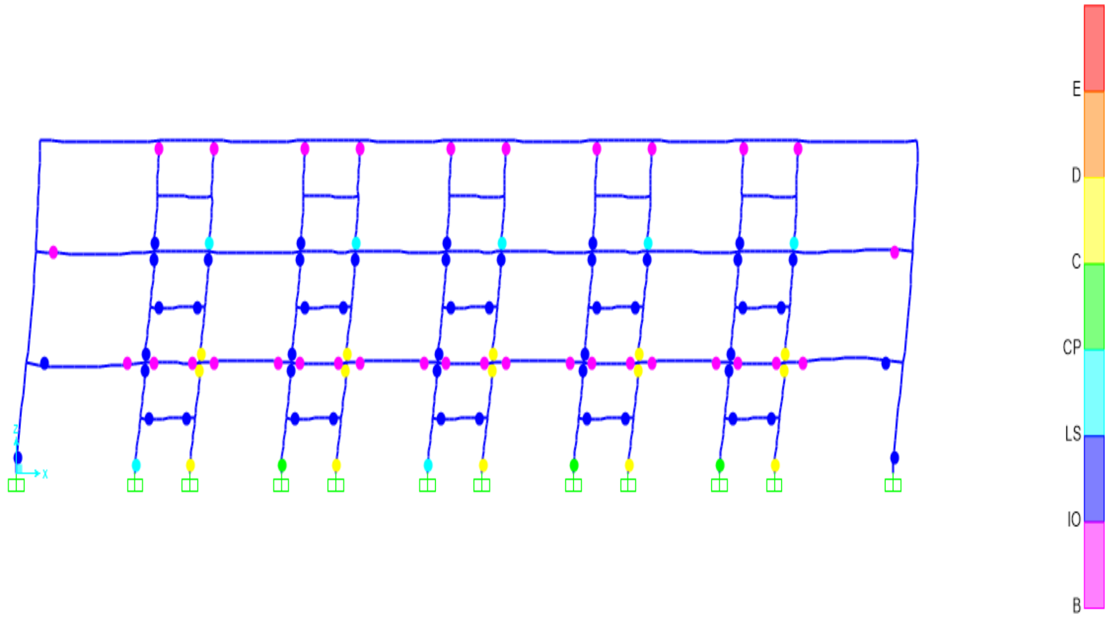

Figure 4.63 Plastic hinge distribution at the final stage of LCF5-3m under effect of Newhall earthquake

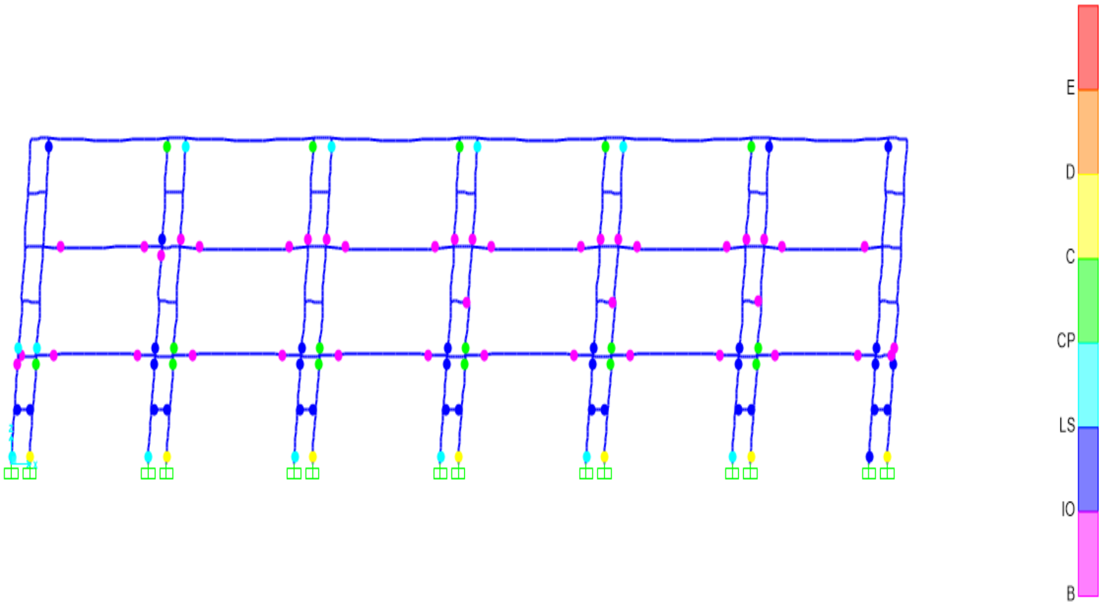

Figure 4.64 Plastic hinge distribution at the final stage of LCF7-1m under effect of Newhall earthquake

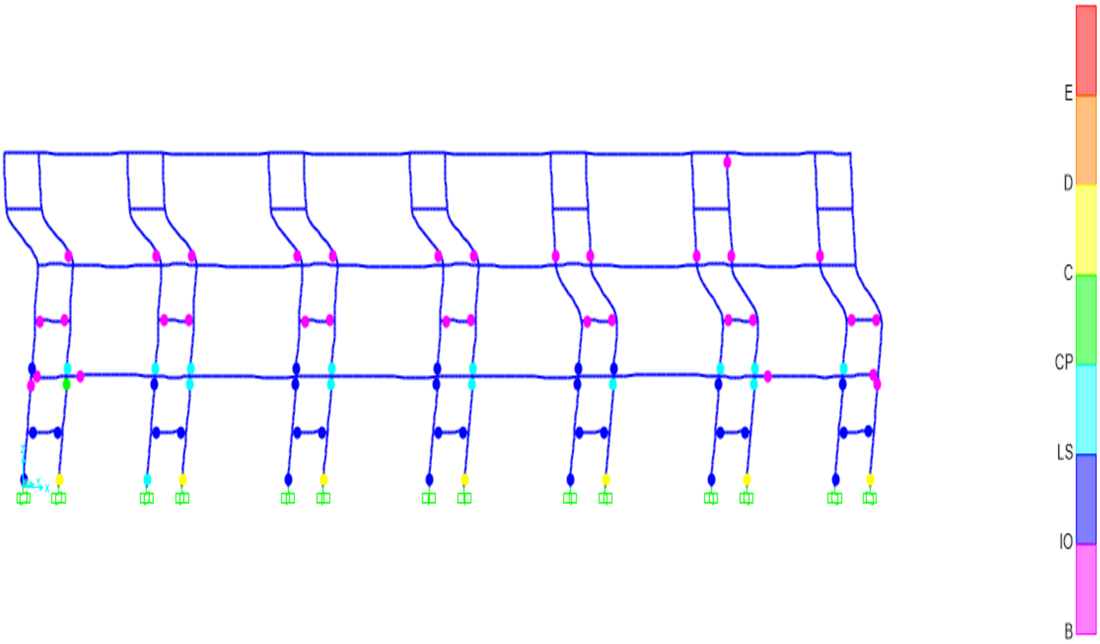

Figure 4.65 Plastic hinge distribution at the final stage of LCF7-2m under effect of Newhall earthquake

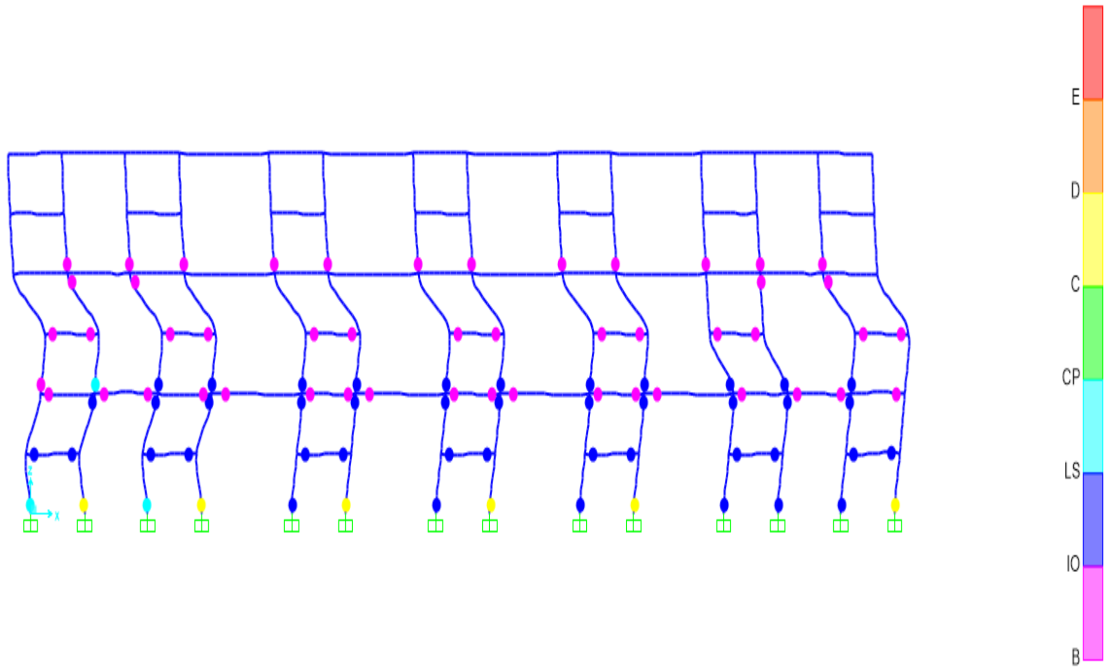

Figure 4.66 Plastic hinge distribution at the final stage of LCF7-3m under effect of Newhall earthquake

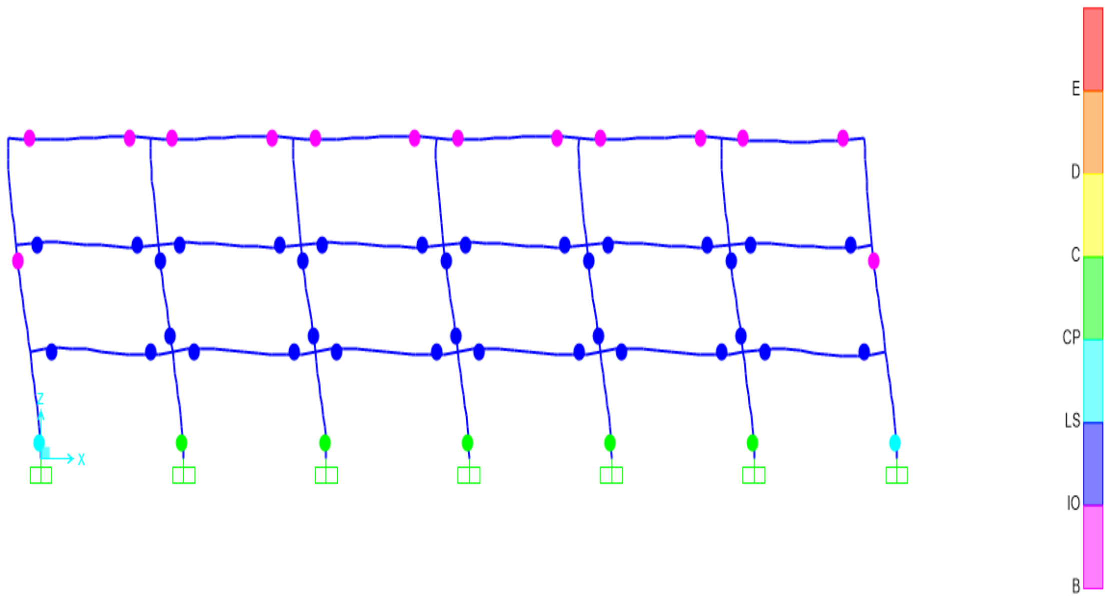

Figure 4.67 Plastic hinge distribution at the final stage of MRF under effect of Petrolia earthquake

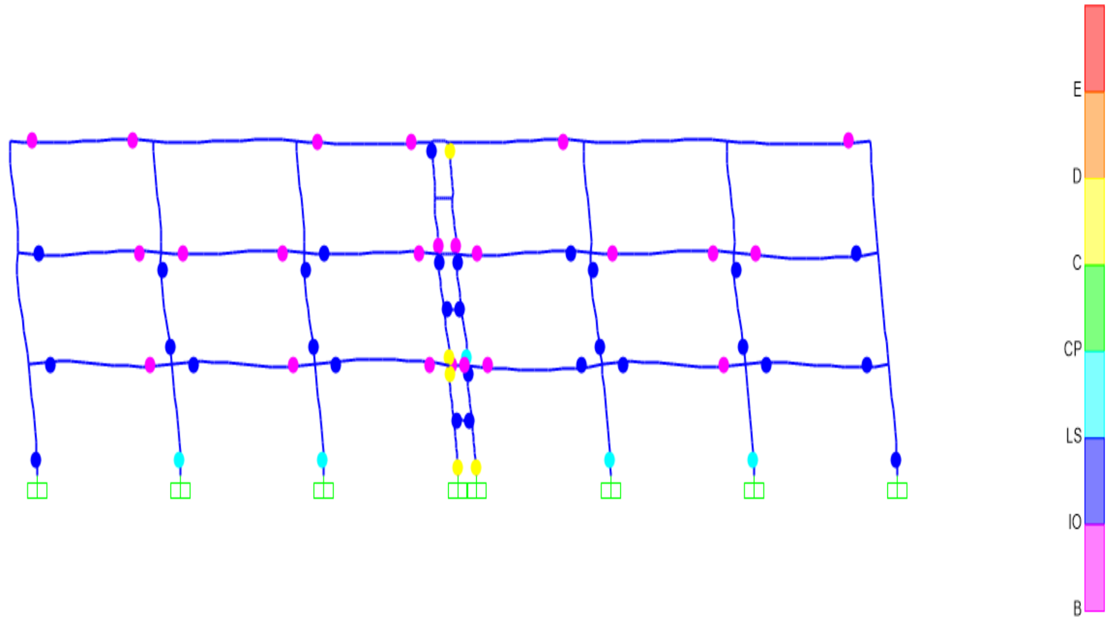

Figure 4.68 Plastic hinge distribution at the final stage of LCF1-1m under effect of Petrolia earthquake

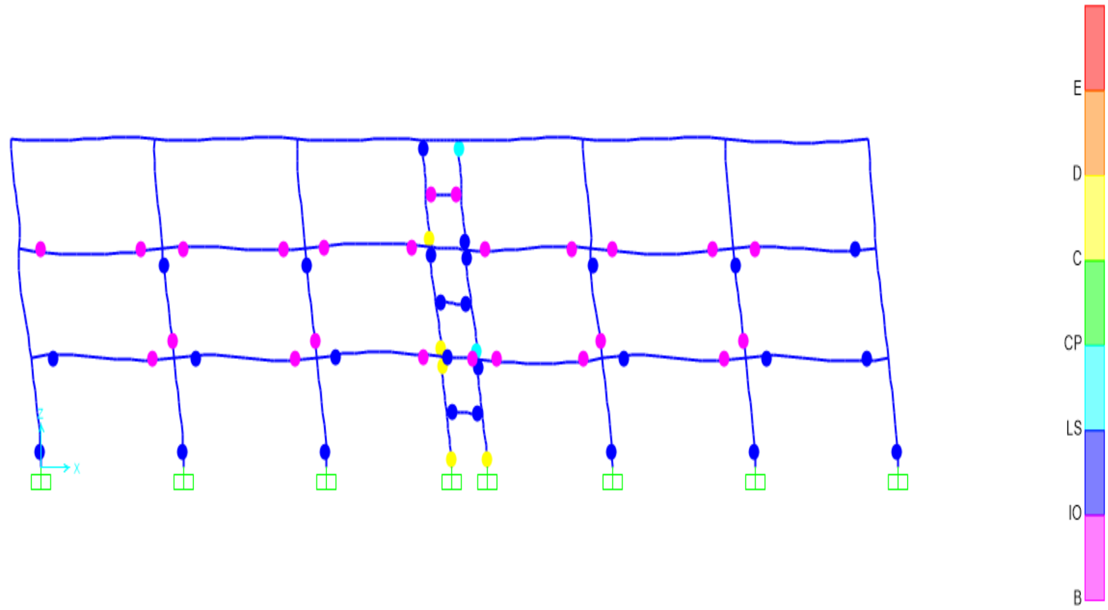

Figure 4.69 Plastic hinge distribution at the final stage of LCF1-2m under effect of Petrolia earthquake

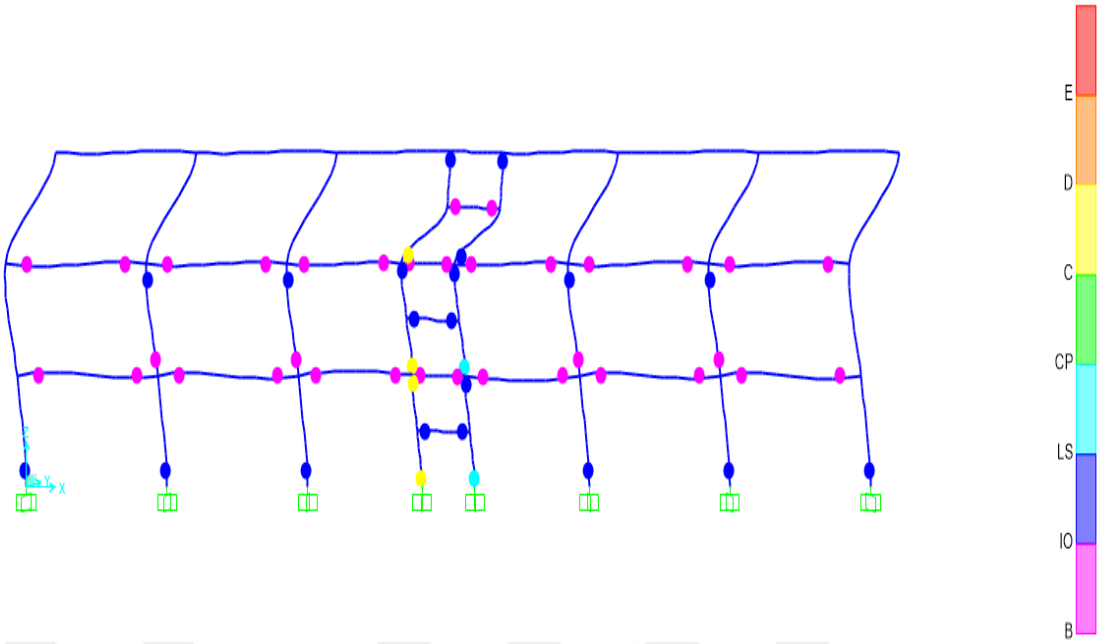

Figure 4.70 Plastic hinge distribution at the final stage of LCF1-3m under effect of Petrolia earthquake

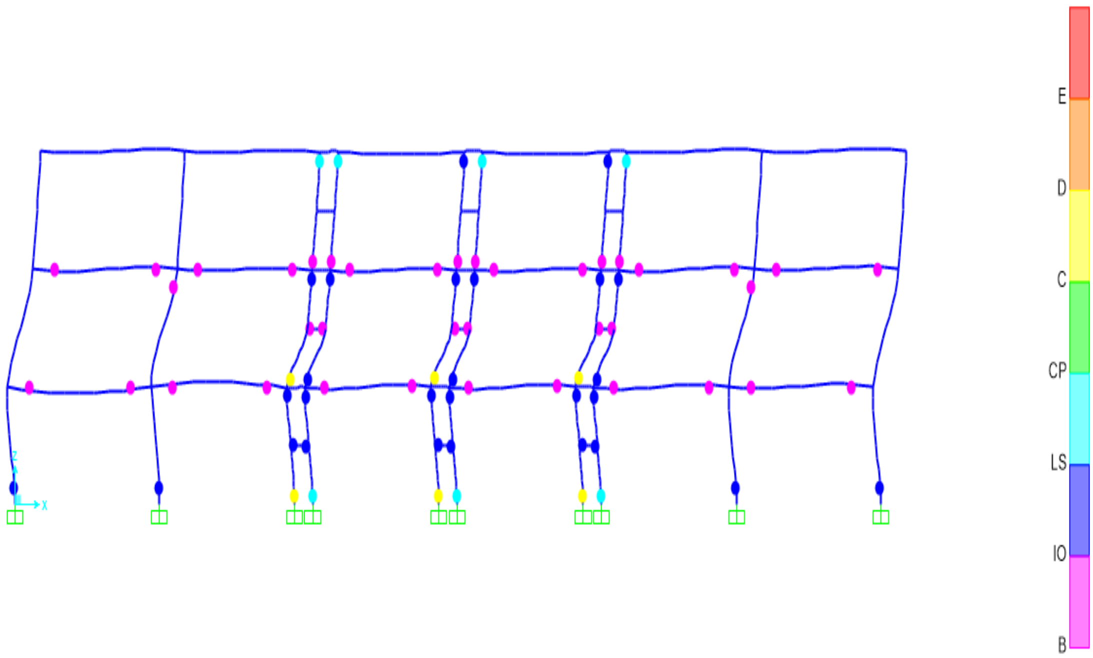

Figure 4.71 Plastic hinge distribution at the final stage of LCF3-1m under effect of Petrolia earthquake

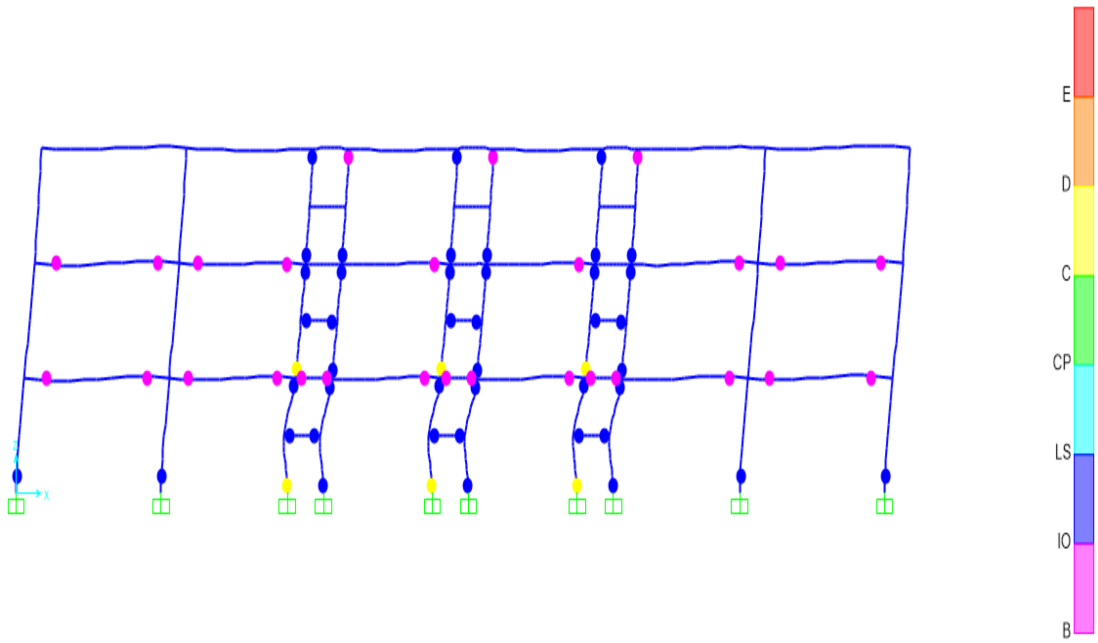

Figure 4.72 Plastic hinge distribution at the final stage of LCF3-2m under effect of Petrolia earthquake

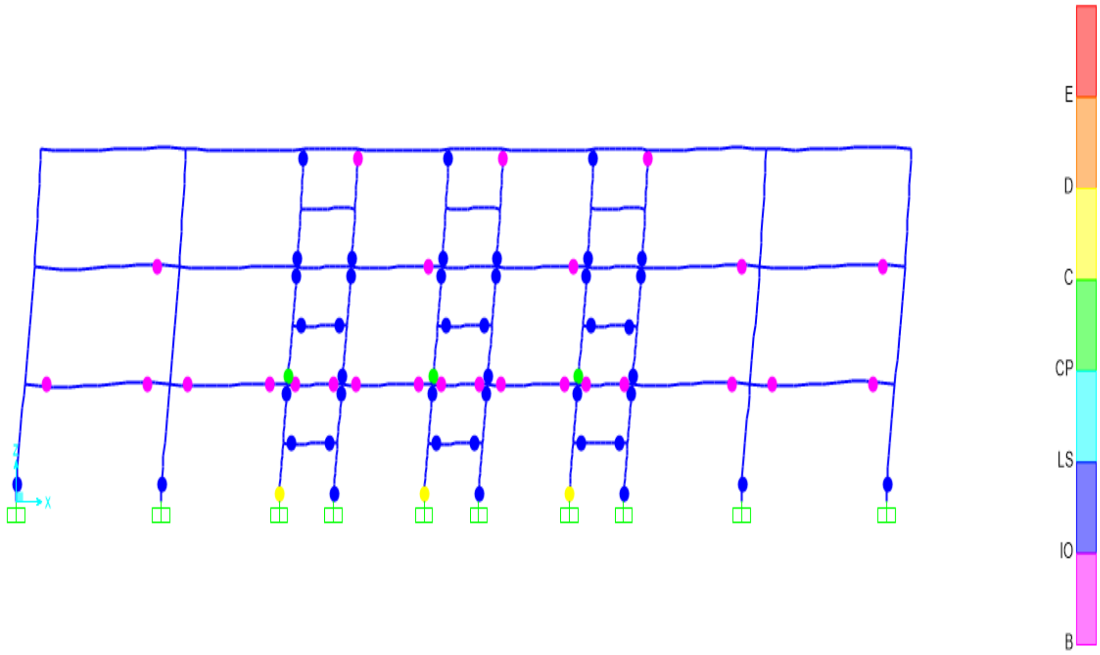

Figure 4.73 Plastic hinge distribution at the final stage of LCF3-3m under effect of Petrolia earthquake

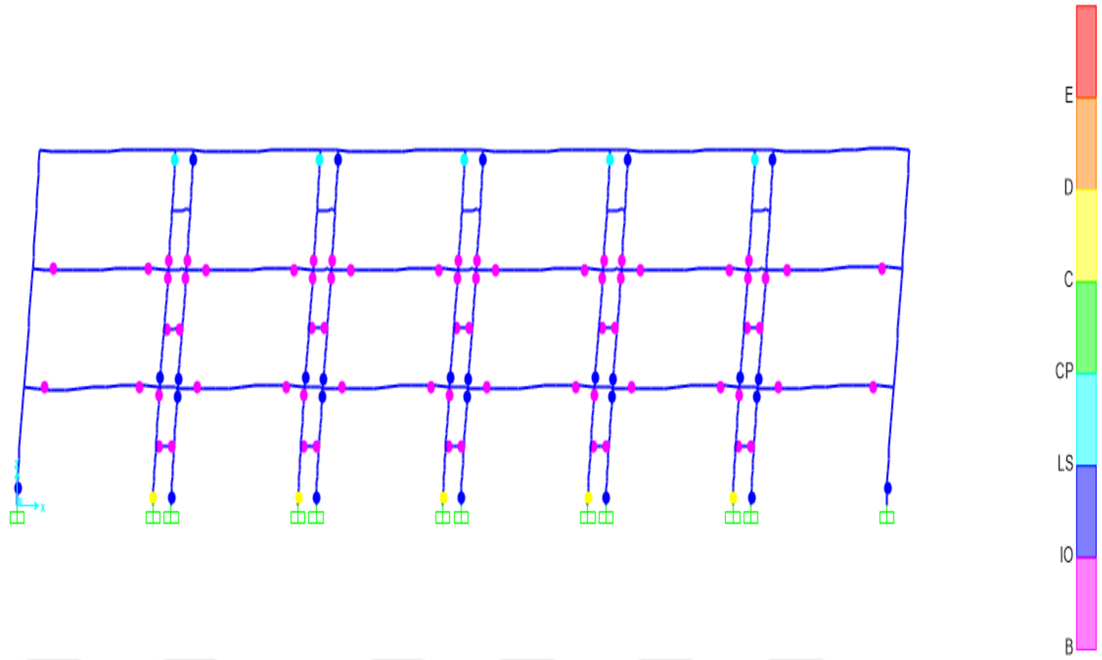

Figure 4.74 Plastic hinge distribution at the final stage of LCF5-1m under effect of Petrolia earthquake

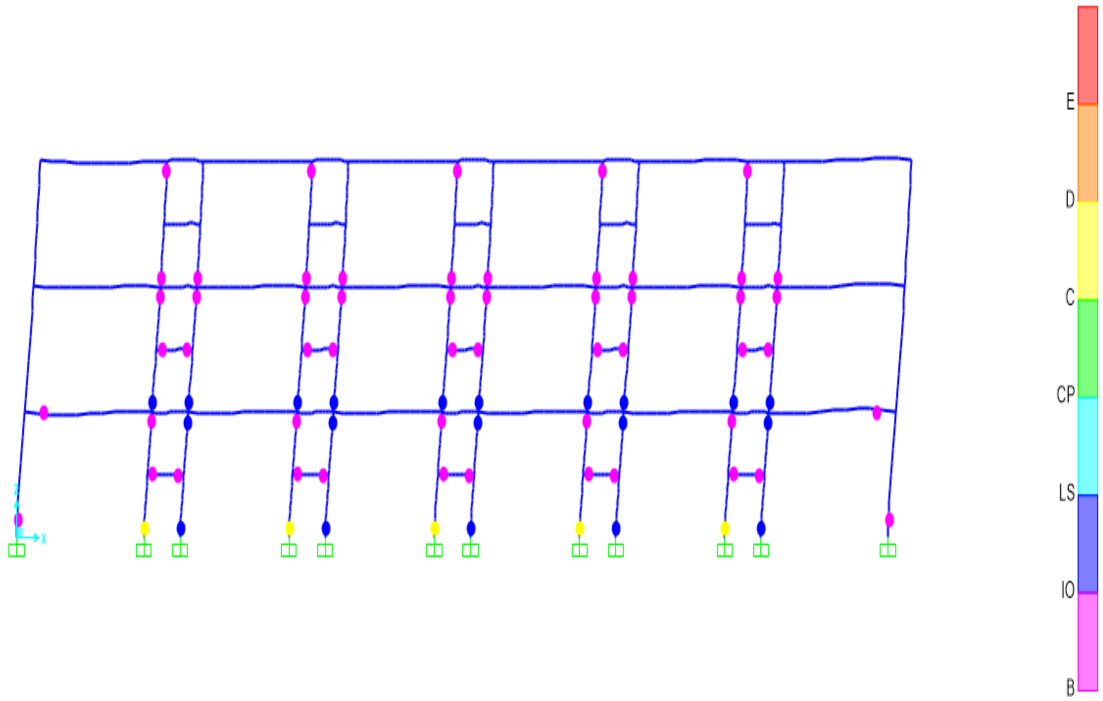

Figure 4.75 Plastic hinge distribution at the final stage of LCF5-2m under effect of Petrolia earthquake

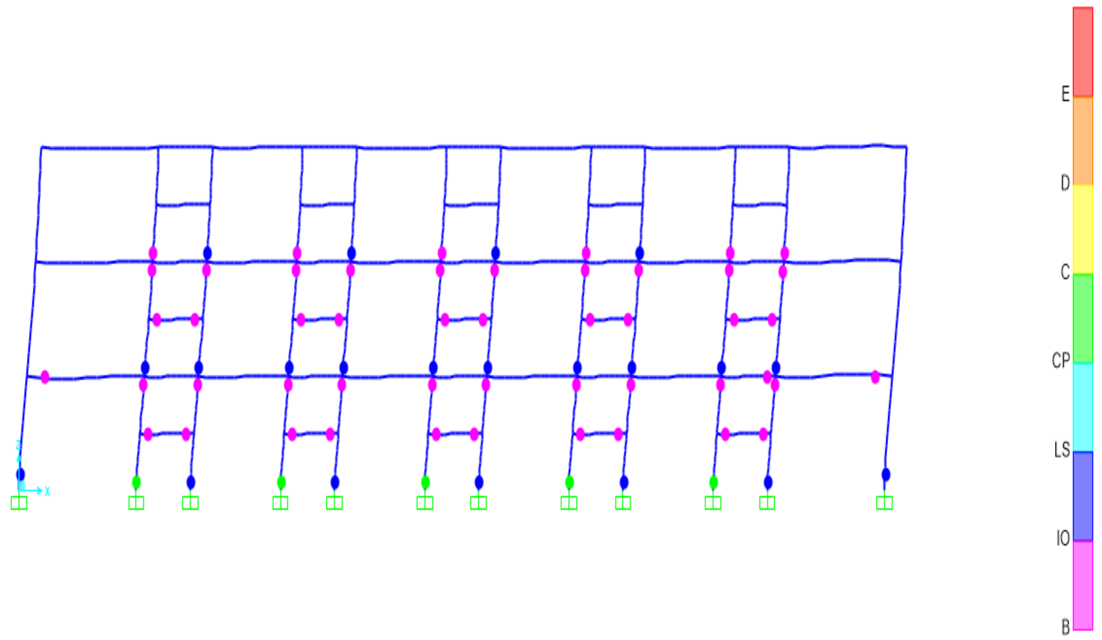

Figure 4.76 Plastic hinge distribution at the final stage of LCF5-3m under effect of Petrolia earthquake

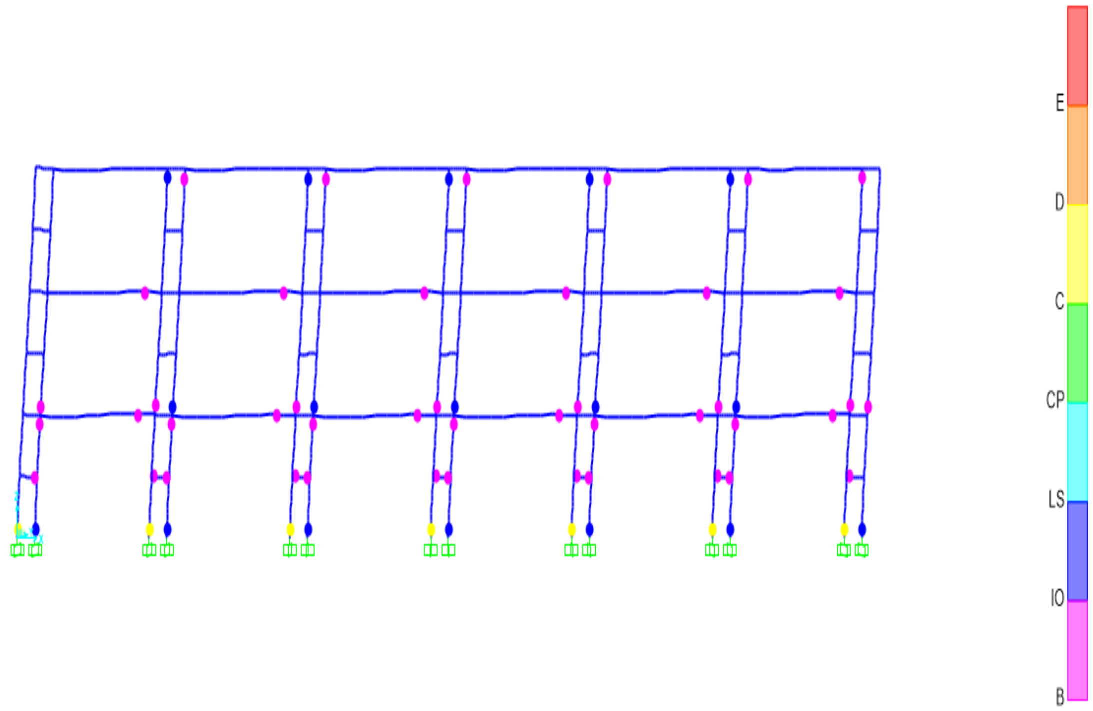

Figure 4.77 Plastic hinge distribution at the final stage of LCF7-1m under effect of Petrolia earthquake

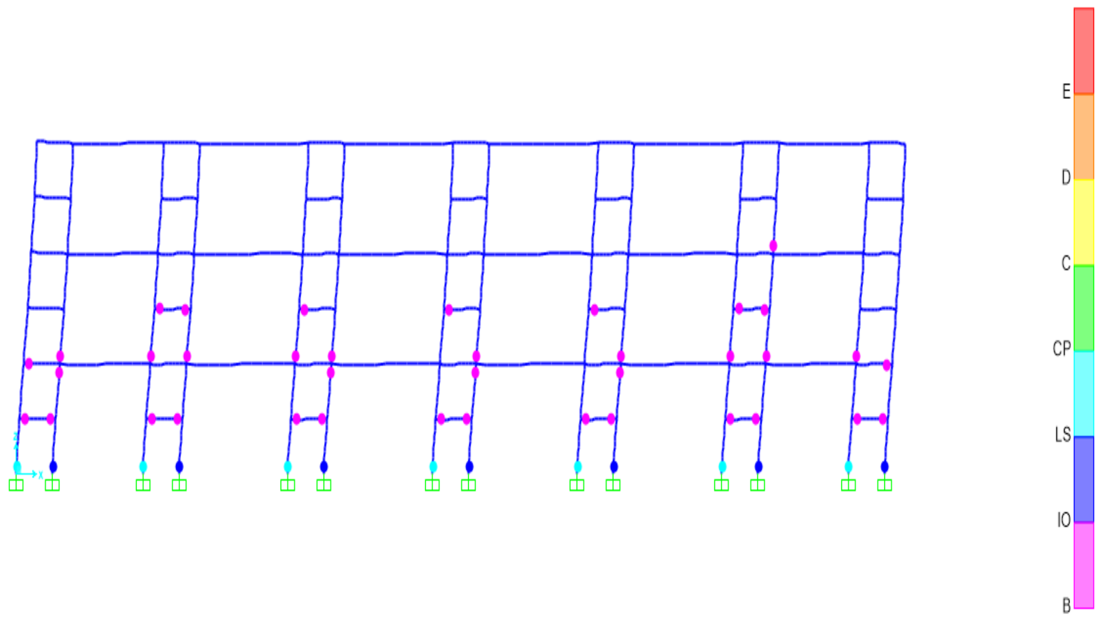

Figure 4.78 Plastic hinge distribution at the final stage of LCF7-2m under effect of Petrolia earthquake

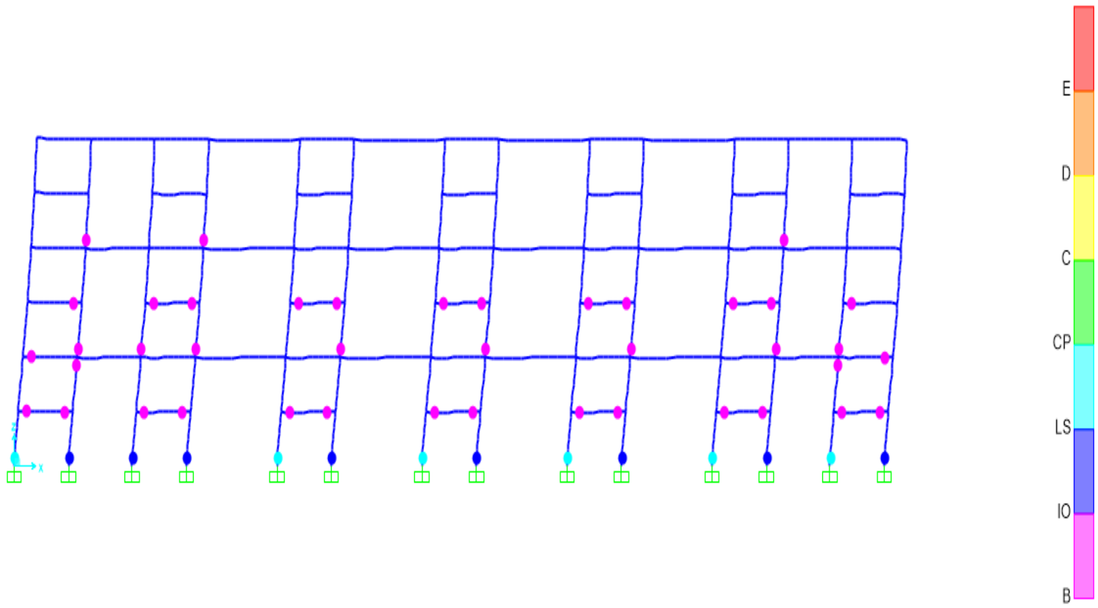

Figure 4.79 Plastic hinge distribution at the final stage of LCF7-3m under effect of Petrolia earthquake

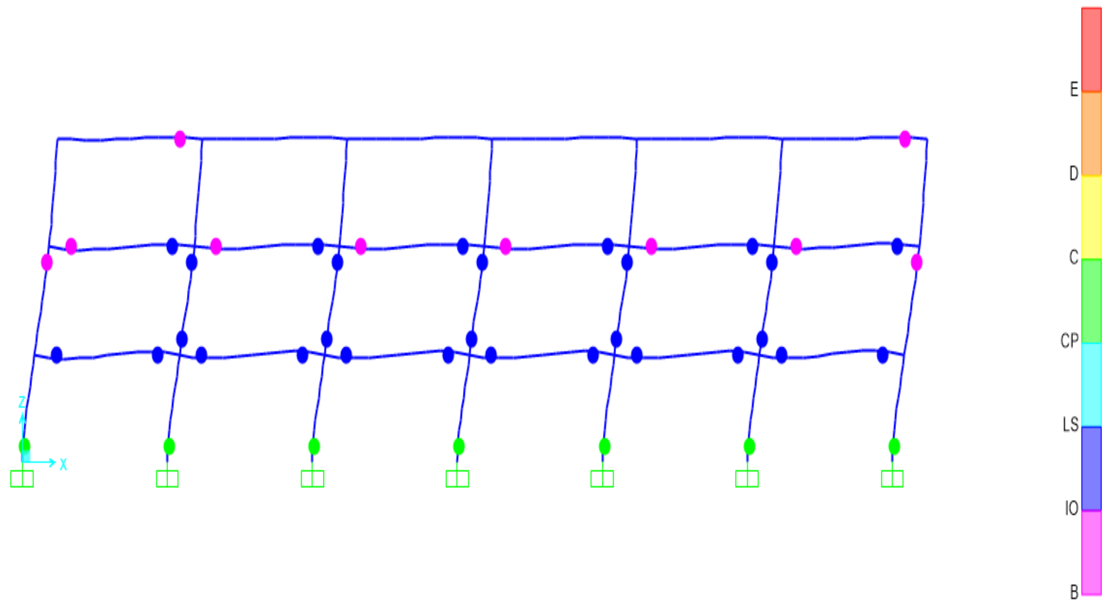

Figure 4.80 Plastic hinge distribution at the final stage of MRF under effect of Holliste earthquake

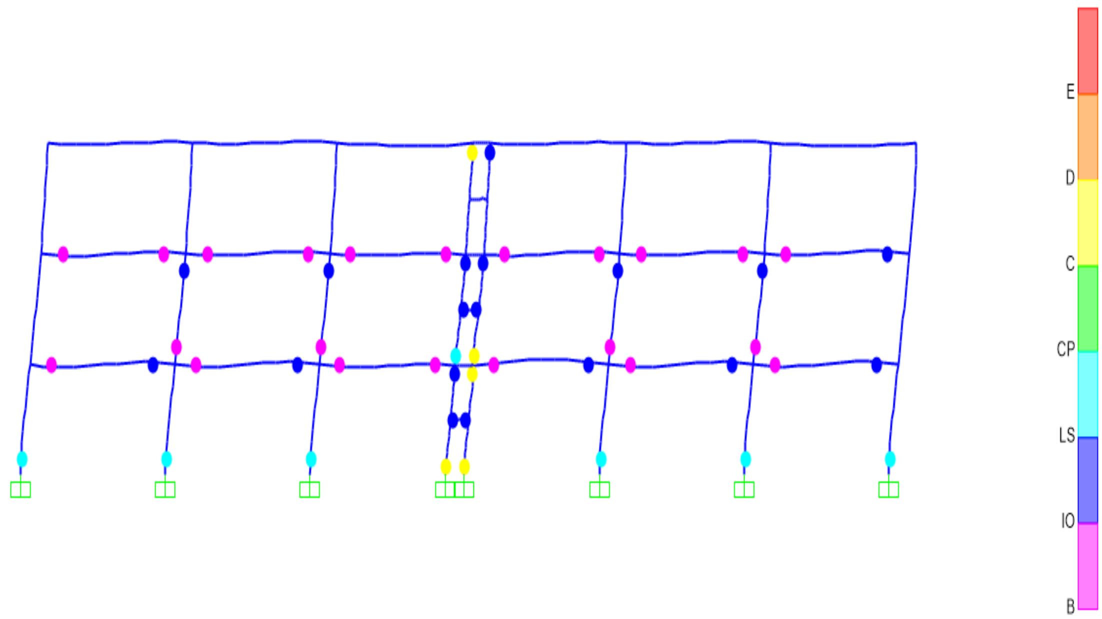

Figure 4.81 Plastic hinge distribution at the final stage of LCF1-1m under effect of Holliste earthquake

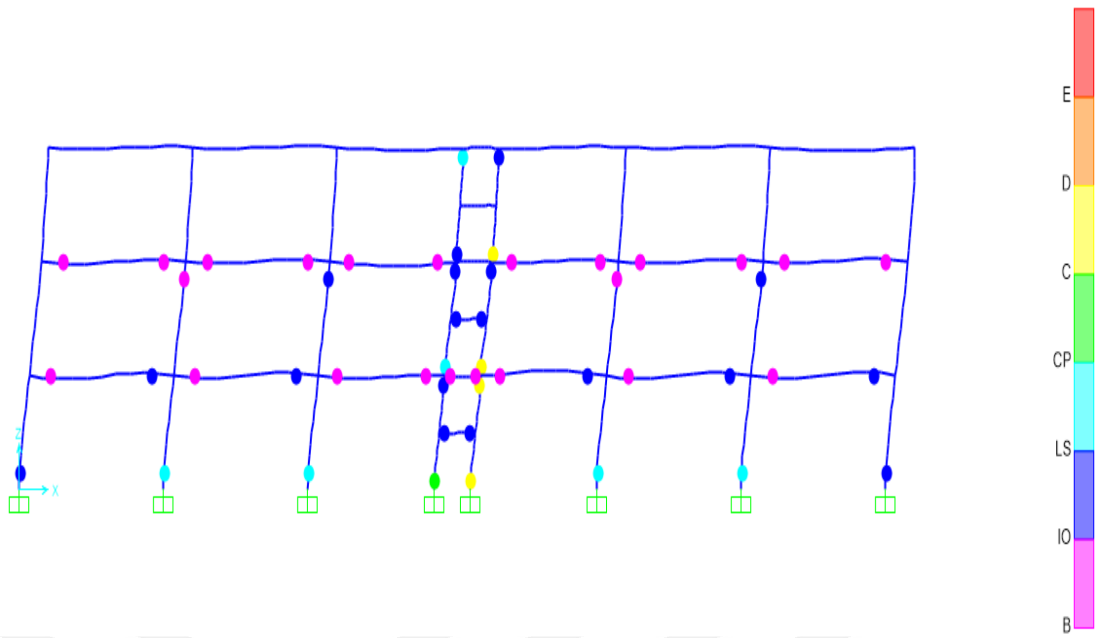

Figure 4.82 Plastic hinge distribution at the final stage of LCF1-2m under effect of Holliste earthquake

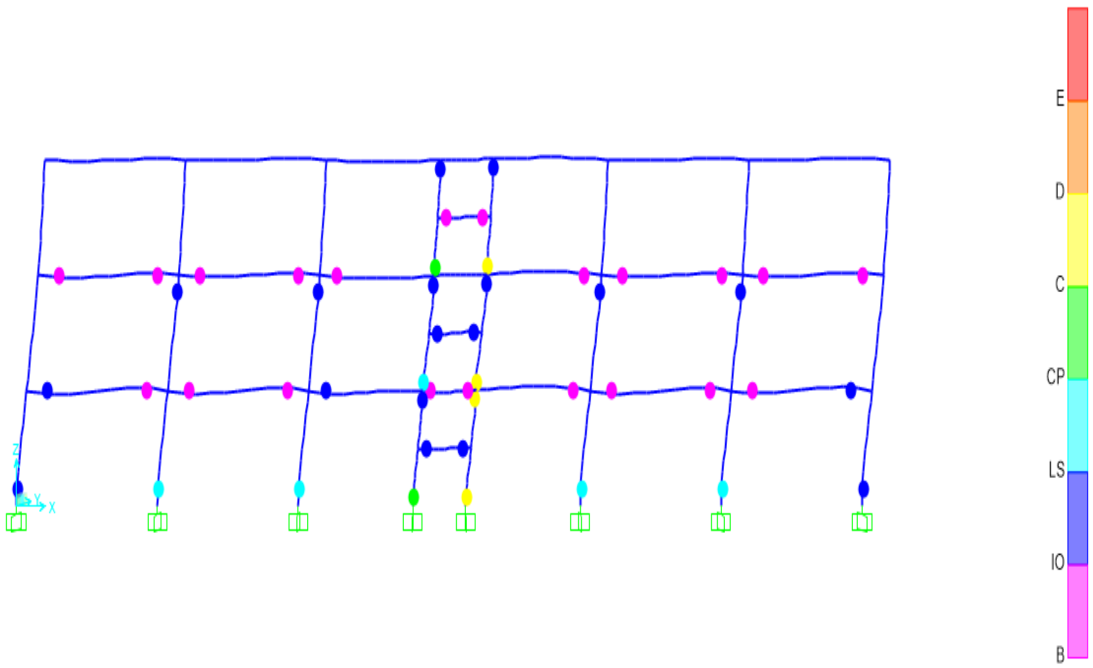

Figure 4.83 Plastic hinge distribution at the final stage of LCF1-3m under effect of Holliste earthquake

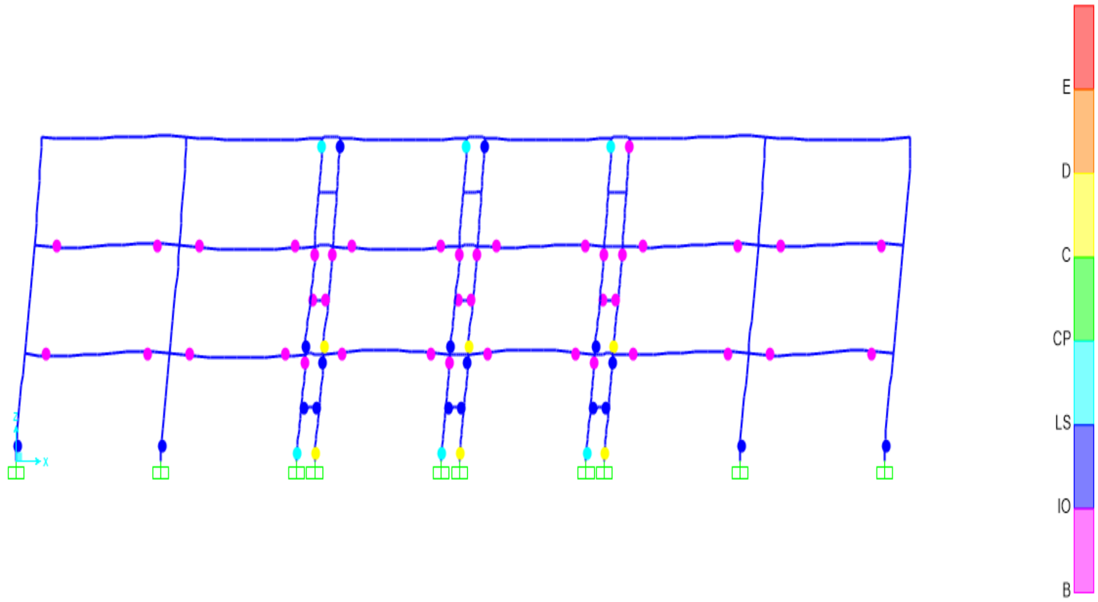

Figure 4.84 Plastic hinge distribution at the final stage of LCF3-1m under effect of Holliste earthquake

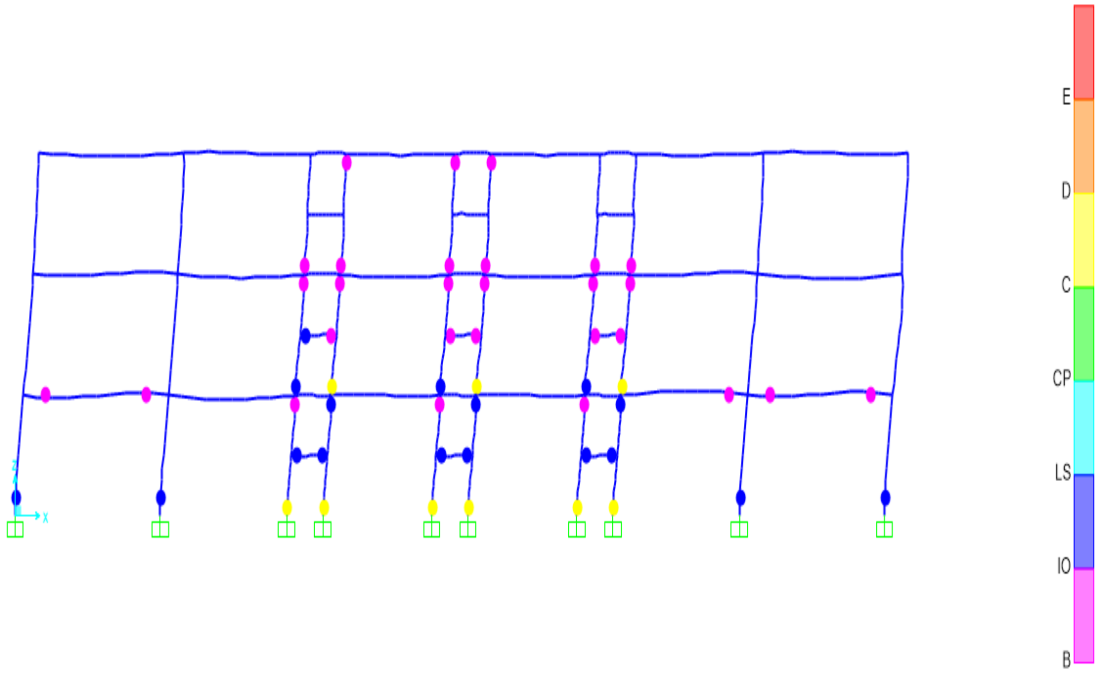

Figure 4.85 Plastic hinge distribution at the final stage of LCF3-2m under effect of Holliste earthquake

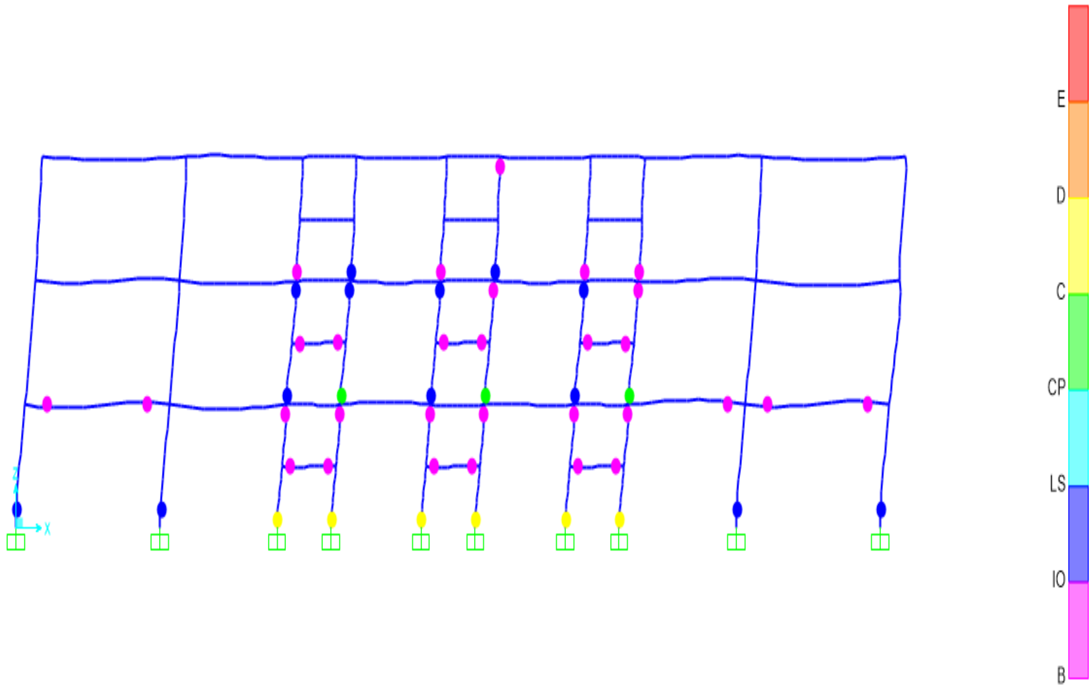

Figure 4.86 Plastic hinge distribution at the final stage of LCF3-3m under effect of Holliste earthquake

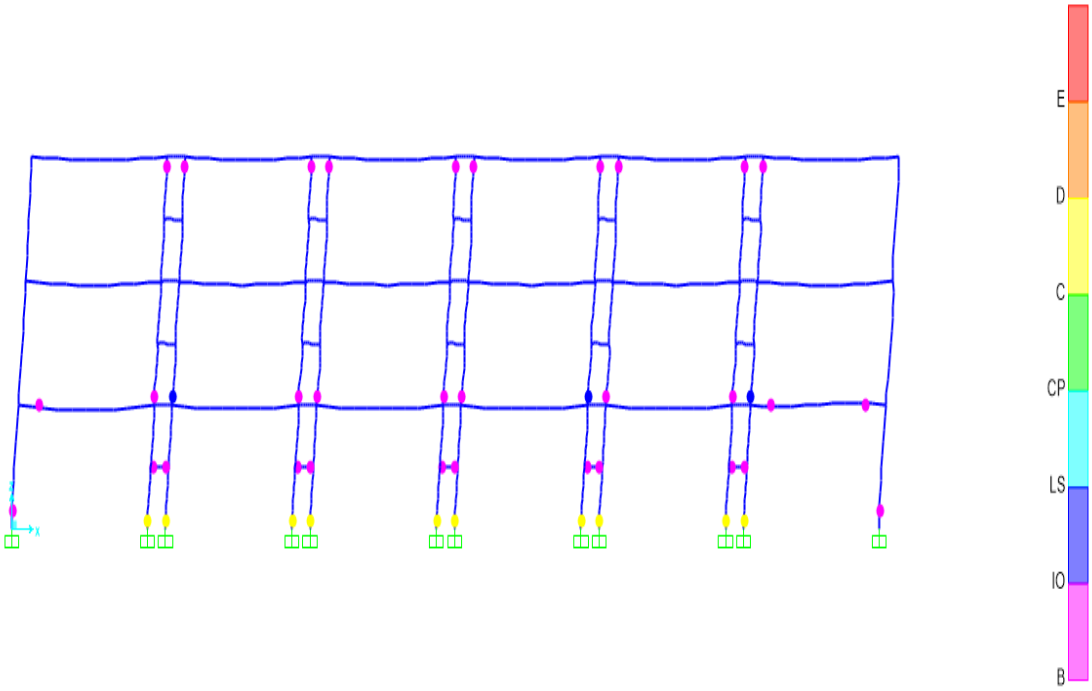

Figure 4.87 Plastic hinge distribution at the final stage of LCF5-1m under effect of Holliste earthquake

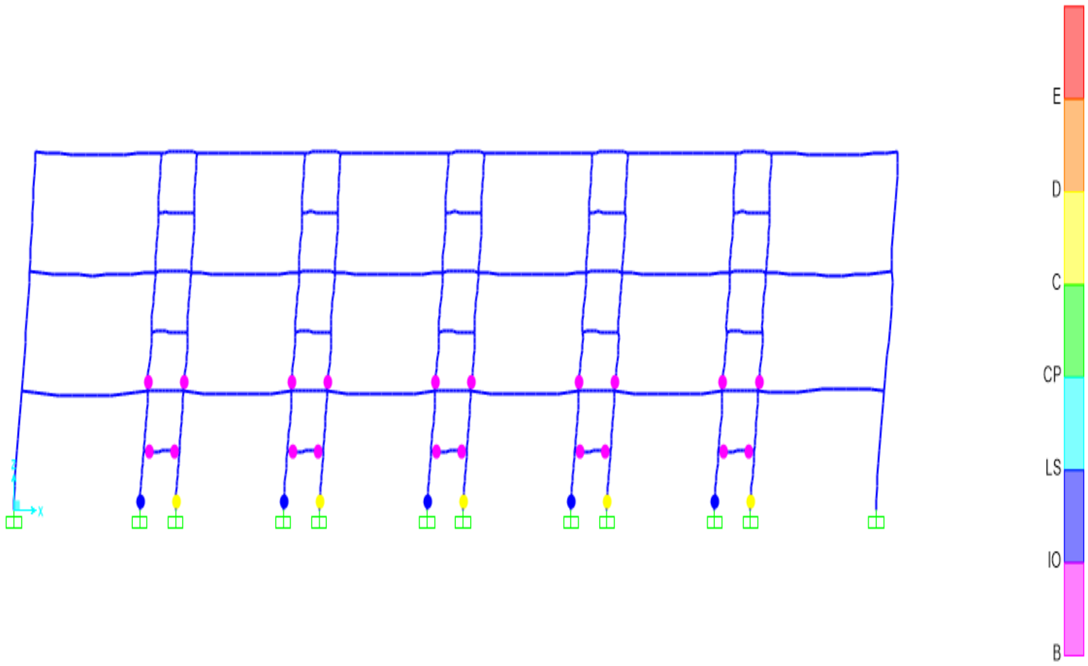

Figure 4.88 Plastic hinge distribution at the final stage of LCF5-2m under effect of Holliste earthquake

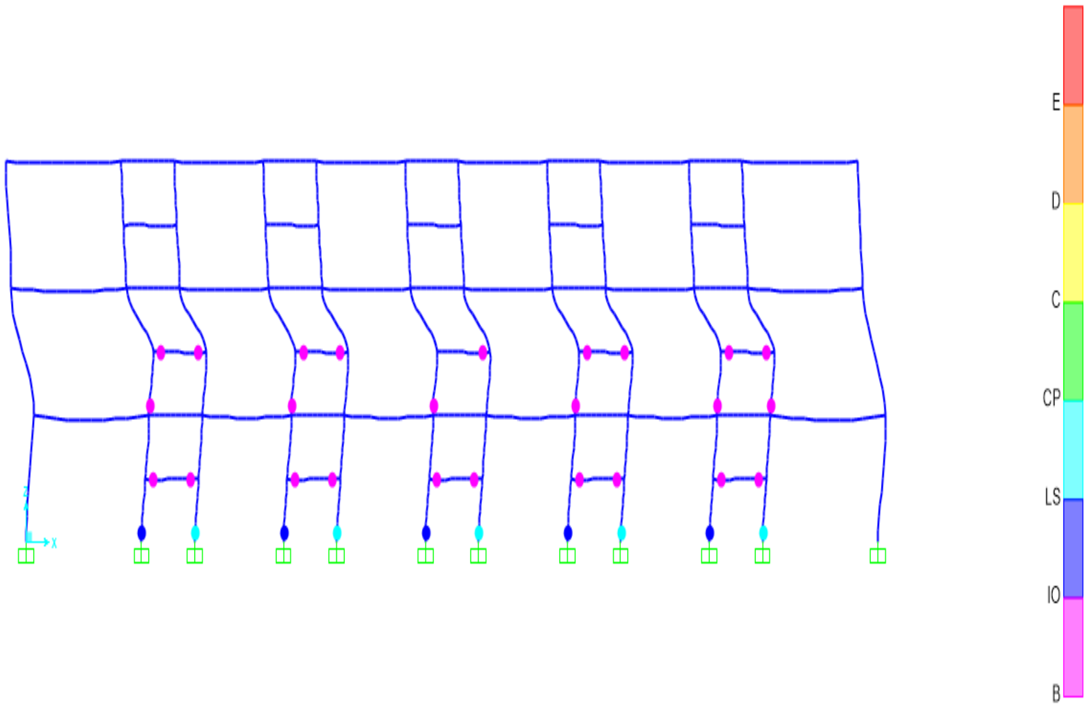

Figure 4.89 Plastic hinge distribution at the final stage of LCF5-3m under effect of Holliste earthquake

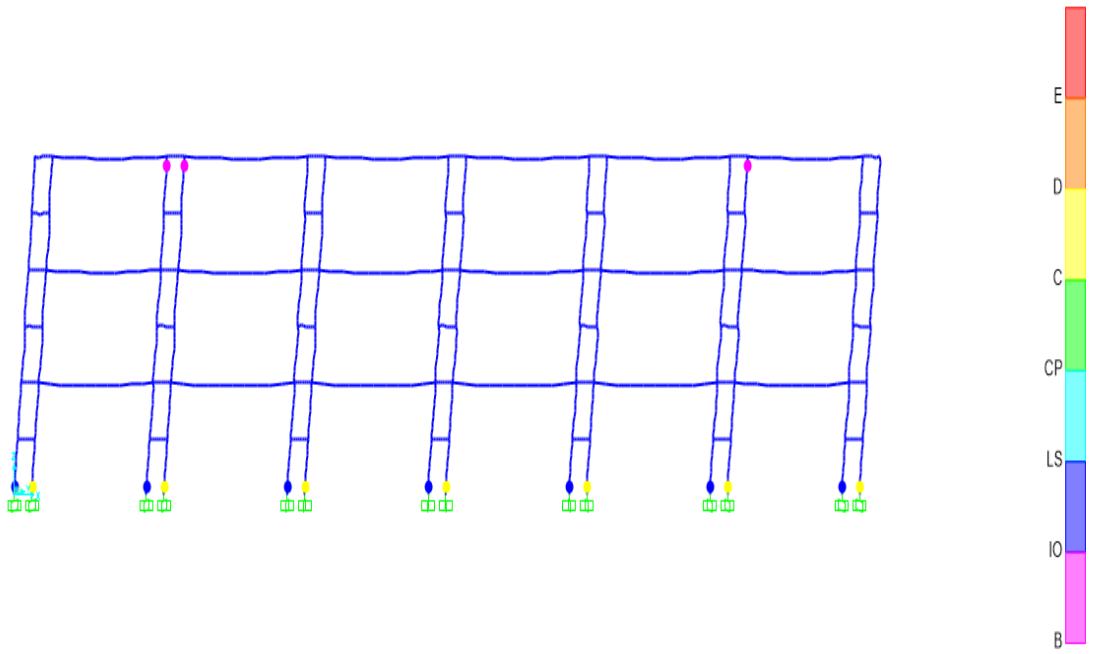

Figure 4.90 Plastic hinge distribution at the final stage of LCF7-1m under effect of Holliste earthquake

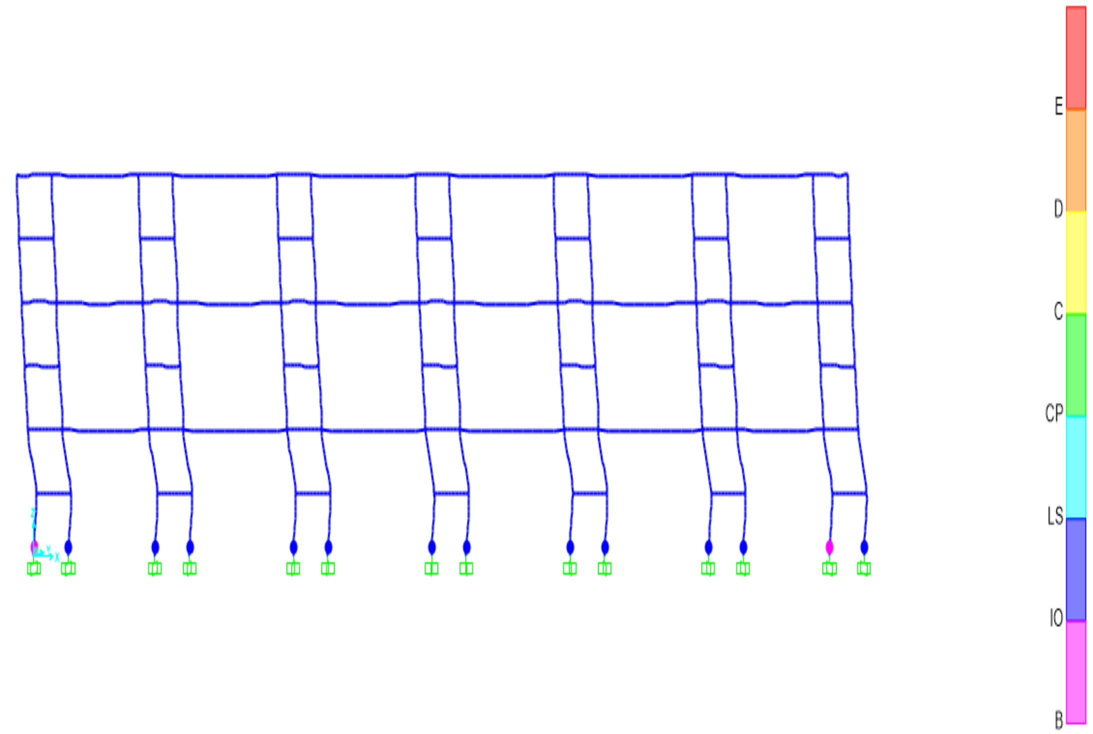

Figure 4.91 Plastic hinge distribution at the final stage of LCF7-2m under effect of Holliste earthquake

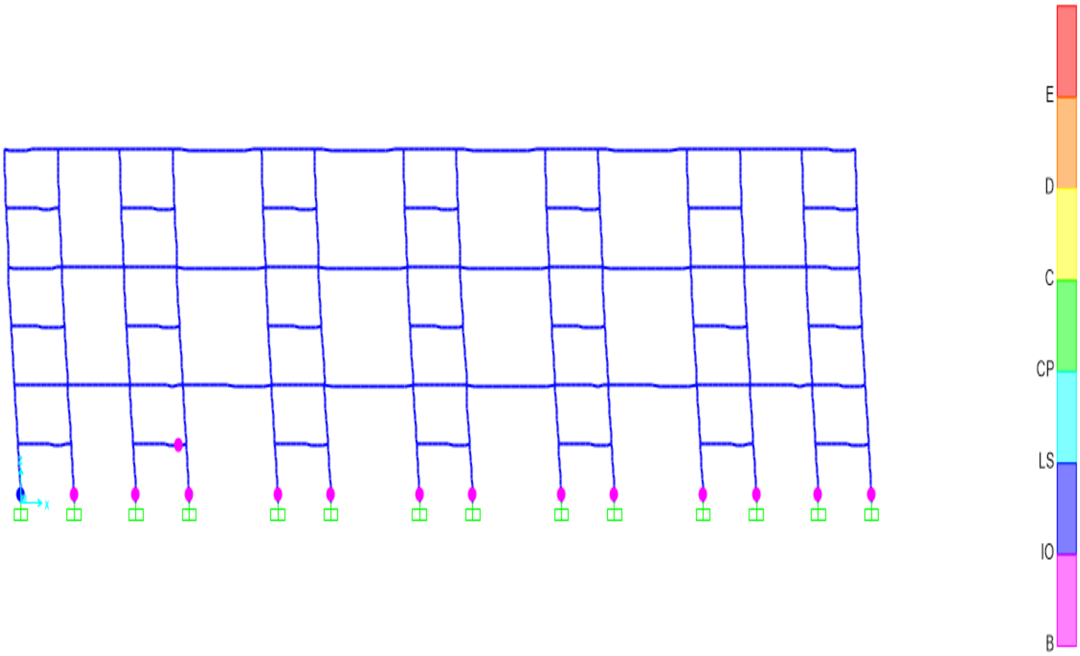

Figure 4.92 Plastic hinge distribution at the final stage of LCF7-3m under effect of Holliste earthquake

CHAPTER 5

CONCLUSIONS

In this study, a MRF and LCFs having different numbers of link columns in the frame system were investigated analytically through nonlinear pushover and time history analysis. The following conclusions were drawn:

- The results of the analysis showed that as the number of link columns in the frame system increased, the base shear capacity and initial stiffness of the structures were increased.

- Also increasing in the base shear capacity and initial stiffness was detected for the same linked column number by changing in dimension of the link beam in all models of the LCFs.

- For pushover analysis less increment in the base shear capacity and initial stiffness detected between the link column spacing of 2 and 3 m as well as more between that of 1 and 2 m.

- From the time history analysis, it was concluded that the link column systems were effective in reducing the displacement demand of the MRF and thus reducing the damage that observed in the structures.

- Like the pushover analysis, in the time history analysis, the maximum displacement was reduced by changing the link beam length from 1 m to 2 m and 3 m, respectively.

- The result of the time history analysis showed that the maximum displacement between 2 m and 3 m link beam was so close which achieved the high results between 1 and 2 m link beam length.

- It was also seen that the link beam length is a parameter that could affect the response of the structure, and it should be decided on both considering the target design performance state and the architectural properties of the structure.

- The analysis of the results showed that the use LCF system as a lateral load resisting system in the case study steel frame upgrades the overall seismic response mostly by providing a plastic hinge concentration on replaceable links.

REFERENCES

AIJ. Architectural Institute of Japan. (1991). Standards for structural calculation of steel reinforced concrete structures, Tokyo, Japan.

AIJ (1995). Performance of steel buildings during the Hyogoken-Nanbu earthquake.

Aiken, I., Clark, P., Tajirian, F., Kasai, K., Kimura, I., Ko, E. (1999). Unbonded braces in the united states - design studies, large-scale testing and the first building application, Proceedings of the International Post-SMiRT Conference Seminar, Vol. I, Korea, Earthquake Engineering Research Center, 317–337.

AISC 341–10 (2010). Seismic Provisions for Structural Steel Buildings, American Institute of Steel Construction.

Arce, G. (2002). Impact of higher strength steels on local buckling and overstrength of links in eccentrically braced frames.

Azizinamini, A., Ghosh, S. K. (1996). Steel reinforced concrete structures in 1995 Hyogoken-Nanbu Earthquake, *Journal of Structural Engineering*, ASCE, **123**(8), 986-990.

Budiono, B., Moestopo, M., Kusumastuti, D., Muslih, M. R. (2017). Residual stress effect on link element of eccentrically braced frame, *Journal of Constructional Steel Research*, **128**, 397-404.

Dargush, G. F., Soong, T. T. (1995). Behavior of metallic plate dampers in seismic passive energy dissipation systems, *Earthquake Spectra*, **11**(4), 545-568.

Detsky, A. S., McLaughlin, J. R., Baker, J. P., Johnston, N. A. N. C. Y., Whittaker, S. C. O. T. T., Mendelson, R. A., Jeejeebhoy, K. N. (1987). What is subjective global assessment of nutritional status?, *Journal of Parenteral and Enteral Nutrition*, **11**(1), 8-13.

DiSarno, L., Elnashai, A. S. (2002). Seismic retrofitting of steel and composite building structures, *Mid-America Earthquake Center CD Release 02-01*.

Doran, B. (2013). Elastic-plastic analysis of R/C coupled shear walls: The equivalent stiffness ratio of the tie elements, *Journal of the Indian Institute of Science*, **83**(3&4), 87.

Dusicka, P., Iwai, R. (2007). Development of linked column frame system for seismic lateral loads, In *Structural Engineering Research Frontiers* (pp. 1-13).

Dusicka, P., Lewis, G. (2010). Investigation of replaceable sacrificial steel links, In *Proceedings of the 9th US National and 10th Canadian Conference on Earthquake Engineering* (Vol. 1659).

Engelhardt, M. D., Popov, E. P. (1992). Experimental performance of long links in eccentrically braced frames, *Journal of Structural Engineering*, **118**(11), 3067-3088.

Federal Emergency Management Agency (2000). State of Art Report on past performance of steel moment frame buildings in earthquakes, Report No. FEMA 355E, Washington, D.C., USA.

FEMA 461 (2007). Interim Testing Protocols for Determining the Seismic Performance Characteristics of Structural and Nonstructural Components, Washington-DC.

FEMA P-749 (2010). Earthquake-Resistant Design Concepts an Introduction to the NEHRP Recommended Seismic Provisions for New Buildings and Other Structures, Washington, DC.

FEMA-350 (2000). Recommended seismic design criteria for new steel moment-frame buildings, Report No. 350, SAC Joint Venture for the Federal Emergency Management Agency, Washington, D.C.

FEMA-351 (2000). Recommended seismic evaluation and upgrade criteria for existing welded steel moment-frame buildings, Report No. 351, SAC Joint Venture for the Federal Emergency Management Agency, Washington, D.C.

FEMA-352 (2000). Recommended postearthquake evaluation and repair criteria for welded steel moment-frame buildings, Report No. 352, SAC Joint Venture for the Federal Emergency Management Agency, Washington, D.C.

FEMA-353 (2000). Recommended specifications and quality assurance guidelines for steel moment-frame construction for seismic applications, Report No. 353, SAC Joint Venture for the Federal Emergency Management Agency, Washington, D.C.

FEMA-354 (2000). A policy guide to steel moment-frame construction. Report No. 354, SAC Joint Venture for the Federal Emergency Management Agency, Washington, D.C.

FEMA-355 C (2001). State of the art report on systems performance of steel moment frames subject to earthquake ground shaking, Report No. 355, Helmut Krawinkler, Team Leader, SAC Joint Venture for the Federal Emergency Management Agency, Washington, D.C.

FEMA-356 (2000). Prestandard and commentary for the seismic rehabilitation of building, Washington, D.C.

Ghobarah, A., Elfath, H. A. (2001). Rehabilitation of a reinforced concrete frame using eccentric steel bracing, *Engineering Structures*, **23**(7), 745-755.

Goodyear, D., Sun, J. (2003). New developments in cable-stayed bridge design, San Francisco, *Structural Engineering International*, **13**(1), 59-63.

Hajjar, J. F., Leon, R. T., Gustafson, M. A., Shield, C. K. (1998). Seismic response of composite moment-resisting connections, II: Behavior, *Journal of Structural Engineering*, **124**(8), 877-885.

Hjelmstad, K. D., Popov, E. P. (1983). Seismic behavior of active beam links in eccentrically braced frames, *NASA STI/Recon Technical Report N*, **84**, 18480.

Iwata, M., Kato, T., Wada, A. (2000). Buckling-restrained braces as hysteretic dampers, *Behavior of Steel Structures in Seismic Areas*, 33-38.

Kasai, K., Popov, E. P. (1986). General behavior of WF steel shear link beams, *Journal of Structural Engineering*, **112**(2), 362-382.

Lewis, G. R. (2010). Replaceable shear and flexural links for the linked column frame system.

Liao, K. W., Wen, Y. K., Foutch, D. A. (2007). Evaluation of 3D steel moment frames under earthquake excitations, I: Modeling, *Journal of structural engineering*, **133**(3), 462-470.

Lopes, A. P., Dusicka, P., Berman, J. (2014, July). Linked column frame steel system performance validation using hybrid simulation, In *Tenth US National Conference on Earthquake Engineering, Anchorage, Alaska*.

Lydia, D. D. H., Hemalatha, G. (2013). Performance of Linked Column System under Seismic forces for Concrete Structures, *Journal of Engineering Research and Applications*, **3**, 1845 - 1849.

Malakoutian, M. (2011). Seismic Response Evaluation of the Linked Column Frame System, Ph.D. partial fulfillment, Civil and Environmental Engineering Dept., University of Washington, Seattle, WA.

Malakoutian, M., Berman, J. W., Dusicka, P. (2013). Seismic response evaluation of the linked column frame system, *Earthquake Engineering & Structural Dynamics*, **42**(6), 795-814.

Malakoutian, M., Berman, J. W., Dusicka, P., Lopes, A. (2012). Seismic Performance and Design of Linked Column Frame System (LCF), In *World Conference on Earthquake Engineering*.

Malakoutian, M., Berman, J. W., Dusicka, P., Lopes, A. (2016). Quantification of Linked Column Frame Seismic Performance Factors for Use in Seismic Design, *Journal of Earthquake Engineering*, **20**(4), 535-558.

Malley, J. O., Popov, E. P. (1983). Design considerations for shear links in eccentrically braced frames, *Earthquake Engineering Research Center*, University of California.

Mazzoni, S., McKenna, F., Scott, M. H., Fenves, G. L. (2006). OpenSees command language manual, *Pacific Earthquake Engineering Research (PEER) Center*.

Minimum Design Loads for Buildings and Other Structures; ASCE 7-10 (2010). American Society of Civil Engineers: Reston, VA, USA.

Miyama, T., Tanaka, K., Meng, L., Kato, Y., Hirasawa, M., Sasaki, M. (1996). Study on the highly damped building with low-yield-point steel shear panel, In *Proceedings of the Eleventh Conference on Earthquake Engineering* (No. 416).

Nader, M., Lopez-Jara, J., Mibelli, C. (2002). Seismic design strategy of the new san francisco-oakland bay bridge self-anchored suspension span, *Proceedings of the Third National Seismic Conference and Workshop on Bridges*, Portland, OR.

Naeim, F. (2001). Seismic Design Handbook 2 ndedn.

Naeim, F., Lew, M., Huang, S. C., Lam, H. K., Carpenter, L. D. (2000). The performance of tall buildings during the 21 September 1999 Chi-Chi earthquake, Taiwan, *The Structural Design of Tall Buildings*, **9**(2), 137-160.

Najafi, L. H., Tehranizadeh, M. (2017). Equation for achieving efficient length of link-beams in eccentrically braced frames and its reliability validation, *Journal of Constructional Steel Research*, **130**, 53-64.

Nakashima, M. (1995). Strain-hardening behavior of shear panels made of low-yield steel, I: test, *Journal of Structural Engineering*, **121**(12), 1742-1749.

Nakashima, M., Akazawa, T., Tsuji, B. (1995). Strain-hardening behavior of shear panels made of low-yield steel, II: model, *Journal of Structural Engineering*, **121**(12), 1750-1757.

Nakashima, M., Inoue, K., Tada, M. (1998). Classification of damage to steel buildings observed in the 1995 Hyogoken-Nanbu earthquake, *Engineering Structures*, **20**(4-6), 271-281.

Nateghi-A, F. (1995). Retrofitting of earthquake-damaged steel buildings, *Engineering Structures*, **17**(10), 749-755.

Nateghi-A, F. (1997). Seismic upgrade design of a low-rise steel building, *Engineering Structures*, **19**(11), 954-963.

Okazaki, T., & Engelhardt, M. D. (2007). Cyclic loading behavior of EBF links constructed of ASTM A992 steel, *Journal of Constructional Steel Research*, **63**(6), 751-765.

Okazaki, T., Arce, G., Ryu, H. C., Engelhardt, M. D. (2005). Experimental study of local buckling, overstrength, and fracture of links in eccentrically braced frames, *Journal of Structural Engineering*, **131**(10), 1526-1535.

Pincheira, J. A., Jirsa, J. O. (1995). Seismic response of RC frames retrofitted with steel braces or walls, *Journal of Structural Engineering*, **121**(8), 1225-1235.

Popov, E. P., Balan, T. A., Yang, T. S. (1998). Post-northridge earthquake seismic steel moment connections, *Earthquake Spectra*, **14**(4), 659-677.

Popov, E. P., Engelhardt, M. D., Ricles, J. M. (1989). Eccentrically braced frames: US practice, *Engineering Journal*, **26**(2).

Precast/Prestressed Concrete Institute. (1992). *PCI Design handbook: Precast and prestressed concrete,* Precast/Prestressed Concrete Institute.

Ramadan, T., Ghobarah, A. (1995). Behaviour of bolted link-column joints in eccentrically braced frames, *Canadian Journal of Civil Engineering*, **22**(4), 745-754.

Richards, P. W. (2004). Cyclic stability and Capacity design of steel eccentrically braced frames.

Richards, P., Uang, C. M. (2002). Evaluation of rotation capacity and overstrength of links in eccentrically braced frames, *Report No. SSRP-2002118. San Diego, CA: Department of Structural Engineering, University of California at San Diego*.

Richards, P., Uang, C. M. (2003). Development of testing protocol for short links in eccentrically braced frames, *Report No. SSRP-2003/08. La Jolla (CA, USA): Department of Structural Engineering, University of California at San Diego*.

Ricles, J. M., Popov, E. P. (1987). Dynamic analysis of seismically resistant eccentrically braced frames, University of California, Earthquake Engineering Research Center.

Roeder, C. W., Popov, E. P. (1977). Inelastic behavior of eccentrically braced steel frames under cyclic loadings, *NASA STI/Recon Technical Report N*, **78**, 20375.

Sabelli, R., Mahin, S., Chang, C. (2003). Seismic demands on steel braced frame buildings with buckling-restrained braces, *Engineering Structures*, **25**(5), 655-666.

Saeki, E., Iwamatu, K., Wada, A. (1996). Analytical study by finite element method and comparison with experiment results concerning buckling-restrained unbonded braces, *Journal of Structural and Construction Engineering*, **484**, 111-120.

SAP. 2000: Static and Dynamic Finite Element Analysis of Structures, Advanced 18.0.0, Structural Analysis Program, Computers and Structures Inc., Berkeley (2009).

Shelton, J. J., Hemalatha, G. (2016). Behavior of Linked-Column System subjected to Seismic Force, *Indian Journal of Science and Technology*, **9**(6).

Shimizu, K., Hashimoto, J., Kawai, H., Wade, A. (1998). Application of damage control structure using energy absorption panel, *Structural Engineering World Wide*.

Shuey, B. D., Engehardt, M. D., Sabol, T. A. (1996). Testing repair concepts for damaged steel moment connections, Experimental investigation of Beam column subassembly ages SAC96-01, SAC Joint Venture, Sacramento, CA.

Stephens, M. T. (2011). Numerical and Experimental Analysis of Composite Sandwich Links for the LCF System.

Tanaka, K., Torii, T., Sasaki, Y., Miyama, T., Kawai, H., Iwata, M., Wada, A. (1998). Practical application of damage tolerant structures with seismic control panel using low yield point steel to a high-rise steel building, *Proceedings, Structural Engineering World Wide, Elsevier, CD-ROM, Paper T190-4*.

Tena-Colunga, A. R., Vergara, A. L. (1997). Comparative study on the seismic retrofit of a mid-rise steel building: steel bracing vs energy dissipation, *Earthquake engineering & structural dynamics*, **26**(6), 637-655.

Tsai, K. C., Chen, H. W., Hong, C. P., Su, Y. F. (1993). Design of steel triangular plate energy absorbers for seismic-resistant construction, *Earthquake spectra*, **9**(3), 505-528.

Turkish Earthquake Code, TEC, (2007). Specification for buildings to be built in seismic zones, *Ministry of Public Works and Settlement, Government of Republic of Turkey*.

Uang, C. M., Bondad, D., Lee, C. H. (1998). Cyclic performance of haunch repaired steel moment connections: experimental testing and analytical modeling, *Engineering Structures*, **20**(4-6), 552-561.

Youssef, N. F., Bonowitz, D., Gross, J. L. (1995). A survey of steel moment-resisting frame buildings affected by the 1994 Northridge earthquake, US National Institute of Standards and Technology.